KTH Electrical Engineering

Interference Mitigation and Synchronization for Satellite Communications

JOEL GROTZ

Doctoral Thesis in Telecommunications
Stockholm, Sweden 2008

KTH, School of Electrical Engineering
Signal Processing Laboratory
SE-100 44 Stockholm
SWEDEN

TRITA-EE 2008:058
ISSN 1653-5146
ISBN 978-91-7415-182-4

Akademisk avhandling som med tillstånd av Kungl Tekniska högskolan framlägges till offentlig granskning för avläggande av teknologie doktorsexamen i telekommunikation 12 December 2008, klockan 10:00 i Amphithéatre B02, Université de Luxembourg, 6 rue Coudenhove-Kalergi, L-1359 Luxembourg.

Tryck: Universitetsservice US AB

Abstract

Within this thesis, the satellite broadcast scenario of geostationary satellites is reviewed. The densely crowded geostationary arc in the common broadcast frequencies may create significant interference from adjacent satellites (ASI). The possible use of multiple-input receivers and of interference processing techniques is analyzed in this specific context. In addition the synchronization problem is studied under interference limited conditions for broadcast as well as broadband satellite systems.

We address fixed satellite broadcast reception with the goal of decreasing the aperture of the receiving antenna. The front-end antenna size is commonly defined by the presence of interference from adjacent satellites. A small antenna aperture leads to interference from neighboring satellites utilizing the same frequency bands. We propose a multi-input reception system with subsequent joint detection which provides reliable communication in the presence of multiple interfering signals. An iterative least square technique is adopted combining spatial and temporal processing. This approach achieves robustness against pointing errors and against changing interference scenarios. Different temporal interference processing methods are evaluated, including Minimum Mean Square Error (MMSE) based iterative soft-decision interference cancellation as well as Iterative Least Square with Projection (ILSP) based approaches, which include spatial and temporal iterations. Furthermore the potential of an additional convolutional channel decoding step in the interference cancellation mechanism is verified.

Also, we demonstrate how to accurately synchronize the signals as part of the detection procedure. The technique is evaluated in a realistic simulation study representing the conditions encountered in typical broadcast scenarios.

In a second part of the thesis the problem of synchronization is reviewed in the context of interference limited scenarios for broadband satellite return channels. Spectral efficiency is of great concern in the return channel of satellite based broadband systems. In recent work the feasibility of increased efficiency by reducing channel spacing below the Symbol Rate was demonstrated using joint detection and decoding for a synchronized system. We extend this work by addressing the critical synchronization problem in the presence of adjacent channel interference (ACI) which limits performance as carrier spacing is reduced.

A pilot sequence aided joint synchronization scheme for a multi-frequency time division multiple access (MF-TDMA) system is proposed. Based on a maximum likelihood (ML) criterion, the channel parameters, including frequency, time and phase are jointly estimated for the channel of interest and the adjacent channels. The impact of ACI on the synchronization and detection performance is investigated. It is shown that joint channel parameter estimation outperforms single carrier synchronization with reasonable additional

computational complexity in the receiver. Based on the proposed synchronization scheme in conjunction with an appropriate joint detection mechanism the carrier spacing can be reduced significantly compared to current systems providing a substantial increase in spectral efficiency.

Acknowledgments

First and foremost I would like to thank Professor Björn Ottersten for his excellent teaching and support throughout my thesis work. He certainly has a busy schedule but nevertheless always finds the time to give good advice and guidance. This work is nearing completion with the help of his active, efficient and professional support. I would also like to thank Dr. Jens Krause from SES ASTRA for his good support and advice throughout my work, despite his loaded schedule.

I am grateful for the financial support I received in the form of a *Bourse Formation Recherche* (BFR) from the Luxembourg Ministry of Higher Education and Culture. Furthermore I would like to thank the *Luxembourg International Advanced Studies in Information Technologies Institute* (LIASIT) and the *Société Européenne des Satellites* (SES) for their active support and help throughout my work. Especially Professor Thomas Engel and Dr. Gérard Hoffmann from LIASIT, who have - certainly among others - been instrumental in building up the LIASIT Ph.D. program.

Also many thanks to the Product Development Group within SES ASTRA and Detlef Schulz, who helped make this work possible and all the colleagues from SES ASTRA and SES Engineering who supported and encouraged this work. I would also like to thank Jean-Pierre Choffray, Dr. Claus-Peter Fischer, Tom Christophory and Joël Ordener from SES for inspiring discussions, support and good advice.

I am grateful for a friendly and supportive work environment at the Signal Processing Group of the *School of Electrical Engineering* (*EE*) at *KTH*, Stockholm and especially to Pandu Devarakota, Cristoff Martin, Jochen Giese and Xi Zhang. All the Ph.D. students at *EE* are highly motivated and hard-working but the very supportive and positive atmosphere is certainly motivating. I would like to thank all my friends and fellow Ph.D. students on *plan 4* for a pleasant collaboration, the interesting discussions and the nice time I had in Stockholm. I am looking forward to the Alumni-days.

I am grateful to Magali Martin from *LIASIT* and to Annika Augustsson and Karin Demin from *EE* at *KTH* for their efficient and excellent support for all administrative work.

It has been a pleasure for me to guide and supervise the Diploma Thesis and also the Master Thesis work of Klaus Schwarzenbarth. Also the work within the related ESA pre-study in collaboration with *Space Engineering S.p.A., Rome* has been very interesting and helped broaden the approach and scope of this work.

I would also like to thank the examination committee members that have the task of reviewing this work, some of which have to travel from far to attend the thesis defense.

Finally I am certainly grateful also to my family and friends for their support and patience throughout the more stressful times of this work.

Joël Grotz
September 2008

Contents

Chapter 1

Introduction

1.1 Motivation

In this thesis we investigate the performance of satellite communication systems under interference limited conditions. Both fix satellite broadcast and broadband systems are reviewed in that perspective. An increased demand for broadcast services (i.e. Video/TV, Audio and Data services) as well as the current strong trend for global and ubiquitous internet services (i.e. broadband access and trunking) increases also the demand for satellite based services. Both broadcast services and broadband access services are considered in the framework of this thesis.
For broadcast systems, the increase in traffic in key frequency bands (e.g. C-band at 4GHz and Ku-band at 12GHz) has created increased interference levels from adjacent satellite systems. The scenarios of fixed satellite communication are revised in the perspective of currently typical interference conditions. The main aim is to address the requirements on the terminal front-end that are defined by interference scenarios. The use of small aperture antennas is of commercial importance, especially for consumer-grade receiving terminals. However small antennas are less spatially selective in their gain pattern and stronger interference from adjacent satellites has to be taken into account.
The work presented in this thesis addresses the specific interference limited detection problems in satellite communication and proposes new techniques for the receivers that help reach high throughput efficiencies while reducing the reception equipment front-end requirements.
In a second part, satellite broadband systems are analyzed, under the aspects of multiple-access interference between users. The need to support a large number of users with high data throughputs drives the requirement for efficient transmission schemes over the limited satellite capacity. Different challenges arise in the development and improvement of multi-user access schemes at different levels of the communication chain. In the framework of this thesis we

focus on the physical layer of the return link. Especially the interference between users and the related synchronization problems in time and frequency are analyzed.

1.2 Satellite Broadcast Systems Background

The fixed satellite reception and fixed satellite two-way systems in satellite allocated frequency bands (C-band, Ku-band and Ka-band) have been developed and studied since decades. The first generation of satellite systems used large reception and transmission earth station antennas to compensate for the low sensitivities and high noise figures of the first generation of reception systems. The development of the high electron mobility transistors (HEMT) [SCD+87] led to the conception of low-noise receiver electronics at very low costs compared to traditional receiver structures [Wei82]. This permitted the use of smaller reception antennas and eventually has been key to the market success of satellite broadcast reception.
The development of digital transmission schemes has decreased considerably the requirements on signal quality for decoding and has permitted the continuation of the trend towards smaller reception terminals. The standards defined by the Digital Video Broadcasting (DVB) standardisation body[1] have gained wide acceptance.
Recent advances in channel coding technology based on Low Density Parity Check Codes (LDPC), first investigated by Gallager [Gal62], later re-proposed by MacKay and Tanner [MN96] [Tan96] [KLF01] have led to the definition of a second generation of these transmission schemes [ETS05a] with a significantly increase spectral efficiency [MR04]. A significant amount of work has since been done on LDPC decoding, especially on reduced complexity decoding schemes, e.g. [FMI99] [Col07] [Lec07].
This previous work has focused on improving the single satellite link to the possible theoretical limit, these are however suboptimal if the link is limited by interference from adjacent systems and not only noise sources. Untreated interference is perceived as a noise source at the receiver, however by exploiting the interference structure the link performance can be improved as demonstrated herein.

1.3 Satellite Broadband Systems Background

We define as *satellite broadband systems* two-way communication systems, centered around a common access system, the *hub* and using satellite capacity to access the hub. In general this satellite capacity is located on a geostationary satellite platform.

[1] see DVB Website: http://www.dvb.org/

Proprietary, so called, very small aperture terminals (VSAT) systems have been developed in the past (1980's) for C-band and Ku-band systems and operated with success for voice, video and data based services. The development of solid-state power amplifiers (SSPA) has allowed the development of transmit electronics that could be fitted to small transmit antennas [FLR94] and have been a major factor for the VSAT proliferation.
The seamless coverage of a geographical area, including all the rural regions, is without doubt one of the main commercial advantages of satellite based broadband systems with respect to its terrestrial competition. Furthermore satellite broadband has through its network topology clear advantages with respect to terrestrial system for multicast based applications. Proprietary VSAT access technologies have been developed for satellite systems based on different approaches, CDMA based access strategies on a defined SCPC as well as multi-frequency time division multiple access (MF-TDMA) based systems. In an effort to improve the efficiency and standardize and harmonize the VSAT based systems, the DVB standardization body launched a working group with the result of DVB Return Channel via Satellite (RCS) [ETS03a]. A major goal of the standardization has been the terminal cost reduction and interoperability.
Also the development of more efficient access technologies has led to a new VSAT standard that defines a common multi-frequency time division multiple access (MF-TDMA) based access policy on the return channel, [ETS03a] and allows for more cost effective and efficient VSAT networks. DVB-RCS based two-way satellite systems have emerged in the last years and are used with success in many civilian and military markets around the world. The main known commercial manufacturers on this satellite broadband market include among others *Newtec Cy N.C.*, *Hughes Network Systems Inc.*, *Gilat Satellite Networks*, *ALCATEL*, *Thales Alenia Space*, *EMS Advantech AMT* and *STM Networks Inc.*
In addition, satellite broadband systems throughput efficiency has increased through the development of novel space segment multiplexing technologies, such as multi-beam coverages and frequency-reuse on these coverage areas. Furthermore the advances in coding theory have also improved the burst mode transmission schemes, especially turbo-based codes [BG96] have proved very effective. In the future, also satellite signal regenerative systems will further improve link efficiencies, [MB02] [HMF02]. Efficiency is understood here as spectral efficiency in terms of throughput per Hertz, bits/s/Hz. We demonstrate herein how the spectral efficiency can be further improved by Multi-User Detection (MUD) based processing in the multi-carrier demodulator of the hub and also specifically by the additional support of joint synchronization methods.

Physical Layer Efficiency

The return channel via satellite is commonly shared among the active terminals within the coverage area on an MF-TDMA basis. The physical layer efficiency

in terms of aggregate throughput rate in bits/s/Hz of the system depends on a number of factors. Assuming that the modulation and coding is defined by the standard [ETS03a], this allows however for a certain number of parameters to be optimized, among others the channel frequency spacing of the MF-TDMA system, the burst training sequence length as well as the timing guard band between the MF-TDMA transmission slots.
In this thesis we focus on the tunable parameters within DVB-RCS that allow to optimize the return channel efficiency and device a receiver mechanism that allows for a tighter fitting of the MF-TDMA slots on the return link and permits smaller training sequence lengths at the same system target performance level.

Network Layer Efficiency

It is worth mentioning that in addition to the physical layer, the network layer is key for efficient return link utilization. The aspects include the capacity allocation on the return link (link layer aspects) as well as higher layer protocols, such as TCP/IP.
The link layer aspects defined in the framework of DVB-RCS consists of a Demand Assignment Multiple Access (DAMA) based capacity framing and allocation. The scheduling of the capacity assignment for the variable, demand based capacity is a major aspect of the overall system efficiency. Dynamic bandwidth allocation is one of the important tools to improve link layer efficiency, see e.g. [CFP04].

On the application layer, the TCP protocol has trouble to perform well over a the long hop delay, which results from the long propagation delay to geostationary satellites. This simple drawback has been the major performance issue in the first DVB-RCS based systems. A number of TCP enhancement solutions have been proposed and are available now, improving as far as possible the network layer performance of two-way systems, e.g. [HK99]. The simplest solutions consist in adapting TCP parameters to accommodate for long access delays and optimize as far as possible the slow-start mechanism. A better alternative is to terminate the TCP connection at the terminal side in a performance enhanced proxy (PEP) and use an optimized communication protocol over the satellite link. This solution is proposed by several non-standard based systems, e.g. *TelliNet* [Tel] or *PEPsal* [CFL07].
In addition, application layer optimizations can be performed for two-way satellite systems that help improve the experienced throughput speed. Especially *HTTP pre-fetching* and content caching have potential to improve the application layer throughput of satellite systems, addressing the problem of fragmented web-pages and repeated transmission of the same content.
In recent work, cross-layer optimization aspects have been investigated. For specific traffic patterns, link layer protocols that take into account the state of the physical layer have proved to outperform the classical separation of the communication problems, [CFK07]. While network and application layer optimizations are worth

mentioning and an important aspect of improving throughput efficiency of the return channel of satellite broadband systems, these aspects are out-of-scope of the presented work, which focuses on physical layer aspects.

Future Broadband Systems

The forward link of two-way satellite systems will benefit considerably from the introduction of adaptive coding and modulation (ACM) with DVB-S2. The ACM capability allows the design of links with a sufficient rainfade margin to maintain the communication link during fading events and permits high throughput rates when no rainfade is experienced, [ETS05a] [RdG04a] [CdGR08]. The fading events on fix satellite links are long-term events, which makes a simple closed-loop system feasible, that adapts the modulation and coding rate to the experienced signal quality level at the receiver side. In a similar manner ACM techniques can be adapted also to the return link of two-way systems to exploit the long-term rainfade variations, [RdG04b].
In addition, the proliferation of satellite broadband will drive the need for further system level optimizations. In large networks the optimization of the space segment can provide additional efficiency increases. Especially the use of spot-beam coverages with frequency reuse between the different spot-beams increases the spatial reuse of the same frequency band. Especially Ka-band based systems promise efficiency increases in that respect, as the spot-beam coverage can be designed to be smaller as compared with Ku-band systems. Also the major drawback of Ka-band systems, which is its high fading induced by rain and atmospheric effects, is largely alleviated with the use of ACM techniques that can help exploit the high rainfade margin that has to be included in the system design. Furthermore, the dynamic allocation of the satellite power to the transmitting terminals further increases the potential throughput of the systems.

Non-GEO based Broadband Systems

Possible further evolutions of satellite broadband include non geostationary (NGEO) based systems that use a number of satellites positioned in low earth orbit (LEO) constellation to form a global coverage or in elliptic orbits covering a large defined geographic area. Such systems have a number of advantages, which include the inherently better link budget due to the satellites that are much closer compared to geostationary satellites. These systems face different additional problems due to the non negligible satellite movements, which requires Doppler shift compensation and satellite tracking, as well as a seamless handover procedure that does not loose the link when one satellite moves out of reach of a given terminal. In these systems , inter-satellite links (ISL) can help reduce the required number of ground gateway stations, see [TKN05].

In addition, there are medium earth orbit (MEO) satellite constellations as well as high elliptical orbits (HEO) that represent a feasible and interesting compromise for global coverage satellite access systems. In fact these satellite constellations can be realized with less satellites than LEO systems while still providing a significant link budget and signal delay improvement over traditional GEO stationary satellite constellations.

Mobile Applications

Current development work is done by extending DVB-RCS based systems to permit mobile and nomadic applications, including usage in e.g. trains, buses, airplanes and ships. A number of technical challenges have to be overcome in that respect, which are mainly in the area of synchronization for connection establishment, related guard-bands in timing and frequency as well as regulatory aspects related to mobile transmitting terminals. The DVB-RCS standard itself provides the necessary flexibility to permit mobile applications in a standard compatible manner.
The integration of mobile two-way satellite systems with future terrestrial wireless systems such as WiMAX[2] and LTE[3] based systems, is a good candidate for the combination of seamless data coverage and high throughput for mobile applications. Indeed current 3G wireless systems and future LTE or *4G* systems, based on OFDMA and spatio-temporal access techniques [OSA99] [SGS08] are good candidates to provide wireless high speed data connections to mobile devices. However the need for a terrestrial network infrastructure means that the high volume services will likely be available in urban areas and only at high costs in other rural sites. Satellite based two-way systems are ideal to complement these terrestrial high speed connections with seamless coverage.

1.4 Satellite Broadcast Reception

The first part of this thesis focuses on the broadcast scenario, e.g. in Ku-band or C-band. Figure 1.1 illustrates the common considered scenario of a geostationary satellite serving a large broadcast receiver population within a large defined broadcast region with a common signal. The signal transmitted bears commonly DVB-S [ETS98] or DVB-S2 [ETS05a] digitally encoded video and audio content, but recently more and more IP based services have become available.
The receivers are considered consumer-grade equipment and are subject to significant cost constraints in that respect. The antenna front-end has a direct impact on the receive signal level through its antenna gain on-axis, the noise

[2]see WiMAX Forum Website: http://www.wimaxforum.org/
[3]see 3GPP Website: http://www.3gpp.org/

figure of the receiving electronics (ie. LNB) and the off-axis gain towards the interfering satellites. This requirement is in contradiction to the strong commercial requirement for small and compact reception antennas. This requirement has been confirmed by market research and is especially strong in urban areas, where large antennas are undesirable.
The possibility to use small reception antennas is consequently seen as a strong commercial advantage, especially with the increased competition from other means of content distribution, e.g. TVoDSL, DVB-T, FTTH. In commonly used broadcast frequency bands, the antenna dimensions are however often limited by the presence of interferers on adjacent satellites using the same frequency band. A reduction of the antenna aperture would inevitably imply an increased level of interference from adjacent satellites. The reduced signal quality could to some degree be counteracted by a lower coding rate on the channel, but only at the detriment of throughput efficiency.

In this context, the presented work analyzes the use of interference processing techniques at the terminal, adapted to the specific scenario of satellite broadcast reception. The use of a multi-input antenna front end is considered that introduces a spatial degree of freedom in the antenna gain diagram. In addition, a nonlinear signal processing step that actively processes the interference is considered and analyzed in detail.

Figure 1.2 illustrates the link budget of a typical broadcast link in Ku-band with two interferers at +3 and -3 degrees spacing from the desired signal direction. This is considered a typical interference scenario, which can be different for specific channels on different broadcast satellites. The impact of the interference increases with smaller antenna sizes and the link becomes interference limited. The typical recommended antenna sizes for DTH reception is around 60cm. This is comparable in performance to a 40cm antenna without interference.

Broadcast receivers can work with channels at various signal-to-noise (SNR) ratios, especially the recent DVB-S2 standard [ETS05a] allows an impressive flexibility in the possibility to select coding and modulation schemes that are best suited for a given SNR region. Adapting the broadcast link to lower signal to noise ratios will however inevitably be linked to a reduced channel capacity and thus throughput. In that respect the benefit of the use of interference mitigation techniques can be evaluated in terms of channel capacity gain, in Shannon's classical [Sha48] terms, as follows:

$$\Delta C = \log_2 (1 + \mathrm{SNR}) - \log_2 (1 + \mathrm{SNIR}) \tag{1.1}$$

if we view the interference as additional additive Gaussian noise source. The considered interference scenario is static and changing only rarely in time. The interferers are in most cases wide-band and of similar signal nature than the wanted signal, i.e. digitally modulated DVB-S/S2 signals. It may occur that the interferers are of

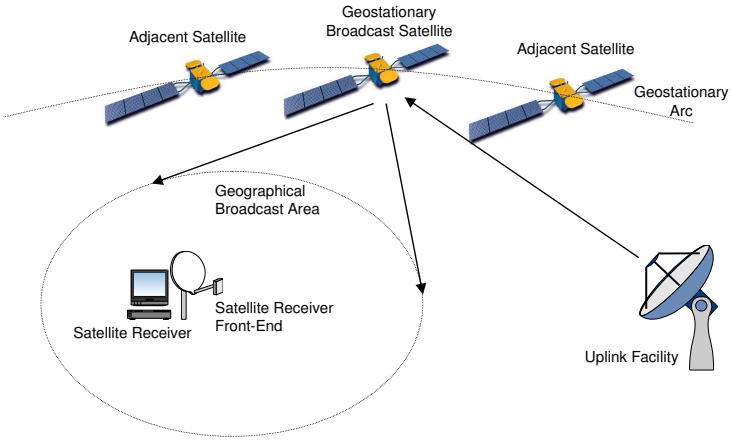

Figure 1.1: Illustration of basic concept of satellite broadcast based on geostationary satellites. A common broadcast signal is received by a large number of receiving satellite terminals. Interference in the same frequency band is experienced by the receiving terminals from the adjacent satellite systems, if a small antenna aperture is deployed at the receiver front-end. Note that the interference situation is quasi-static and a measurement at the uplink facility can help the receivers with the interference detection and classification in terms of modulation type, symbol rate and standard compliance.

different signal nature or multi-carrier narrow-band transmissions. The nature of the interferer has an impact on the possible mitigation techniques, which is taken into account in the approach outlined in the following chapters of this thesis. For digitally modulated signals, the receiver exploits the signal structure and interference cancellation approaches are possible that are not feasible with other signal types. Since we are assuming a quasi-static interference scenario, the modulation parameters of the digitally modulated signals, including modulation type, symbol rate, standard compliance, coding rate, power levels and coarse frequency estimation are determined at a central control point and communicated to the receivers, via e.g. a dedicated private section in a DVB table. This hub support alleviates the need for interference parameter detection and reduces the burden on the broadcast receiver processing. This mechanism has also additional advantages in terms of a reduced processing requirements in the receiver.

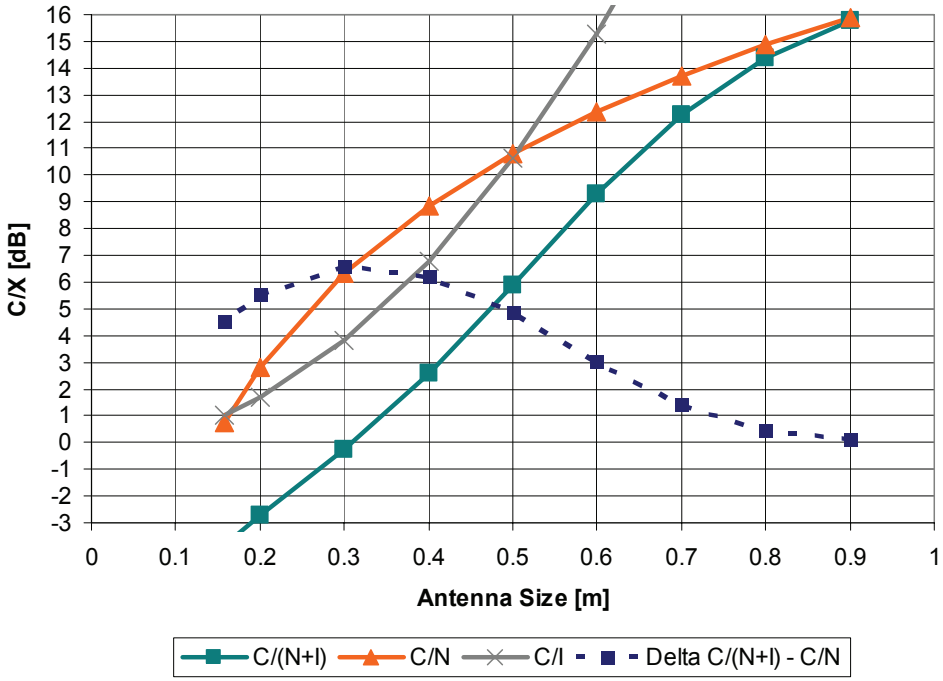

Figure 1.2: Impact of interference on the link budget of small reception antenna as a function of the antenna size. Two interferers were assumed, spaced at +3 and -3 degrees offset with the same power level as the desired signal. Here, C/N is the signal to noise ratio at reception, C/I the signal to interference ratio and C/(N+I) represents the combined signal to noise and interference ratio at reception. Delta C/(N+I) - C/N represents the potential gain of active interference processing.

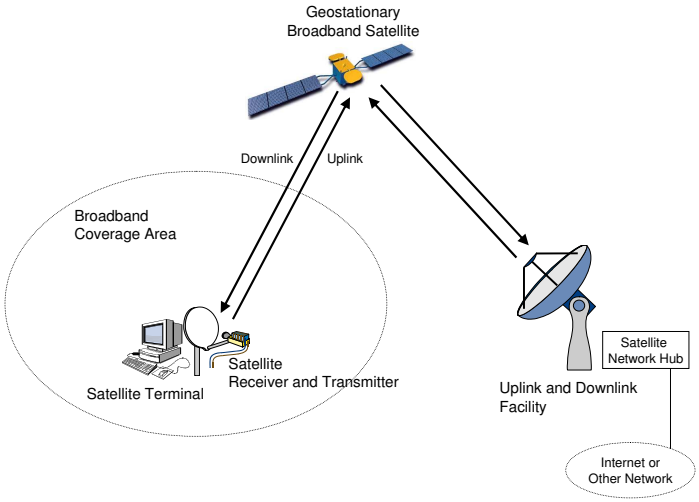

Figure 1.3: Satellite Broadband Basic Scenario. A large number of interactive broadband terminals are connected via a shared satellite capacity to a common network hub.

1.5 Satellite Broadband Networks

In two-way satellite broadband systems, such as DVB-RCS [ETS03a] [ETS03b] based systems, the MF-TDMA scheme foresees a burst based access on the return channel that is shared among the different transmitting terminals.

The return channel from the terminal to the receiving hub station is MF-TDMA based. MF-TDMA is a version of frequency and time multiplexing access scheme, where the carrier frequency transmitted by a particular user can change from burst to burst. The frame structure of this MF-TDMA link can be flexibly adapted to different channel spacings and the duration of a burst is also a configurable parameter. The efficiency of this multi-user return link depends on the choice of operational parameters and which must be compatible with the common receiving hub station.

The spectral efficiency depends on the slot spacing in the frequency band of the MF-TDMA scheme, see Figure 1.4. In the first implementations of the DVB-RCS systems, a channel spacing factor of 1.0-1.5 $\times$ signal symbol rate (ie. burst bandwidth) has been used to eliminate the adjacent channel interference (ACI) from the interference budget. The spectral efficiency of the system as a whole is however directly proportional to the channel spacing. A denser slot spacing results in a

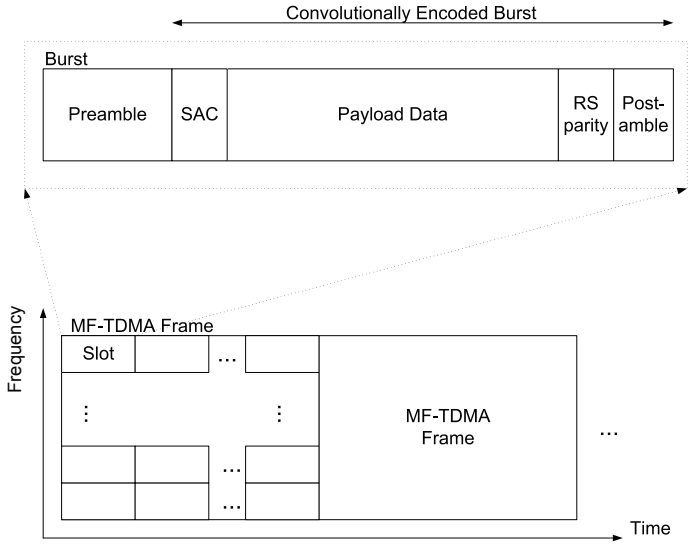

Figure 1.4: Illustration of the MF-TDMA time and frequency slot subdivision for multiple access. Different terminals access the same return link capacity on predefined time and frequency slots using transmission by bursts. The training sequence is located in the 'Preamble'. An MF-TDMA frame is subdivided into slots that represent a transmit opportunity for the accessing terminals. A transmitted burst is composed of a preamble part that contains the known symbol sequence followed by a Satellite Access Control (SAC) field and the encoded payload in ATM cells or in MPEG transport stream format. The payload is followed by a Reed-Solomon (RS) parity check sequence and eventually a postamble.

higher spectral efficiency of the return channel system. The use of joint detection techniques is considered in this thesis in conjunction with a significantly reduced channel spacing factor and specifically the resulting problem of burst synchronization under reduced channel spacing. Ineed, the dense packing of bursts increases the interference from the adjacent channel (ACI) and increases the detection errors on each burst. The problem of synchronizing under these conditions is studied within the this thesis.

Synchronization in symbol timing and carrier frequency offset is a crucial problem, especially for burst based data transmission, since a very limited amount of symbols have to be used for the synchronization and ultimately data detection. Training sequences are used to estimate the synchronization parameters, before a reliable data detection is feasible. This obviously reduces the efficiency of the

transmission as a certain part of the burst length has to be allocated to training data and only the remaining part is used for data transmission.
This synchronization problem under interference limited conditions is examined in detail in this thesis. A joint synchronization mechanism is presented that improves the frequency and timing synchronization performance and improves in that manner the detection performance.
It is important to distinguish between the synchronization of the broadband receiver to the incoming bursts in symbol-timing, phase and frequency and the system-level synchronization between the transmitting terminals that enables the MF-TDMA operation. Indeed a higher level synchronization process is required in satellite MF-TDMA systems, that coordinate the burst transmission timing and the adjustment of the transmit frequencies of the different accessing terminals. This synchronization level ensures that the different transmission delays from the terminal to the central hub receiver and the satellite movements are compensated and taken into account to map the incoming bursts on the MF-TDMA frame structure at the input of the receiver. This mechanism is supported in DVB-RCS [ETS03a] by a specific acquisition and synchronization bursts. In addition to this system level MF-TDMA synchronization, which has inherently lower precision requirements, the above-mentioned receiver symbol-timing, phase and frequency synchronization is required for burst reception synchronization within the burst demodulator system of the receiving hub station.

1.6 Interference Cancellation Background

This section gives a general introduction to the background context of interference cancellation. A more detailed outline of the specific background work considered as basis for this thesis is presented in section 1.11.

Detection and Interference Processing

Sharing the frequency resources in a communication system among different systems or users can be organized in several manners with advantages depending on the application and channel conditions. It has been demonstrated by past work that the use of receivers that process jointly the communicating signals outperform in terms of spectral efficiency systems that avoid interference and process on only one signal source at the receiver side, see [Ver98]. The joint detection in the receiver involves a more complex processing for the signal detection step, which is the tradeoff required for the potentially higher spectral efficiency. Joint detection and decoding systems have emerged in the form of multi-user systems, where a large number of users access the same common resource. Especially for Code Division Multiple Access (CDMA) based wireless systems, joint reception of the CDMA access terminals has proved very practical and effective, [Mos96] [TR06].
Joint multiuser detection has been studied extensively and a significant gain over

single user detection can be obtained in general. The optimal detection in multi-user systems is in most cases too complex and intractable in practice as it involves searches over large sets of possible symbol combinations or the optimization over non-convex objective functions, see [Ver98]. In practice it is often resolved to suboptimal techniques that are in theory suboptimal but less complex. Linear interference cancellation techniques use the linear filtering of the received signal to minimize the effect of the interferer under the channel conditions experienced. For example the decorrelating detector or the minimization of the mean square error (MMSE) assumes a linear receiver structure for which the parameters have to be selected such that the received signal detection performance is optimized under the given constrains.
Nonlinear interference cancellation techniques are commonly decision driven interference processing systems such as Successive Interference Cancellation (SIC) and Parallel Interference Cancellation (PIC) are built on an iterative approach that loops over tentative symbol estimates to reconstruct and cancel an interference signal estimate, [WP99]. These iterations can be based on soft- or hard-decision based symbol estimates.
A further degree of complexity involves the joint decoding of the signals. Exploiting the redundancy that is included in the channel coding of the signals increases the potential improvement over symbol detection based mechanisms. These methods involve turbo-based iterative decoding of the different signals involved in combination with interference suppression [BC02].

Spatial Signal Processing

In more recent work, the interference processing task has been combined with multiple antenna systems, that permit a spatial directivity in wireless systems, see e.g. [HTR$^+$02]. Recent developments in coding strategies such as Space-Time Block Codes (STBC), see [KO05] try to use the additional spatial degree of freedom to further optimize the diversity and coding gain.
In the present thesis the principle of joint spatial-temporal interference processing is adapted to satellite reception under interference from adjacent satellites. A suboptimal, reduced complexity interference mitigation processing is derived and analyzed in detail. A spatial filtering step is proposed as first stage of the receiver, allowing a limited amount of freedom in the combination of the wanted signal and the main adjacent interferers. A second temporal interference cancellation step further reduces the impact of the main interferers on the wanted signal. Details are discussed in Chapter 2 and 3.

1.7 Synchronization Background

A general background of the synchronization context is given here below. A more detailed outline of the specific background work considered in the synchronization

part of this thesis is presented in the following section 1.11.

In the context of data communication the synchronization parameters are commonly modeled as random nuisance parameters that need to be estimated in conjunction or prior the detection of the data on the received signal. Synchronization is required at different levels in the communication system. At the physical layer it involves, depending on the modulation type, symbol timing, frequency and phase estimation, [MS84] [MA90].
For burst mode multiple access systems, the synchronization task is considerably more challenging as it requires the parameter estimation on a finite small length of consecutive symbols. The required estimation accuracy has to be met with the limited amount of symbols available for the estimation task. For continuous transmissions under extremely slow changing channel conditions as experienced by fix satellite reception, the estimation effort of frequency and timing can be subdivided into acquisition and tracking of the synchronization parameters. The tracking achieves high accuracy through continuously refined estimations using of long symbol sequences and slow responding estimation loops, [MA90] [MD97].
Optimal synchronization from a Maximum Likelihood (ML) criteria is achieved under joint estimation of all unknown nuisance parameters at the receiver side. This however is practically unfeasible due to the multi-dimensioned and nonlinear nature of the ML cost function, which also exhibits many local minima. An exhaustive search is practically often unfeasible and simpler techniques are used, often relying simplification of the cost function and with the help of coarse estimates which are iteratively refined.
In digital receivers that work with samples of the received signal, the symbol timing is of crucial importance at different stages. Indeed, the sampling rate itself might need to be piloted by the recovered symbol timing to help the system work in a symbol synchronous manner.

The present thesis considers DVB-S/S2 based continuous data transmission in the context of broadcast scenarios and burst mode, DVB-RCS based systems in the context of broadband systems. These standards define (mandatory or optional) data-aided synchronization mechanisms using pilot sequences.

In the context of this work, the data aided synchronization mechanism is reviewed under interference limited conditions. The burst based return channel of a DVB-RCS broadband systems is considered in Chapter 8. The received multi-channel burst sequence at the receiver is limited by adjacent channel interference. A cost function for the joint multi-channel synchronization is derived and a simplified, computationally tractable mechanism is proposed that improves the synchronization over single channel burst synchronization.

Synchronization in Interference Processing Systems

In the context of strong interference also the synchronization task of the receiver in frequency and symbol timing is considerably more difficult. Estimating these nuisance synchronization parameters jointly on the main signal and all the interferers has the potential to outperform the synchronization approach on a single signal. The symbol timing, frequency offset and signal phase for coherent detection need to be estimated for all signals involved in the interference processing. This is generally a considerable task but often not considered in the work on multi-user detection (MUD) and interference processing.
Furthermore, the signal processing methods involved in interference cancellation however often require superior synchronization accuracies to work well compared to the synchronization requirements of single user detection. The symbol timing and frequency offset synchronization problem is taken into account in the work presented in the following Chapter 7 in conjunction with interference processing mechanisms.
Based on the synchronization approach presented in this thesis in the context of broadband systems, as outlined in Chapter 8, an additional synchronization task is included in the iterative interference processing mechanism presented in Chapter 3. Using the defined pilot sequences in DVB-S2, a synchronization step in symbol timing and in frequency is triggered at the detection of the pilot sequences in one of the received signals (main signal or one of the processed interferers).

1.8 Satellite Channel Model

The satellite channel link budget for satellite reception can be subdivided into the following different elements [MB02], see Figure 1.5:

- Uplink thermal noise
- Transponder amplifier nonlinearity and filter distortions
- Downlink thermal noise
- Interference contributions from other links

For fix satellite reception, the uplink and downlink attenuation is caused by long term weather induced fading. For broadcast systems with a small reception antenna at the end-user terminal side, the link is usually strongly downlink noise limited and by interference from adjacent satellites. On the other hand, the broadband return channel with its small antenna on the uplink side is limited in capacity by uplink thermal noise and, depending on the system dimensioning, by interference from other users in the same access environment.
The impact of the transponder nonlinearity and filter distortions depends on the dimensioning of the link and modulation used. If the symbol rates are significant with respect to the transponder bandwidth, the group delay of the Input Multiplex

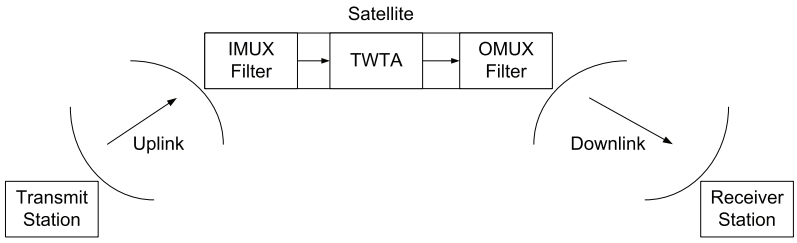

Figure 1.5: Illustration of relevant channel parts of a satellite link. The transmitted signal is impeded by additive noise on the uplink and downlink. The Input Multiplex Filter (IMUX) and the Output Multiplex Filter (OMUX) filters distort the signal by their nonlinear phase response that cause group delay and inter-symbol interference. The traveling wave tube amplifier (TWTA) causes a signal distortion, if it is operated with little backoff close to its saturation point.

Filter (IMUX) filters distorts the signal. This is especially the case for so-called 16/32-APSK (Amplitude Phase Shift Keying) *higher order modulations* as defined in DVB-S2, where several symbol amplitude levels are defined, which are distorted in amplitude by the nonlinearity of the Traveling Wave Tube Amplifier (TWTA) and by inter-symbol interference generated by the group delay of the filters. A pre-distortion of the signal at the transmitter side becomes necessary to reduce these effects, which can only be partially compensated by equalization on the receiver side.
Similarly in multi-carrier systems approaching the capacity limit of the transponder the transponder TWTA amplifier nonlinearity degrades the signal through out-of-band inter-modulation products. These can be well modeled using nonlinear system theory [Sch81] and specifically using Volterra series [BBD79] [BB83]. Alternatively, a more practical approach relies on noise power ratio (NPR) tests and the modeling of a large number of multi-carriers as a single large signal [RBL$^+$00]. This gives very satisfying results in practice for most applications.
These transponder degradations can be well included in the link budget with the help of an equivalent signal-to-noise ratio. In many scenarios the link budget degradation is dominated by only a few of the mentioned signal impediments. In this thesis two different scenarios are considered, first the broadcast scenario with a downlink noise limited link with significant interference from adjacent satellite systems and second the broadband scenario with an uplink noise limited link budget with additional significant intra-system interference from other users accessing on the adjacent frequency channel in the MF-TDMA frames. The transponders are assumed to be operated in linear mode and consequently the TWTA nonlinearities are negligible in this context.

Table 1.1: This table summarizes the on-axis antenna gains computed for the different antenna sizes assumed in the context of the numerical evaluations of the broadcast reception scenario in this thesis.

Ant. Size [cm]	10	15	20	25	30	35
Gain [dBi]	20.5	24.1	26.7	28.9	30.5	31.9
Ant. Size [cm]	40	45	50	55	60	65
Gain [dBi]	33	34	34.5	35	35.5	36

Table 1.2: Link budget assumptions that serve as basis for the numerical evaluations of the broadcast reception scenarios outlined in this thesis.

Parameter	Def. value	Parameter	Def. value
Satellite EIRP	53 dBW	Symbol Rate	30 MSymb./s
Free Space Loss	205 dB	Rain Attenuation	2 dB
LNB Noise Temperature	120 Kelvin	Frequency	11.75 GHz

1.9 Link Budget Assumptions

Numerical simulations were performed with different mechanisms to verify the feasibility of the proposed concepts and the interference processing in particular, assuming a Ku-band based broadcast scenario.

A model of a front-end antenna gain pattern was computed using *GRASP*, a physical optics based antenna modeling tool by TICRA, for antenna reflector sizes ranging from 10cm to 65cm. The detector array was placed at focal point of the parabolic reflector to generate symmetrical patterns in both azimuth offset directions. The maximal nominal on-axis gains in Ku-band of the antennas are listed in Table 1.1.

To consider realistic conditions, link budget assumptions were chosen which are typical for a geostationary satellite broadcasting in Ku-band. The parameters are listed in Table 1.2.

Note that this link is not fading statistically over time, as it is commonly assumed for mobile terrestrial wireless systems. The channel is modeled as non-fading. A long term margin accounting for rain attenuation and equivalent to the target availability of the link results in a worst case perspective for the performance evaluation is taken into account in accordance with the applicable ITU recommendations, [ITU07].

We assume that all signals are either DVB-S or DVB-S2 [ETS05a] [ETS05b] compliant signals and this implies also that the signal shaping as defined in (2.3) is a root raised cosine filter (RRCF), split into two equal filters at the transmit and receive side as square root raised cosine (SRRCF) matched filter.

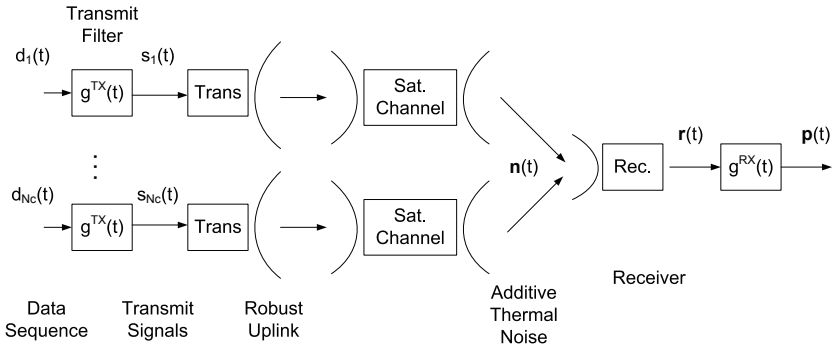

Figure 1.6: Illustration of the satellite broadcast reception scenario. The main signal of interest is interfered by signals from adjacent satellites. The link is downlink thermal noise and interference limited.

1.10 Signal Model

For both the continuous time broadcast signal and the burst return channel system, a Phase Shift Keying (PSK) based linear modulation is used. The satellite channel is assumed dominated by the uplink and downlink noise parts with the signal degradations in the transponder being negligible.

Interference Limited Broadcast Reception

Figure 1.6 illustrates the considered scenario for the broadcast reception under interference conditions. A wanted signal is interfered by $N_C - 1$ signals from adjacent satellites. The receiver is composed of a multiple input antenna with M elements and a signal detection stage with spatial and temporal processing. The M input elements include a down-conversion step from the RF frequency to the intermediate frequency (IF). One possible configuration comprises a configurable analogue signal combination step at this intermediate frequency prior to the receiver input and A/D conversion for subsequent temporal processing. An alternative configuration comprises a digital processing on all M signal elements and consequently M receivers for each input signal and subsequent A/D conversion of each input signal.

The received signal can be expressed as follows:

$$\begin{aligned}\mathbf{r}(t) &= \begin{bmatrix} r_1(t) \\ \vdots \\ r_M(t) \end{bmatrix} = [\mathbf{a}_1 \dots \mathbf{a}_{N_C}] \begin{bmatrix} s_1(t) \\ \vdots \\ s_{N_C}(t) \end{bmatrix} + \mathbf{n}(t) \\ &= \sum_{i=1}^{N_C} \mathbf{a}_i(t) s_i(t) + \mathbf{n}(t) = \mathbf{A}\mathbf{s}(t) + \mathbf{n}(t)\end{aligned} \tag{1.2}$$

Here N_C signals $s_i(t)$, coming from N_C different satellites that are closely spaced around the wanted satellite signal source, are received at different amplitude and phase levels $\mathbf{a}_i$ on M inputs at the receiver side, with M spatially different antenna input elements. The signal $s_i(t)$ is linearly modulated and we define with $g^{TX}(t)$ the transmit filter and $g^{RX}(t)$ the receive filter of the link. These can be arbitrary in principle, but are defined by the applicable DVB standards as root-raised cosine (RRCF) filters, see e.g. [Pro00]. We denote with $r_i(t)$ the complex valued received symbol sequence of the i-th out of the M input elements. The $M \times 1$ vector $\mathbf{r}(t)$ represents the combination of the M complex-valued received symbol sequences in baseband and is potentially oversampled. It is specifically stipulated when an oversampled signal is required.
The additive noise is regrouped in the $M \times 1$ vector $\mathbf{n}(t)$. Note that the noise components on the M input elements are partially correlated due to the correlated input elements of the antenna. The additive noise is thus composed of noise received by the antenna elements, which is partially correlated on the M input elements and a noise component from the M amplification stages in the receiver, which is uncorrelated on the M input elements.

Antenna Modeling

In the context of this work, the antenna front-end has been included in necessary detail in the analysis. A physical optics (PO) and physical theory of diffraction (PTD) based antenna model using the simulation software General Reflector and Antenna Farm Analysis Software, GRASP[4], has been elaborated and used to determine the gain pattern and maximal on-axis gain of the devised antenna. An offset circular parabolic reflector has been assumed with typical geometrical parameters, $f/D = 0.5 - 0.6$ (focal length divided by the antenna's diameter). The assumed tapering of the feed gain on the reflector surface is assumed a Gaussian distribution with -12dB tapering at the reflector edge.
Example antenna gain pattern plots are depicted on the Figures 3.1 and 5.1. The azimuth angle η dependent signal amplitude at reception $\mathbf{a}(\eta)$ can be computed from this model. From these, the signal amplitudes at the reception of different

[4]GRASP is a software by TICRA, http://www.ticra.com/

satellite positions assumed, $\mathbf{A}(\boldsymbol{\eta}) = [\mathbf{a}(\eta_1) \cdots \mathbf{a}(\eta_{N_C})]$, are determined by link budget calculation taking into account the modeled reception antenna system gain pattern.
The received noise level $\mathbf{n}(t)$ also depends on the assumed antenna parameters. This is taken into account in the numerical evaluations in the sequel of this work in the sense. As mentioned, the input noise to the antenna system is assumed correlated by the determined correlation factor that the antenna geometry generates for the overlapping antenna gain patterns. The noise level generated inside the MLNB by the independent amplification of the different input streams is assumed uncorrelated. The received noise correlation $E\{\mathbf{n}(t)\mathbf{n}(t)^*\} = \mathbf{R_n}$ is derived from this evaluation.

Performance Evaluation

In the context of the numerical performance evaluations of the proposed broadcast reception system, as defined in Chapters 3, 5 and 7, detailed simulation models were the basis. The orbit and antenna geometry is the basis for the signal power levels and path delays assumed at the input of the receiver. The goal here is to not only compare receiver algorithms but to draw system level conclusions on the achievable performance and to make recommendations for the possible design parameters of the proposed receiver. These include the possible antenna aperture, the number of MLNB input elements as well as the element spacing of these input feeds. Furthermore on the second step of interference processing the initialization parameters of the proposed algorithm can be adjusted and fine tuned for the considered interference scenarios, especially the initial spatial weighting elements, as described in details in Chapter 5.

Synchronization Parameters

The receiver detection mechanism has to work in an environment of parameters in frequency offset $\Delta\mathbf{f} = [f_1 \cdots f_{N_C}]^T$ and symbol timing offset $\Delta\mathbf{t} = [t_1 \cdots t_{N_C}]^T$, $N_C \times 1$ vectors, where f_i and t_i are respectively the frequency and timing offset of the i-th input signal. These can be regrouped in the parameters vectors $\boldsymbol{\theta} = \left[\Delta\mathbf{f}^T\ \Delta\mathbf{t}^T\right]^T$. This is included in the signal model as follows:

$$\mathbf{r}(t) = \mathbf{A}(\boldsymbol{\eta})\mathbf{s}(t, \Delta\mathbf{f}, \Delta\mathbf{t}) + \mathbf{n}(t) \tag{1.3}$$

The transmitted signal on the ith carrier can be expressed as follows ($\star$ denotes the convolution operator):

$$s_i(t, \Delta f_i, \Delta t_i) = g_i^{TX}(t, \Delta f_i) \star d_i(t - \Delta t_i) \tag{1.4}$$

Here, $d_i(t - \Delta t_i)$ represents the symbol sequence of the ith carrier with a symbol timing offset of Δt_i. The transmit signal shaping filter impulse responses $g_i^{TX}(t)$ of

the ith carrier can be expressed as follows, including the frequency offset Δf_i and phase ϕ_i:

$$g_i^{TX}(t, \Delta f_i) = g_{MF}(t) e^{j(2\pi \Delta f_i t + \phi_i)} \tag{1.5}$$

The received symbol vector $\mathbf{r}(t)$ is observed for consecutive symbol times $t = 1 \dots N_d$. We assume that the signal amplitudes $\mathbf{A}(\boldsymbol{\eta})$ are well estimated and that the interference scenario is known, with support from information from a central monitoring station as explained in Section 1.4. The noise covariance $\mathbf{R_n} = E\{\mathbf{n}(t)\mathbf{n}(t)^*\}$ is also well defined from the known antenna and MLNB calibration parameters. Indeed the fact that the interference scenario is considered quasi-static, it is considered feasible to perform a good covariance matrix estimation using sample covariance estimation methods.

The broadcast reception part of the thesis discusses the detection problem of the wanted data stream $s_1(t)$ from the observation of $\mathbf{r}(t)$, $t = 1 \dots N_d$, including the synchronization parameters $\Delta\mathbf{f}$ and $\Delta\mathbf{t}$. In a first part of the work (Chapter 3, 5 and 6), perfect synchronization is assumed and the joint detection is analyzed. The synchronization problem in symbol timing and carrier frequency is then, in a second step (Chapter 7), also taken into account.

Synchronization in Return Channel Systems

The context of multi-access satellite systems using an MF-TDMA based access strategy is the basis assumed for these scenarios. Figure 1.7 illustrates this setup. A large number of terminals access the common satellite capacity. A small frequency spacing between the MF-TDMA channels will increase the capacity of the system but introduce inter-channel interference between frequency-adjacent bursts. Simultaneously transmitted bursts then interfere though partially frequency overlapping channels.

For the development of the proposed synchronization mechanism, as elaborated in Chapter 8, the transmitted MF-TDMA on N_C frequency adjacent carriers can be expressed as follows:

$$s(t) = \sum_{i=1}^{N_C} a_i s_i(t) + n(t) \tag{1.6}$$

For the purpose of the elaboration of the synchronization mechanism development in this work, we are particularly interested in the pilot sequence $c_0(t)$ containing L pilot symbols situated at the beginning of each burst. The timing offset on the ith burst is denoted with Δt_i and the frequency offset $\Delta f_i = f_i^c + f_i$, where f_i^c is the center frequency of the ith channel and f_i the frequency error. We can then express $s_i(t)$ as follows:

$$s_i(t) = c_0(t - \Delta t_i) e^{2\pi j (t - \Delta t_i)(f_i^c + f_i)} \tag{1.7}$$

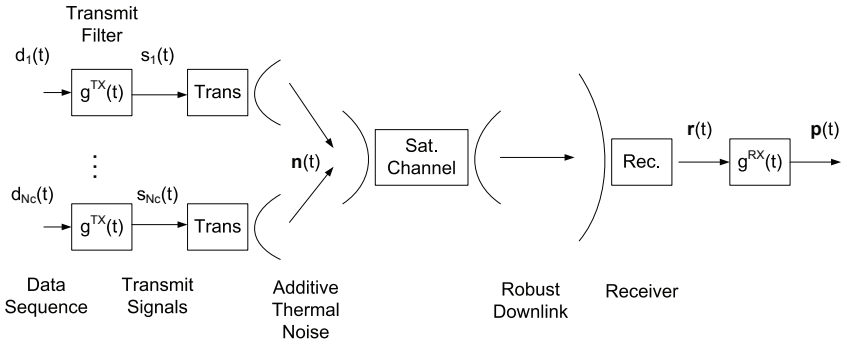

Figure 1.7: Illustration of the broadband access system. A common satellite capacity is accessed by a number of terminals transmitting in an time and frequency division MF-TDMA slotted scheme. The link is limited by intra-system interference and uplink thermal noise.

We consider as baseband signal the jth signal and relate the adjacent channels, indexed i, to the considered baseband signal. The timing offsets can then be expressed relative to the jth signal as $\tau_i = \Delta t_i - \Delta t_j$, with $\tau_j \equiv 0$. The signal after the receive filter can then be expressed as a convolution as follows:

$$s_i^f(t, \tau_i, f_i) = g_{MF}(t) \star s_i(t, \tau_i, f_i) \tag{1.8}$$

The sampled received sequence can then be expressed as follows for the mth sample time interval:

$$x(m) = g_{MF}(t) \star \sum_{k=1}^{N_C} s_k(t) a_k + n'(t)|_{t=mT_S} \tag{1.9}$$

The filtered noise process is expressed here as $n'(t) = g_{MF}(t) \star n(t)$. Taking advantage of the fact that the interference is clearly dominated by the direct neighbours of the considered channel, we can express the received sequence as follows:

$$\mathbf{x} = \begin{bmatrix} x(1) \\ \vdots \\ x(L) \end{bmatrix} \simeq \begin{bmatrix} \mathbf{s_{i-1}^f} & \mathbf{s_i^f} & \mathbf{s_{i+1}^f} \end{bmatrix} \cdot \begin{bmatrix} a_{i-1} \\ a_i \\ a_{i+1} \end{bmatrix} + \begin{bmatrix} n'(1) \\ \vdots \\ n'(L) \end{bmatrix} \tag{1.10}$$

Here a_i is the amplitude of the signal from the i-th terminal and $\mathbf{s_i^f} = [s_i^f(1) \cdots s_i^f(L)]^T$ is the $L \times 1$ vector regrouping the L consecutive symbols of the i-th channel.

The synchronization parameters in symbol timing and in frequency can also be taken into account here as follows:

$$\mathbf{x}(\boldsymbol{\tau}, \mathbf{f}, \mathbf{a}) = \mathbf{S}(\boldsymbol{\tau}, \mathbf{f})\mathbf{a} + \mathbf{n}' \tag{1.11}$$

Where we define:

$$\mathbf{S}(\boldsymbol{\tau}, \mathbf{f}) = \left[\begin{array}{ccc} \mathbf{s}_{\mathbf{i-1}}^{\mathbf{f}} & \mathbf{s}_{\mathbf{i}}^{\mathbf{f}} & \mathbf{s}_{\mathbf{i+1}}^{\mathbf{f}} \end{array} \right] \tag{1.12}$$

$$\mathbf{a} = \left[\begin{array}{c} a_{i-1} \\ a_i \\ a_{i+1} \end{array} \right] \tag{1.13}$$

and

$$\mathbf{n}' = \left[\begin{array}{c} n'(1) \\ \vdots \\ n'(L) \end{array} \right] \tag{1.14}$$

The synchronization parameters in amplitude, frequency and symbol timing are regrouped in the vectors $\mathbf{a}$, $\Delta\mathbf{f}$ and $\Delta\mathbf{t}$ respectively, with $\mathbf{f} = \left[\begin{array}{ccc} f_{i-1} & f_i & f_{i+1} \end{array} \right]^T$ and $\boldsymbol{\tau} = \left[\begin{array}{ccc} \tau_{i-1} & \tau_i & \tau_{i+1} \end{array} \right]^T$. The received signal is composed of the multi-carrier burst sequence of the N signals $s_i(t, \Delta f_i, \Delta t_i, \mathbf{a})$, as defined in (1.7). The amplitude $\mathbf{a} = [a_{i-1} a_i a_{i+1}]^T$ is however also considered an unknown in this case. Indeed, even though the channel is not fading rapidly and that even a power control mechanism might be in place to level the transmission power of the different users, the burst mode transmission from different terminals generates amplitude variations at the receiver that require amplitude fine adjustment.

1.11 Work Overview and Contributions

Interference Limited Broadcast Reception

The interference processing considered in this thesis comprises different linear and nonlinear detection and decoding based approaches in conjunction with a first spatial pre-filtering step. These approaches include linear processing techniques based on minimum mean square error (MMSE), hard-decision and soft-decision based interference processing approaches as well as decoding based interference cancellation. In addition timing and frequency synchronization is taken into account, the performance in interference overloaded scenarios is analyzed, and a robust iterative procedure is presented that combines the detection and the linear spatial selection steps. Herein, the algorithms are tailored to the satellite broadcast problem previously described and a detailed performance analysis is carried out for the considered scenario.
The problem of detecting multiple signals with an antenna array has also been considered in the past [ORK89] [OVK92] [LX97]. Wang et al. [WP99] have presented a space-time CDMA based multiuser receiver and demonstrated substantial gain by detecting jointly multiuser signals. A considerable amount of work has since been appeared in space-time detection and decoding [WFGV98] [PP97] [CCC00] [HtB03]; [TV05] provides a comprehensive overview. Most of these techniques were conceived in the context of multiuser detection in Multiple Input Multiple Output (MIMO) systems and in typically a rich scattering environments. An interesting recent work concentrates on ground based adaptive beamforming for mobile satellite systems, [ZK05].
The maximum likelihood (ML) detector is generally intractable and recently efficient and powerful suboptimal methods were derived that approach ML performance, like the list sequential detector (LISS) [BHW03], sphere decoding extension of the V-BLAST algorithm [DCB00] [HC05] and semi-definite relaxation of the ML problem [VB96].
The considered problem differs from this previous work in the sense that almost no scattering is assumed over the satellite link and only one specific signal is of interest in an interference overloaded multi-input reception system. The joint use of a linear pre-processing step followed by and nonlinear interference cancellation step has proved to be an attractive setup for overloaded systems, see [HTR$^+$02], [GC98] and [GSM$^+$97]. A most promising technique in this respect is the introduction of the iterative least square with projection (ILSP), [TPV96] [TPV97].
Inspired among others by these works [TPV96], [HTR$^+$02] and [BGK02], we adapt the ILSP concept to a joint spatial and temporal detection mechanism that performs well for the considered broadcast reception scenarios. Simulations of realistic scenarios are used to verify the performance of the proposed scheme for broadcast reception scenarios in Ku-band.

In addition the synchronization problem is reviewed in a second part of this

work. The pilot symbol based synchronization problem specific to DVB-S2 has been investigated in [BC07]. This work is extended and adapted to the broadcast reception scenario with multiple adjacent satellite interfering signals. A linear spatial pre-processing is introduced that helps deal with the overloaded interference system and adds robustness to the receiver setup. A subsequent temporal processing step is proposed, to detect the symbol sequence of the wanted signal in the interference overloaded received signals.

The frequency and symbol timing synchronization issue is considered and an iterative joint detection and synchronization method is presented. Numerical examples demonstrate that the proposed methods can be used to reduce the selectivity requirements of receiving antennas and thereby reduce the antenna size and increase reception robustness.

Synchronization in Broadband Return Channel Systems

In an effort to increase the spectral efficiency of MF-TDMA systems such as satellite based DVB-RCS (Digital Video Broadcasting Return Channel via Satellite, see [ETS03a]) systems, the synchronization problem of frequency, phase and time estimation in MF-TDMA based multi-user systems is considered. Spectral efficiency is central to the commercial success of two-way satellite systems. The introduction of DVB-S2 [ETS05a] will considerably improve the efficiency on the forward link. The efficiency of the return link will depend mostly on the satellite system structure and the performance of the receiving hub system of which synchronization is an essential part.

The joint detection in multiuser systems is in general well studied and documented, see Verdu [Ver98]. These techniques, applied to multi user systems, can provide a substantial increase in spectral efficiency [BGK02] by allowing reduced carrier spacing. Most joint detection work considers a synchronized system, which is not realistic on the return link of a satellite broadcast system. The acquisition of channel parameters, including frequency, time and phase is critical and often the limiting factor for detection performance in interference limited situations.

Single carrier synchronization under noise limited conditions is well studied, see [MA90] [MD97] and [MMF98] for a description of the state of the art methods. However the specific problem of joint channel synchronization in multi-user systems which is considered herein has not been considered in known work so far. In the current application, the interference is well structured and exploiting this knowledge allows much higher tolerance against adjacent channel interference (ACI) as compared to generic synchronization methods. Joint synchronization in conjunction with joint detection allows tighter channel spacing without an increase in training overhead.

In particular, in multi user systems with small carrier spacing, the resulting ACI limits the performance of the communication link. In general, the feasibility of interference limited operation has been studied in previous work for cellular systems, see Klang [KO02]. Arslan [AGB98] has studied the successive cancellation

in GSM like systems. Janssen [JS02] has investigated the applicability of nonlinear successive interference rejection methods. Petersen [PF94] has studied the ability of linear and decision-feedback equalizers to suppress all received adjacent-channel interference. Also for satellite systems, the application of these techniques to the joint detection of adjacent multi user signals with close channel spacing (considerably below 1 x Symbol Rate) has been demonstrated, see [BGK02]. Based on these and similar results it can be concluded that a satellite DVB-RCS system can well be operated at channel spacings below 1 x Symbol Rate, provided that the receiver can establish synchronization to the multiple users.

The synchronization problem specific to typical multi user satellite systems has been addressed in, e.g. [MYBM01]. Ko [KZC05] has studied ML-based frequency estimation of frequency hopping signals without pilot symbols. Koo [KL02] has analyzed the joint frame synchronization. Channel estimation and specifically data-aided frequency estimation of MF-TDMA bursts in noise limited cases has been considered in other studies, for example [LR95]. The synchronization problem in channels with co-channel interference has been considered for the specific case of multi-antenna receivers (see [AJS99]) and the Cramér-Rao bound has been studied in detail for the practical synchronization related estimation processes, [NSM02] and [NSM04].
However the problem of joint synchronization in interference limited scenarios has been given little attention to date for the specific case of multi user satellite systems, like DVB-RCS systems described above. The only work known to the author is by Yachil, Davidson and Bobrovsky [YDB06].

Herein, the synchronization task is analyzed under the assumption of multi-access interference caused by a reduced channel spacing. The synchronization performance is assessed for common techniques based on data-aided synchronization. Under the multi-access interference scenario, a cost function is derived to estimate the synchronization parameters jointly for the received burst sequence of frequency adjacent bursts. A computationally tractable iterative estimation procedure is derived from this optimization formulation. The performance is analyzed and compared to applicable theoretical estimation bounds in terms of frequency and timing synchronization. Furthermore these results are used to assess the error rate performance of the data symbol detection step and the achievable improvements. The simulation scenarios are detailed and realistic in the sense that a multi-channel burst structure is constructed with computed link budget noise and interference levels.

1.12 Thesis Outline and Publications

As already mentioned, we treat both the broadcast reception scenario and the broadband return link within this thesis. Chapters 2 to 7 treat the broadcast reception scenario while Chapter 8 focuses on the broadband return link. Chapter

2, 3, 4 and 5 build upon each other and introduce in steps and details the proposed concept of spatial and temporal signal detection in the context of interference limited broadcast reception. Chapter 6 is reflecting results that illustrate performance with an additional decoding in the reception chain and is not directly related to the work presented in the previous Chapters 2 to 5.
The synchronization is the focus of the Chapters 7 and 8. In Chapter 8 a synchronization method is introduced and elaborated in details in the context of an MF-TDMA based return channel of a satellite broadband system. In Chapter 7, this concept is adapted to the special case of DVB-S2 based interfering broadcast signals received with a proposed receiver as outlined in Chapters 2 to 5.

To summarize, the sequel of the thesis can be outlined as follows:

Chapter 2 - Satellite Interference Mitigation

The interference limited broadcast reception scenario is analyzed in this part of the thesis. A system with adjacent satellite interference is assumed and a reception scenario with a small size receive antenna that receives the wanted signal as well as the adjacent interferences in band is presented. A receiver structure is proposed with a spatial degree of freedom that permits to direct the antenna gain within a certain range. The performance of this spatial processing based mechanism is analyzed in detail. In combination with the spatial front-end processing a second level signal processing is considered at symbol detection level and channel decoding level. While the optimal symbol detection problem is considered intractable, a suboptimal symbol detection based processing stage is considered and proposed.

Chapter 3 - Linear Pre-Processing

The spatial configuration step is analyzed in this part. A linear pre-processing (LPP) mechanism is introduced that defines the spatial weighting parameters on a defined optimization criterion. The performance of this system is analyzed in detail under the assumption of overloaded and non-overloaded systems.

Chapter 4 - MMSE based Interference Processing

Based on an approach from the literature by Beidas et al. [BGK02], a soft-decision based iterative MMSE based interference processing step developed and tested for adjacent channel interference in broadband systems, is adapted to the scenario of broadcast reception. This entails the specific frequency offset and amplitude difference as well as the challenge of different symbol rates on the main signal and the interferer. Furthermore phase noise impairments are assumed and simulated as well.
The simulations within this part do not include a spatial linear pre-processing

(LPP) step and assume a certain signal to noise and interference ratio at the input of the interference processing algorithm.

This work has been published in the following conference paper and is part of the Diploma Thesis of Klaus Schwarzenbarth, which has been supervised by the author of this thesis:

- [SGO07], K. Schwarzenbarth, J. Grotz, B. Ottersten, MMSE Based Interference Processing for Satellite Broadcast Reception, *Proceedings IEEE Vehicular Technology Conference*, Dublin, March 2007.

Chapter 5 - Spatio-Temporal Interference Processing

The interference processing step is introduced and analyzed in detail. The system is working on symbol detection level. The interference cancellation step is combined with the spatial pre-processing step in a joint mechanism. The performance of this joint detection mechanism is analyzed in detail. In particular the joint processing is demonstrated to outperform the simple combination of the separate steps, spatial pre-processing and subsequent interference processing.

The work presented in these Chapters is partially included in the following publications:

- [GOK06], J. Grotz, B. Ottersten, J. Krause, Applicability of Interference Processing to DTH Reception, *9th International Workshop on Signal Processing for Space Communications*, Noordwijk, The Netherlands, September 2006.

- [GOK08], J. Grotz, B. Ottersten, J. Krause, Signal detection and synchronization for interference overloaded satellite broadcast reception, *IEEE Transactions on Wireless Communications*, July 2008, Submitted.

Chapter 6 - Interference Processing with Decoding

In this part of the thesis, the additional channel decoding is taken into account, based on the assumption that the signals are standard based transmissions, e.g. DVB-S [ETS98]. The benefit of the interference cancellation with additional decoding is analyzed in details. A second step in this part is to consider the DVB-S2 based LDPC decoding step in an iterative interference processing mechanism. As in previous steps, the performance of this system is evaluated through computer simulations.

The following conference and journal publications partially present the work on Satellite Interference Mitigation with Decoding, outlined in this Chapter of the thesis:

- [GOK05], J. Grotz, B. Ottersten, J. Krause, Decision-Directed Interference Cancellation Applied to Satellite Broadcast Reception, *Proceedings IEEE Vehicular Technology Conference*, Dallas, September 2005.

The following work, which has been done in collaboration with Space Engineeging S.p.A. in the framework of an ESA funded prestudy project (ARTES-1 contract number 18070/04/NL/US). Its major additional contribution has been to assess the feasibility of joint LDPC decoding in DVB-S2 streams that interferer and to verify the results with an additional LPP pre-processing step as proposed in previous work by the author of this thesis, [GOK06].

- [CGG08], E. Casini, G. Gallinaro, J. Grotz, Reduced Front-End Reception Requirements for Satellite Broadcast using Interference Processing, *IEEE Transactions on Consumer Electronics*, November 2008.

Chapter 7 - Synchronization in Broadcast Systems

The synchronization mechanism of the satellite broadcast reception under interference conditions is considered in this section. The considered joint spatial-temporal processing introduced in Chapter 5 is extended, taking into account the symbol synchronization aspects. Based on the presented joint interference processing method introduced in the following Chapter 8, the synchronization is taken into account in the iterative reception procedure as additional step. As illustrated by computer simulations, an improved symbol timing estimate and frequency offset synchronization is achieved.

Chapter 8 - Synchronization in Broadband Systems

The satellite broadband return channel is considered in this part of the thesis. A common multi-user return channel sharing capacity according DVB-RCS specified MF-TDMA scheme is analyzed in the perspective of reduced channel spacing between the frequency channels. The introduced adjacent channel interference (ACI) degrades the perceived signal to noise and interference ratios of the received bursts. A joint synchronization and detection technique is elaborated that helps reduce the requirements on the training sequence length under a channel spacing factor that is below the burst bandwidth and that generates consequently ACI. The performance of this mechanism is analyzed in detail from its synchronization perspective and also from a symbol detection perspective.

The following conference and journal publications partially present the work on Synchronization under Interference Limited Conditions, which is included in this Chapter of the thesis :

- [GO05], J. Grotz, B. Ottersten, Data-Aided Frequency Synchronisation under Interference Limited Conditions, *Proceedings IEEE Vehicular Technology Conference*, Stockholm, May 2005.

- [GOK07], J. Grotz, B. Ottersten, J. Krause, Joint Channel Synchronization Under Interference Limited Conditions, *IEEE Transactions on Wireless Communications*, October 2007.

Chapter 9 - Conclusions and Future Work

The main contributions of the previous chapters are summarized in this part of the thesis. An outline of additional aspects for possible future work is presented.

Reading Guide

The assumptions and approaches in the different chapters in the sequel are summarized in the following table to help keep an overview of the work presented within this thesis. The assumptions and the basis of the formalism considered is also mentioned in the introduction of each chapter separately in details.

Chapter Overview

Chapter	Assumptions	Comments	Ref. Chapter
2	N.A.	Joint LPP-SIC problem statement and formulation.	N.A.
3	N.A.	LPP Problem statement and evaluation.	2
4	$M = 1$	MMSE based iterative interference cancellation with single input antenna.	N.A.
5	$N_C > M$	Joint spatio-temporal processing (LPP-SIC) for overloaded systems.	2,3
6	$M = 1, 2$	DVB-S and DVB-S2 decoding steps within interference processing step.	N.A.
7	$N_C > M$	Synchronization for DVB-S2 broadcast systems based on joint spatio-temporal filtering proposed in Chapter 5.	2,3,5,8
8	N.A.	Synchronization of the return channel in the context of broadband systems.	N.A.

1.A Notation

The following notation is used throughout the text. Plain letters, e.g. x and X, are used for scalars. Boldface letters are used for vectors and matrices, e.g. $\mathbf{x}$ is a (column) vector and $\mathbf{X}$ is a matrix.

$E\{\ \}$	The expected value of a random variable.
$Var\{\ \}$	Variance of a random variable.
$\mathbf{x}^{\mathrm{T}}$, $\mathbf{X}^{\mathrm{T}}$	The transpose of a vector, $\mathbf{x}$, or matrix, $\mathbf{X}$.
$\mathbf{x}^*$, $\mathbf{X}^*$	The Hermitian transpose of a vector, $\mathbf{x}$, or matrix, $\mathbf{X}$.
$\mathbf{X}^{-1}$	Inverse of a square full rank matrix $\mathbf{X}$.
$\mathbf{X}^{-*}$	Inverse of $\mathbf{X}^*$.
$\mathbf{X}^{\dagger}$	Moore-Penrose generalized inverse. (pseudo-inverse)
$\|\mathbf{x}\|$	The *Euclidean* norm of a vector $\mathbf{x}$.
$\|\mathbf{X}\|$, $\|\mathbf{X}\|_F$	The *Frobenius* norm of a matrix $\mathbf{X}$.
$\mathbf{X} \otimes \mathbf{Y}$	The Kroneker product of the matrices $\mathbf{X}$ and $\mathbf{Y}$. [HJ85]
$\mathrm{rank}(\mathbf{X})$	The rank of a matrix, $\mathbf{X}$.
$\mathrm{Tr}(\mathbf{X})$	Trace of a matrix.
$\mathrm{vec}(\mathbf{X})$	A column vector containing successively all the columns of the matrix $\mathbf{X}$
$\mathrm{diag}(\mathbf{X})$	A column vector with the diagonal elements of $\mathbf{X}$.
$\mathbb{R}, \mathbb{C}$	The sets of real and of complex numbers.
$\arg\{x\}$	Argument (angle) of complex valued scalar x.
$\arg\max_x f(x)$	The argument of the maximal value of $f(x)$ over its defined region.
$\arg\min_x f(x)$	The argument of the minimal value of $f(x)$ over its defined region.
Ω	Set of communication symbols for linearly modulated signal. $\Omega \subset \mathbb{C}$.
$\mathbf{f}[N]$	A row vector containing as elements the evaluations of the function $f(i)$, with $i = 1 \ldots N$.
$\mathbf{I}_N$	Identity matrix of dimension $N \times N$
$\mathbf{0}_{N_1 \times N_2}$	A matrix of dimensions $N_1 \times N_2$ containing only 0 elements.
$\mathbf{1}_{N_1 \times N_2}$	A matrix of dimensions $N_1 \times N_2$ containing only 1 elements.
$\mathbf{P}_{\mathbf{A}}$	The projection matrix on the column space of $\mathbf{A}$.
$\mathbf{P}_{\mathbf{A}}^{\perp}$	The projection matrix on the orthogonal complement of the column space of $\mathbf{A}$.
$x(t) \star y(t)$	Convolution of the two functions x(t) and y(t), $x(t) \star y(t) = \int_{-\infty}^{+\infty} x(\tau) y(t-\tau) d\tau$

1.B Acronyms

DVB	Digital Video Broadcasting (Standardisation Organisation)
DVB-RCS	Digital Video Broadcasting - Return Channel via Satellite (Standard), [ETS03a]
DVB-S	Digital Video Broadcasting via Satellite (Standard), [ETS98]
DVB-S2	Digital Video Broadcasting via Satellite, Second Generation Standard, [ETS05a]
DVB-T	Digital Video Broadcasting Terrestrial (i.e. via terrestrial transmission), Standard
MF-TDMA	Multiple Frequency Time Division Multiple Access
LPP	Linear Pre-Processing
ASI	Adjacent Satellite Interference
ACI	Adjacent Channel Interference
LNB	Low Noise Block Down Converter
MLNB	Multiple Input LNB
MIMO	Multiple-Input Multiple-Output
MUSIC	Multiple Signal Classification
ML	Maximum Likelihood
ROA	Region Of Attraction
MMSE	Minimum Mean Square Error
MUD	Multiuser detection
PSK	Phase Shift Keying
QPSK	Quadrature Phase Shift Keying
APSK	Amplitude Phase Shift Keying
SNR	Signal to Noise Ratio
SNIR	Signal to Noise and Interference Ratio
V-BLAST	Vertical - Bell Labs Layered Space Time
BER	Bit Error Rate
SER	Symbol Error Rate
IC	Interference Cancellation
SIC	Successive Interference Cancellation
PIC	Parallel Interference Cancellation
LISS	List Sequential Detector
BCJR	Bahl-Cocke-Jelinek-Raviv
GN	Gauss-Newton Gradient Step
CRB	Cramér-Rao Lower Bound
MCRB	Modified Cramér-Rao Bound
L&R	Luise and Reggiannini Frequency Estimation Method
ILSP	Iterative Least Square with Projection
AWGN	Additive White Gaussian Noise
RF	Radio Frequency
IF	Intermediate Frequency

TVoDSL	Television over Digital Subscriber Line
LDPC	Low Density Parity Check Codes
FTTH	Fiber To The Home
Ku-band	Microwave electromagnetic spectrum between 11.7 and 12.7 GHz (downlink)
C-band	Microwave electromagnetic spectrum between 3.7 and 4.2 GHz (downlink)
L-band	Microwave electromagnetic spectrum between 1.0 and 2.0 GHz (roughly), IEEE definition
TCP/IP	Transmission Control Protocol/Internet Protocol
VSAT	Very Small Aperture Terminal
DAMA	Demand Assignment Multiple Access
CDMA	Code Division Multiple Access
WiMAX	Worldwide Interoperability for Microwave Access (Standard)
LTE	Long Term Evolution (3GPP Project Name)
3GPP	Third Generation Partnership Project
ETSI	European Telecommunications Standards Institute
ACM	Adaptive Coding and Modulation
TWTA	Traveling Wave Tube Amplifier
IMUX	Input Multiplex Filter
OMUX	Output Multiplex Filter
NPR	Noise Power Ratio
STBC	Space Time Block Code
MEO	Medium Earth Orbit
HEO	Highly Elliptical Orbit
GEO	Geostationary Orbit
GBBF	Ground Based Beamforming

Chapter 2

Satellite Interference Mitigation

2.1 Introduction

The scenario of broadcast reception with interferers on adjacent satellites is considered in this chapter, as defined in the Introduction part 1.9. As outlined in the previous section, satellite reception systems have to compete efficiently with other means of data delivery. In that respect the reduction in antenna aperture size is of considerable commercial interest. The recent introduction of new improved digital transmission standards, like DVB-S2 [ETS05a], has allowed for transmission parameters aiming at lower signal-to-noise ratios in the link budget and potentially relaxing the reception antenna size requirements. However, the interference from adjacent satellites (ASI) limits the system performance in large parts of the broadcast spectrum when the antenna size is reduced. Additionally, for antennas designed to just meet the reception requirements, the necessary pointing accuracy is considerable for consumer grade products in case close adjacent satellites transmit at the same frequency.

We consider a satellite broadcast system with a fixed reception terminal and a small front-end antenna system. Reducing the antenna front-end aperture, the interference from adjacent satellites increases and becomes the main limiting factor for signal reception. A receiver structure with multiple-input low noise block down converters (MLNB) and linear pre-processing (LPP) on these M inputs and subsequent interference processing is proposed to mitigate the impact of the interferers. Different subsequent interference processing steps are proposed and analyzed for different interference scenarios.

The receiver structure is outlined in detail and the detection problem with the proposed receiver structure is elaborated in this chapter.

The formalism of the general interference mitigation problem under overloaded conditions is derived in this chapter, which has not been addressed by known work to date. The subsequent chapters 3, 5, 7 are based on the formalism derived in this part.

2.2 System Overview

The proposed system here is composed of a multi-input low noise block down converter (MLNB) followed by a receiver which we structure in three blocks; a linear preprocessing unit; a matched filter block and a nonlinear part performing successive interference cancellation (SIC). Figure 2.2 illustrates the reception chain. A wanted signal of interest, $s_1(t)$, is interfered by signals from adjacent satellites $s_2(t) \dots s_{N_C}(t)$, since the aperture is considered too small to isolate the wanted signal completely. The antenna front-end is composed of M separate inputs with pointing directions spaced by a variable amount in azimuth, nominally 3.0 degrees. This is the typical range of orbital separation between broadcast satellites in Ku-band. Note that typically $M = 2, 3$ is a realistic number of inputs considered in the sequel, [GOK06]. For the development herein, the number of input elements M is however arbitrary. The system is assumed overloaded in the sense that the number of signals (wanted and interferers) N_C is generally larger than the number of antenna elements M. This is due to the assumed dense placement of satellites in the geostationary orbit around the wanted satellite.

The spatial selectivity of the antenna front-end captures the N_C satellite signals. Figure 2.1 illustrates the considered setup of the recevier with N_C satellites in the field of view of the receiver.

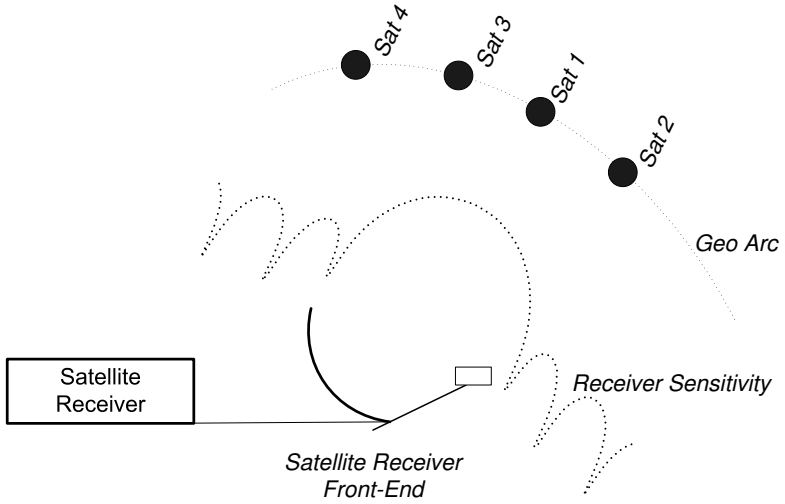

Figure 2.1: A satellite broadcast receiver with an antenna front-end that receives the wanted signal 1 in combination with interferers on adjacent satellites 2, 3 and 4. Here *Geo Arc* denotes the geostationary Earth orbit.

Data Model

After down conversion to the baseband representation of the wanted signal, $s_1(t)$ and symbol sampling of the received signals, the receive sequence is regrouped in the $M \times 1$ vector $\mathbf{r}(t)$ and can be expressed as follows:

$$\begin{aligned}\mathbf{r}(t) &= \begin{bmatrix} r_1(t) \\ \vdots \\ r_M(t) \end{bmatrix} = [\mathbf{a}_1 \dots \mathbf{a}_{N_C}] \begin{bmatrix} s_1(t) \\ \vdots \\ s_{N_C}(t) \end{bmatrix} + \mathbf{n}(t) \\ &= \sum_{i=1}^{N_C} \mathbf{a}_i(t) s_i(t) + \mathbf{n}(t) = \mathbf{A}\mathbf{s}(t) + \mathbf{n}(t)\end{aligned} \tag{2.1}$$

Here the antenna response, $\mathbf{A}$, is a complex valued matrix containing the relative antenna sensitivity for the N_C carriers by the M input elements and $\mathbf{n}(t)$ is a vector modeling the noise on the M input streams. Note that the noise samples are spatially correlated to a certain extent, as the antenna beams overlap partially. The noise is further assumed to be zero mean and temporally white.

The signal, $s_i(t)$, represents a linearly modulated communication signal composed of the filtered output of a complex data sequence $d_i(t)$ from the complex symbol set $\mathbf{\Omega}$. The shaping filter (typically a root-raised cosine filter) has impulse response $g_i^{TX}(t)$. The complex symbol set is defined by the transmission standards used, typically DVB-S or DVB-S2 [ETS05a], often QPSK or 8PSK for broadcast transmissions. The ith signal can then be expressed as follows ($\star$ denotes the convolution operator):

$$s_i(t) = g_i^{TX}(t) \star d_i(t) \tag{2.2}$$

We define the signal $s_1(t)$ as the wanted signal and the other signals as interferers. We choose to incorporate the frequency offset Δf_i in the matched filter response, $g_i^{TX}(t)$, of the signal $s_i(t)$ in the baseband of $s_1(t)$:

$$g_i^{TX}(t) = g_{MF}(t) e^{\jmath(2\pi \Delta f_i t + \phi_i)} \tag{2.3}$$

Here $g_{MF}(t)$ is the matched filter impulse response (assumed the same for all signals) is shifted in frequency to the offset of the i-th carrier relative to the wanted first carrier. The phase error ϕ_i is included in the definition of $g_i^{TX}(t)$.

Assuming that we have N_C signals (wanted and interfering signals), (2.1) can be reformulated as:

$$\mathbf{r}(t) = \mathbf{A} \begin{bmatrix} g_1^{TX}(t) \star d_1(t) \\ \vdots \\ g_{N_C}^{TX}(t) \star d_{N_C}(t) \end{bmatrix} + \mathbf{n}(t) \tag{2.4}$$

Expressing the transmit signal shaping in the discrete time domain and assuming an FIR filter, we can reformulate (2.2) as follows using N_d consecutive samples of

$g_i^{TX}(t)$ and $d_i(t)$:

$$s_i(t) = \mathbf{g}_i^{TX}[N_d]\mathbf{d}_i(t) \tag{2.5}$$

Here $\mathbf{d}_i(t) = [d_i(t) \dots d_i(t - N_d + 1)]^T$ is the $N_d \times 1$ vector containing the discrete time data sequence of the ith signal and $\mathbf{g}_i^{TX}[N_d] = [g_i^{TX}(1) \dots g_i^{TX}(N_d)]$ is the $1 \times N_d$ transmit filter sample vector of the ith signal, including the frequency offset of (2.3). We combine all the N_d data sequences from the N_C carriers in the $N_d N_C \times 1$ vector $\bar{\mathbf{d}}_{\mathbf{all}}(t) = \left[\mathbf{d}_1^T(t) \dots \mathbf{d}_{N_C}^T(t)\right]^T$.

Define the $N_C \times N_C N_d$ transmit filter matrix as:

$$\mathbf{G}^{TX} = \begin{bmatrix} \mathbf{g}_1^{TX}[N_d] & 0 & \dots & 0 \\ 0 & \mathbf{g}_2^{TX}[N_d] & 0 & \vdots \\ \vdots & & \ddots & 0 \\ 0 & \dots & 0 & \mathbf{g}_{N_C}^{TX}[N_d] \end{bmatrix} \tag{2.6}$$

We can then reformulate the sampled transmit filtering (2.5) for all the N_C signals as follows:

$$\mathbf{s}(t) = \mathbf{G}^{TX}\bar{\mathbf{d}}_{\mathbf{all}}(t) \tag{2.7}$$

The sampled received signal, as defined in (2.1) can then be expressed as follows:

$$\mathbf{r}(t) = \mathbf{A}\mathbf{G}^{TX}\bar{\mathbf{d}}_{\mathbf{all}}(t) + \mathbf{n}(t) \tag{2.8}$$

2.3 Problem Formulation and Receiver Structure

To improve reception under interference conditions, the proposed receiver structure consists of a multi-input LNB with a spatial linear pre-processing (LPP) step, followed by nonlinear interference cancellation (IC) step in the temporal processing domain, see Figure 2.2. Since the satellite broadcast signal is received as a line-of-sight signal, the signal dispersion is very small and the temporal correlation is mainly due to signal shaping, see (2.2). Thus the receiver structure can be decomposed in a spatial part (LPP) followed by a subsequent temporal processing part without loss in performance. The considered scenario comprises an overloaded system with a number of interferers that is generally larger than the number of receive antenna elements ($N_C > M$). Therefore, only linear processing for interference rejection is in general not adequate, [GOK06]. The following Chapter 3.3 illustrates the performance of only a linear processing step for overloaded and not overloaded systems.

In overloaded systems, linearly suppressing some interference will inevitably lead to increased sensitivity in other directions potentially causing interference from other satellites at other orbital locations. To address this, a nonlinear interference processing step is considered as second temporal processing step, after the linear spatial pre-processing (LPP) step.

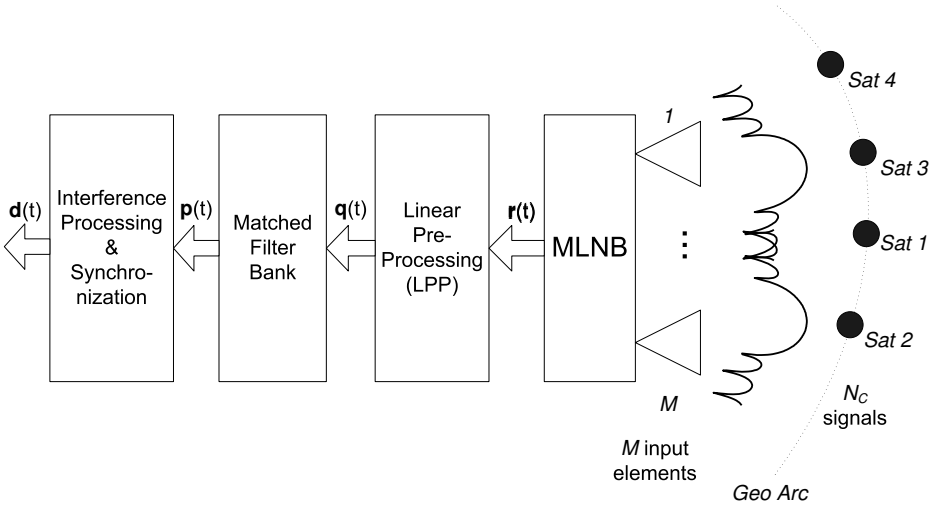

Figure 2.2: Receiver structure overview. A desired signal source on satellite Sat 1 is received in combination with interference on adjacent satellites Sat 2 to Sat N_C. A low noise block down converter (LNB) with M inputs that are directed in different spatial directions receive the signal combination for subsequent spatial linear processing and temporal nonlinear processing.

To allow a good operation of the iterative nonlinear processing, a spatial linear pre-processing step (LPP) pre-conditions $\mathbf{r}(t)$, allowing multiuser detection on a subset of the signals and suppressing the rest.

The spatial processing is represented by an $M \times M$ weighting matrix, $\mathbf{W} = [\mathbf{w}_1 \dots \mathbf{w}_M]$, applied on the received signals $\mathbf{r}(t)$. Multiple simultaneous weighting elements can be applied to optimize the subsequent processing step for each one of the processed carriers, which is discussed further in the subsequent sections. The outputs of the linear weighting steps are denoted as $q_1(t)$ to $q_M(t)$. In total, the M strongest carriers of the N_C are selected to be processed jointly, the wanted signal plus the dominating DVB-S/S2 compliant interferers. The remaining $N_C - M$ carriers are filtered out as far as possible by the spatial processing step. Based on the previous introduced expression (2.1), we can subdivide the received signal accordingly into the "desired" part of M signals, which is processed subsequently, $\mathbf{s}^d(t)$ and the spatially filtered "interference" part, $\mathbf{s}^i(t)$:

$$\mathbf{r}(t) = \mathbf{A}\mathbf{s}(t) + \mathbf{n}(t) = \begin{bmatrix}\mathbf{A}^d & \mathbf{A}^i\end{bmatrix} \begin{bmatrix}\mathbf{s}^d(t) \\ \mathbf{s}^i(t)\end{bmatrix} + \mathbf{n}(t) = \mathbf{A}^d\mathbf{s}^d(t) + \mathbf{A}^i\mathbf{s}^i(t) + \mathbf{n}(t) \quad (2.9)$$

Here, $\mathbf{A}^d$ has dimension $M \times M$ and $\mathbf{A}^i$ has dimension $M \times (N_C - M)$.

Detection Problem Formulation

Below we will start by only considering the detection problem, assuming synchronization has been achieved. The received signal $\mathbf{r}(t)$ from (2.1) is processed in the receiver to detect the symbol sequence $d_1(t)$ of the wanted signal $s_1(t)$ that is degraded by additive noise and interference from adjacent satellite signals.
In the following we consider processing of N_d consecutive symbols on all M inputs. After the spatial weighting step, the signal output on the M carriers can be expressed as follows[1]:

$$\mathbf{q}(t) = \mathbf{W}^*\mathbf{r}(t) = \mathbf{W}^* \left(\mathbf{A}^d\mathbf{s}^d(t) + \mathbf{A}^i\mathbf{s}^i(t) + \mathbf{n}(t)\right) \tag{2.10}$$

Since joint detection on all N_C signals is not considered feasible, the purpose of the spatial filtering, $\mathbf{W}$, is to suppress $\mathbf{s}^i(t)$ and $\mathbf{n}(t)$ to allow joint detection of $\mathbf{s}^d(t)$. The choice of pre-filtering $\mathbf{W}$ will be discussed in Section 3. Assuming that the interference $\mathbf{s}^i(t)$ is suppressed, we adopt a simplified signal model in which the M "desired" dominating signals are considered from which joint detection will be performed:

$$\mathbf{q}(t) = \mathbf{W}^*\mathbf{A}^d\mathbf{s}^d(t) + \mathbf{n}'(t) = \mathbf{W}^*\mathbf{A}^d\mathbf{G}^{TX,d}\mathbf{d}^d(t) + \mathbf{n}'(t) \tag{2.11}$$

where $\mathbf{G}^{TX,d}$ is the $M \times MN_d$ transmit matrix corresponding to $\mathbf{s}^d(t)$, see (2.6) and $\mathbf{d}^d(t) = \left[\mathbf{d}_1^T(t) \dots \mathbf{d}_M^T(t)\right]^T$ is $MN_d \times 1$ and $\mathbf{n}'(t) = \text{vec}\{\mathbf{W}^*\mathbf{n}(t)\}$ is the resulting noise term. After matched filtering, the received signal on carrier i can be expressed as:

$$p_i(t) = [g_i^{RX}(1) \dots g_i^{RX}(N_d)] \begin{bmatrix} q_i(t) \\ \vdots \\ q_i(t - N_d + 1) \end{bmatrix} = \mathbf{g}_i^{RX}[N_d]\mathbf{q}_i(t) \tag{2.12}$$

Defining the receive filtering on the sampled output of the LPP step as matrix operation, we define first, similar to (2.6):

$$\mathbf{G}^{RX} = \begin{bmatrix} \mathbf{g}_1^{RX}[N_d] & 0 & \dots & 0 \\ 0 & \mathbf{g}_2^{RX}[N_d] & 0 & \vdots \\ \vdots & & \ddots & 0 \\ 0 & \dots & 0 & \mathbf{g}_M^{RX}[N_d] \end{bmatrix} \tag{2.13}$$

and can write the receive filter $M \times 1$ vector output as:

$$\mathbf{p}(t) = [p_1(t) \cdots p_M(t)]^T = \mathbf{G}^{RX}\bar{\mathbf{q}}(t) \tag{2.14}$$

with $\bar{\mathbf{q}}(t) = \left[\mathbf{q}_1^T(t) \cdots \mathbf{q}_M^T(t)\right]^T = \text{vec}\{[\mathbf{q}(t) \cdots \mathbf{q}(t - N_d + 1)]^T\}$.

[1] $(\,)^*$ denotes the conjugate transpose.

Note that we can write from (2.11):

$$\bar{\mathbf{q}}(t) = \text{vec}\{\left[\mathbf{W}^* \mathbf{A}^d \mathbf{G}^{TX,d} \left[\mathbf{d}^d(t) \cdots \mathbf{d}^d(t - N_d + 1)\right]\right]^T\} + \mathbf{n}''(t) \tag{2.15}$$

where $\mathbf{n}''(t)$ contains samples of $\mathbf{n}'(t)$ in a vector. Let $\mathbf{D}(t) = \left[\mathbf{d}^d(t) \cdots \mathbf{d}^d(t - N_d + 1)\right]$ which is $MN_d \times N_d$ and contains $M(2N_d - 1)$ unique data symbols. Using properties of the Kronecker product, $\otimes$, we have:

$$\begin{aligned} \bar{\mathbf{q}}(t) &= \text{vec}\{\mathbf{W}^* \mathbf{A}^d \mathbf{G}^{TX,d} \left[\mathbf{d}^d(t) \cdots \mathbf{d}^d(t - N_d + 1)\right]^T\} + \mathbf{n}''(t) \\ &= \text{vec}\{\mathbf{D}^T(t) \left(\mathbf{W}^* \mathbf{A}^d \mathbf{G}^{TX,d}\right)^T\} + \mathbf{n}''(t) \\ &= \left[\left(\mathbf{W}^* \mathbf{A}^d \mathbf{G}^{TX,d}\right) \otimes \mathbf{I}_{N_d}\right] \text{vec}\{\mathbf{D}^T(t)\} + \mathbf{n}''(t) \end{aligned} \tag{2.16}$$

Here $\mathbf{I}_{N_d}$ is the $N_d \times N_d$ identity matrix. Since $\mathbf{D}(t)$ contains $M(2N_d - 1)$ unique data symbols, we can write:

$$\text{vec}\{\mathbf{D}^T(t)\} = \mathbf{S}\bar{\mathbf{d}}(t) \tag{2.17}$$

where $\mathbf{S}$ is an $MN_d^2 \times M(2N_d - 1)$ mapping matrix representing the structure of the data in $\mathbf{D}^T(t)$ and contains only "1" and "0" entries and

$$\bar{\mathbf{d}}(t) = [d_1(t) \cdots d_1(t - 2N_d + 2) \cdots d_M(t) \cdots d_M(t - 2N_d + 2)]^T \tag{2.18}$$

which is $M(2N_d - 1)$ and are the unique data symbols to be detected on the M carriers. The matrix $\mathbf{S}$ is defined in the appendix 5.A.

Consequently, the symbol samples at the receive filtering output of the M carriers can be expressed as follows:

$$\begin{aligned} \mathbf{p}(t) &= \mathbf{G}^{RX} \bar{\mathbf{q}}(t) \\ &= \mathbf{G}^{RX}(\left[\left(\mathbf{W}^* \mathbf{A}^d \mathbf{G}^{TX,d}\right) \otimes \mathbf{I}_{N_d}\right] \mathbf{S}\bar{\mathbf{d}}(t)) + \bar{\mathbf{n}}(t) \\ &= \mathbf{G}(\mathbf{W})\bar{\mathbf{d}}(t) + \bar{\mathbf{n}}(t) \end{aligned} \tag{2.19}$$

where $\bar{\mathbf{n}}(t)$ is the filtered noise sequence. The matrix $\mathbf{G}(\mathbf{W}) = \mathbf{G}^{RX}[\mathbf{W}^* \mathbf{A}^d \mathbf{G}^{TX,d} \otimes \mathbf{I}_{N_d}]$ combines the spatial and temporal part of the received data sequence model. Note that $\mathbf{W}$ enters linearly in (2.19).

Using (2.19), we can group N consecutive symbols on each of the M carriers into a $M \times N$ block that is processed jointly:

$$\mathbf{p}[N] = \mathbf{G}(\mathbf{W})\mathbf{S}\bar{\mathbf{d}}[N] + \bar{\mathbf{n}}[N] \tag{2.20}$$

On the basis of the signal model defined here, the detection problem can then be formulated as follows:

$$[\hat{\mathbf{W}}, \hat{\bar{\mathbf{d}}}] = \arg \min_{\mathbf{W}, \bar{\mathbf{d}}[N] \in \mathbf{\Omega}^{M(2N_d - 1) \times N}} ||\mathbf{p}[N] - \mathbf{G}(\mathbf{W})\mathbf{S}\bar{\mathbf{d}}[N]||_F^2 \tag{2.21}$$

Note that we consider here a simplified problem by using unitary weighting (Frobenius norm) for the cost function, ignoring the structure of the noise process $\bar{\mathbf{n}}(t)$.

The cost function of the problem is non-convex and the optimal solution requires exhaustive search through the symbol sequence set. This is of course intractable and a suboptimal approach has to be followed in practice. Note that the problem is similar to a multi-user detection problem with an additional spatial degree of freedom. Extensive references describe suboptimal optimization approaches, see e.g. [Ver98] for a good overview. In the subsequent section we elaborate on a nonlinear suboptimal optimization approach, including the spatial degree of freedom in the optimization procedure.

2.4 Conclusion

In this chapter the interference problem considered for broadcast reception has been formulated in details and a receiver structure has been proposed. The receiver consists of both a spatial filtering step and a secondary temporal interference mitigation step. The spatial filtering step considered is a linear pre-processing (LPP) step. The system considered here is overloaded ($N_C > M$) and based on this receiver structure a cost function is derived for the joint symbol detection problem.
This problem formulation is used in the subsequent developments of Chapter 3, 5 and 7.

Chapter 3

Linear Pre-processing, (LPP Step)

3.1 Introduction

In this chapter the receiver system defined in the Chapter 2 is considered. The performance of the linear pre-processing step (LPP) is analyzed. The detection problem is reformulated for the specific linear pre-processing problem. The resulting weighting factors are used to verify the performance in terms of typical interference limited reception conditions. The considered antenna design parameters defined in the Section 1.10 are varied under these aspects, specifically the antenna diameter and the angular spacing between the MLNB input elements. Simulation results are presented that illustrate the LPP performance under non-overloaded and overloaded, $N_C > M$, conditions. Specifically the limitations of the LPP method under overloaded conditions are studied in details.

This Chapter uses the formalism introduced in the previous Chapter 2 and focuses specifically on the linear pre-processing problem statement. The results of this Chapter are used in the subsequent development of Chapter 5 and 7.

3.2 LPP Mechanism

The antenna front-end is assumed to be fixed and not mechanically steerable. To condition the signal to noise and interference ratio at the right level for the subsequent temporal interference cancellation step, an initial spatial linear pre-processing is proposed in the receiver system with the selection of the weighting matrix, $\mathbf{W}$, to facilitate subsequent signal detection. An algorithm to iteratively update $\mathbf{W}$ is described below. First we will describe an initialization procedure for $\mathbf{W}$.

Since the noise is uncorrelated with the signals, the covariance matrix of the receiver output can be expressed as follows:

$$\mathbf{R} = E\{(\mathbf{A}\mathbf{s}(t) + \mathbf{n}(t))\,(\mathbf{A}\mathbf{s}(t) + \mathbf{n}(t))^*\} = \mathbf{A}E\{\mathbf{s}(t)\mathbf{s}^*(t)\}\mathbf{A}^* + \mathbf{R}_\mathbf{n} \tag{3.1}$$

The related $M \times M$ noise receive correlation matrix is denoted $\mathbf{R}_\mathbf{n} = E\{\mathbf{n}(t)\mathbf{n}^*(t)\}$.

Note that all signals are assumed uncorrelated and independent. Based on the separation into *desired* and *interfering* signals, we define the covariance of the desired signal $\mathbf{R}^d = \mathbf{A}^d E\{\mathbf{s}^d(t)\mathbf{s}^{d*}(t)\}\mathbf{A}^{d*}$ and of the interfering signal part $\mathbf{R}^i = \mathbf{A}^i E\{\mathbf{s}^i(t)\mathbf{s}^{i*}(t)\}\mathbf{A}^{i*}$. The received signal covariance can then be expressed as:

$$\mathbf{R} = \mathbf{R}^d + \mathbf{R}^i + \mathbf{R_n} \tag{3.2}$$

Following similar steps as in [Win84], the maximization of the power in the desired signal component as cost function for the selection of $\mathbf{W}$ can be expressed as a generalized eigenvector problem:

$$\begin{aligned} \mathbf{W}_1 &= \arg \max_{\substack{\mathbf{W} \\ \text{s.t.}\mathbf{W}\mathbf{W}^*=\mathbf{I}_M}} \frac{\mathrm{Tr}\{\mathbf{W}^*\mathbf{R}^d\mathbf{W}\}}{\mathrm{Tr}\{\mathbf{W}^*\mathbf{R}^i\mathbf{W} + \mathbf{W}^*\mathbf{R_n}\mathbf{W}\}} \\ &= \arg \max_{\substack{\mathbf{W} \\ \text{s.t.}\mathbf{W}\mathbf{W}^*=\mathbf{I}_M}} \frac{\mathrm{Tr}\{\mathbf{W}^*\mathbf{R}^d\mathbf{W}\}}{\mathrm{Tr}\{\mathbf{W}^*(\mathbf{R} - \mathbf{R}^d)\mathbf{W}\}} \end{aligned} \tag{3.3}$$

The application of the weighting factor $\mathbf{W}_1$ maximizes the total power in the processed signals (wanted and interference). Alternatively, the maximal signal-to-noise-and-interference ratio (SNIR) for each j of the M carriers processed can be considered:

$$\mathbf{w}_{2,j} = \arg\max_{\mathbf{w}} \frac{\mathbf{w}^*\mathbf{R}_j^d\mathbf{w}}{\mathbf{w}^*(\mathbf{R} - \mathbf{R}_j^d)\mathbf{w}} \tag{3.4}$$

With $\mathbf{R}_j^d = \mathbf{A}_j^d E\{s_j^d(t)s_j^{d*}(t)\}\mathbf{A}_j^{d*}$, the covariance matrix of the considered j-th signal. We regroup the M weighting vectors $\mathbf{w}_{2,j}$ in $\mathbf{W}_2 = [\mathbf{w}_{2,1} \dots \mathbf{w}_{2,M}]$. To compute the initial weights in (3.3)-(3.4), estimates of the covariance matrices must be obtained. We assume that the antenna responses $\mathbf{a}_j, j = 1, \dots, M$ are known as well as the noise covariance $\mathbf{R}_n$. This is a reasonable assumption in a quasi static reception environment as the one considered here. The noise covariance can be estimated using sample covariance matrix estimation over long time-frames as well as the received signal amplitudes.

By combining this method later with the subsequent temporal processing in Chapter 5, we show that the proposed method is robust against small initialization errors in the antenna response when included in an iterative method.
Note that the weighting $\mathbf{W}_1$ provides the best linear spatial weighting for a joint detection decision all processed carriers, while the weighting matrix $\mathbf{W}_2$ provides the best linear spatial weighting for an isolated detection decision step on each one of the carriers separately. Both weighting matrices $\mathbf{W}_1$ and $\mathbf{W}_2$ will subsequently be used in the proposed processing steps.

This weighting factor is applied to the received signals $r_1(t) \dots r_M(t)$ to yield the outputs $q_1(t) \dots q_M(t)$ as follows:

$$\mathbf{q}(t) = [q_1(t) \cdots q_M(t)]^T = \mathbf{W}^*[r_1(t) \cdots r_M(t)]^T = \mathbf{W}^*\mathbf{r}(t) \tag{3.5}$$

Note that if the LPP step is able to separate well the signal sources and the matrix $\mathbf{W}^*\mathbf{A}^d$ is approximately diagonal, then the spatial and temporal steps can be well separated. We can define $\mathbf{V}$ as the matrix containing all the diagonal elements of $\mathbf{W}^*\mathbf{A}^d$ and $\mathbf{V}'$ as the matrix with all the off-diagonal elements, such that $\mathbf{V} + \mathbf{V}' = \mathbf{W}^*\mathbf{A}^d$. Assuming that $\mathbf{V} \approx \mathbf{W}^*\mathbf{A}^d$, then we can reformulate the detection problem formulation (2.21) as follows, with $\mathbf{T} = \mathbf{V} \otimes \mathbf{I}_{N_d^2}$ and $\mathbf{G} = \mathbf{G}^{RX}(\mathbf{G}^{TX,d} \otimes \mathbf{I}_{N_d})$:

$$[\hat{\mathbf{T}}, \hat{\bar{\mathbf{d}}}] = \arg \min_{\mathbf{T}, \bar{\mathbf{d}}[N] \in \mathbf{\Omega}^{M(2N_d-1)\times N}} ||\mathbf{p}[N] - \mathbf{GTS}\bar{\mathbf{d}}[N]||_F^2 \tag{3.6}$$

The estimates of the weighting matrix $\hat{\mathbf{W}}$ can be directly derived from $\hat{\mathbf{T}}$. This results in the temporal filtering step being applied only after the spatial weighting of the signals.

3.3 LPP Performance Evaluation

In this section we investigate the performance of the linear pre-processing based on the spatial filtering of the adjacent interference as outlined in Section 3.2. A fixed satellite reception scenario with typical performance in Ku-band is considered as outlined in Section 1.9 with adjacent satellite interference. The receiving antenna consists of a conventional parabolic reflector antenna with a multi-input low noise block down-converter (MLNB) as active receiving element. The MLNB regroups several feed input elements with a certain spacing between the elements to generate closely spaced spatially separate beams.
The following Figure 3.1 illustrates the antenna gain patterns generated by a three element MLNB system. Using the defined LPP combination method as outlined in Section 3.2, the equivalent beam pattern is illustrated assuming the presence of two interferer at both sides of the wanted signal. The combined LPP pattern is computed by optimizing for the SNIR ratio using the expression (3.4) and assuming a known covariance matrix $\mathbf{R}$, as defined in 3.1.

The performance of a two and three element MLNB system with one and two interferers is assessed for different antenna sizes on Figures 3.2-3.5. A conventional reference antenna system with a single LNB input and perfectly pointed to the wanted satellite signal, denoted with *ref* on the presented results, is compared in performance to the proposed receiver structure with several input elements and with a subsequent linear pre-processing step (LPP). The signal to noise and interference ratio is denoted with C/(N+I), the signal to noise ratio with C/N and the signal to interference ratio with C/I. The achievable improvement of the proposed method compared to the reference antenna is denoted with *LPP impr.* It can be clearly derived form these results that a two element MLNB system does not yield significant improvement, using only the LPP mechanism deviced in this section. A

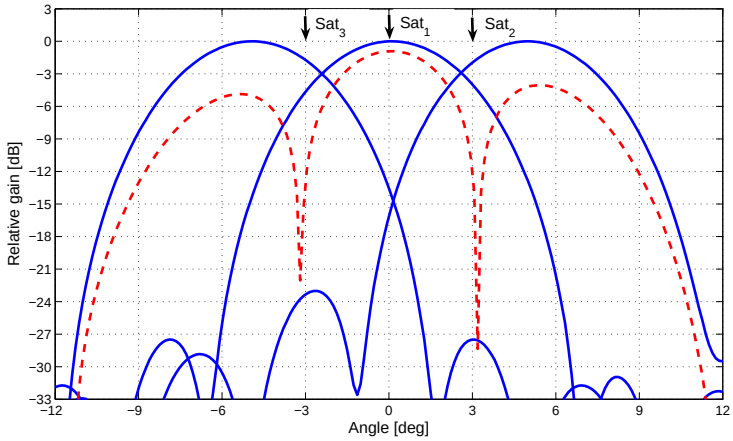

Figure 3.1: Gain pattern of a three element MLNB antenna system with 35cm aperture size and feed elements spaced such that the gain pattern intersection point lies at -3dB. Assuming two interferer at +3 and -3 degrees offset with the same power density level as the wanted signal, the equivalent gain pattern for the LPP combined signal is plotted also (red dashed line).

three element MLNB system however can eliminate the interference quite significantly. Indeed, a target C/(N+I) of 8dB - which is for example required (with implementation margin) for DVB-S QPSK 3/4 - is achievable with a 35cm antenna instead of a 55cm antenna compared to the reference system.

For a given interferer scenario an optimal spacing of the feed elements in terms of output C/(N+I) can be determined for a given antenna size. Figures 3.6-3.8 illustrate the optimization of the feed spacing for two and three element antenna systems. The two element system has a best setup with closely spaced feed elements that allow a small spatial variation in the beam pattern to avoid the interference. The three element system yields best performance for elements that have gain patterns overlapping at 2dB. Note that an intersection at 3dB generates a reception system with a constant (flat) maximal gain pattern over the angular range defined by the arrangement of the MLNB elements. Comparing the results for $M = 2$ and $N_C = 2$ on Figure 3.6 and for $M = 3$ and $N_C = 2$ on Figure 3.7, it is clear that a dual input system is very sensitive in performance to the interferer spacing relative to the feed angle spacing. A three input element MLNB system depends less on the feed spacing in performance improvement results.

Fixing the spacing of the MLNB elements to the optimal position as determined in the previous Figures 3.6-3.8, the performance improvement of the LPP system compared with a conventional reception antenna for different antenna sizes and

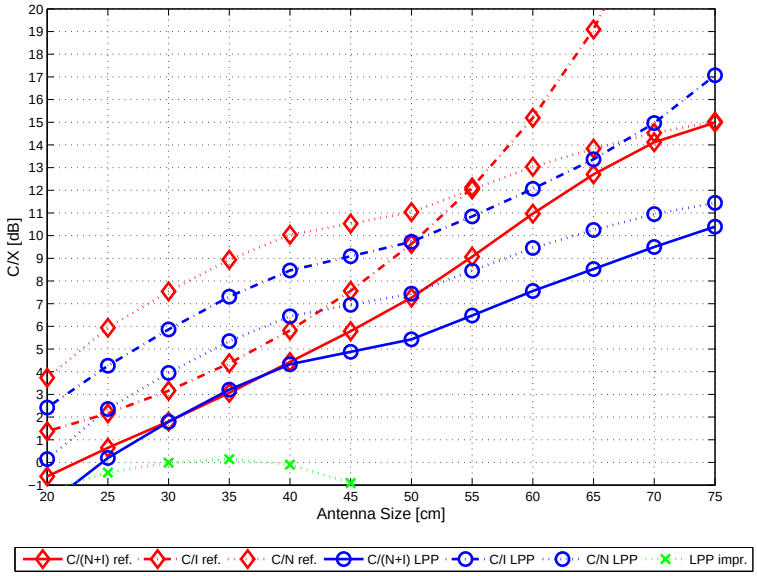

Figure 3.2: Performance of the LPP step compared to a reference antenna system with a single feed at the center. This assumes a single interferer located at 3 degrees offset and a dual input MLNB with subsequent LPP combination. *C/X* denotes the signal to noise ratios and signal to interference and noise ratios as stipulated in the labels. *C/(N+I) ref*, *C/N ref* and *C/I ref* denote the signal to noise and interference, the signal to noise and the signal to interference ratios respectively of the reference antenna system. *C/(N+I) LPP*, *C/N LPP* and *C/I LPP* denote the signal to noise and interference, the signal to noise and the signal to interference ratios of the considered dual input MLNB with a subsequent linear pre-processing (LPP) step. ($M = 2$, $N_C = 2$)

interferer offsets is displayed in Figures 3.9-3.11. Antennas with apertures larger than 55cm have sufficient spatial discrimination towards the neighboring satellites if the interferer is located at 3 degrees offset or more. For a single interferer, a two element MLNB system can eliminate the interference and yield a substantial gain compared to the reference single input antenna, see Figure 3.9. However for two interferer on either side of the wanted signal, a significant gain can be reached with three element systems, see Figure 3.11, while with two element combinations, the interference cannot be eliminated completely and significantly less improvement over the single input reference scenario can be reached with the LPP method, see Figure 3.10.
In general, as in accordance with expectations [BK80] [Win84] [CFS97], the LPP

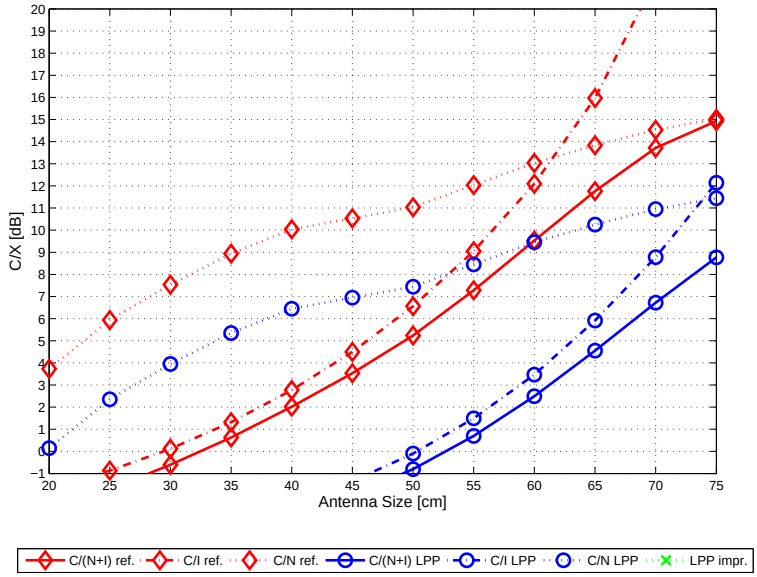

Figure 3.3: Performance of the LPP step compared to a reference antenna system as on Figure 3.2, but with two interferers located at +3 degrees and -3 degrees offset from the wanted signal. C/X refers to the signal and noise and interference ratios as defined in the labels below the Figure. The labels are defined as in Figure 3.2. ($M = 2$,$N_C = 3$)

step works well for $N_C < M$, but for overloaded systems with a number of carriers (wanted and interferer) larger than the number of input elements, $N_C > M$, the LPP system cannot eliminate all the impact of the interference. Additional measures are necessary in that case to reach high interference suppression performance. The results were obtained with a known covariance matrix $\mathbf{R}$ and $\mathbf{R}^d$. This is a reasonable assumption in the sense that the fixed reception scenario is a static situation and it is not varying statistically over time. An iterative improvement of the covariance matrix estimates is therefor feasible and the optimal weighting settings can be reached with high accuracy.

In the subsequent Section 5.3 the additional use of interference processing is proposed to increase detection performance for overloaded systems, $N_C > M$.

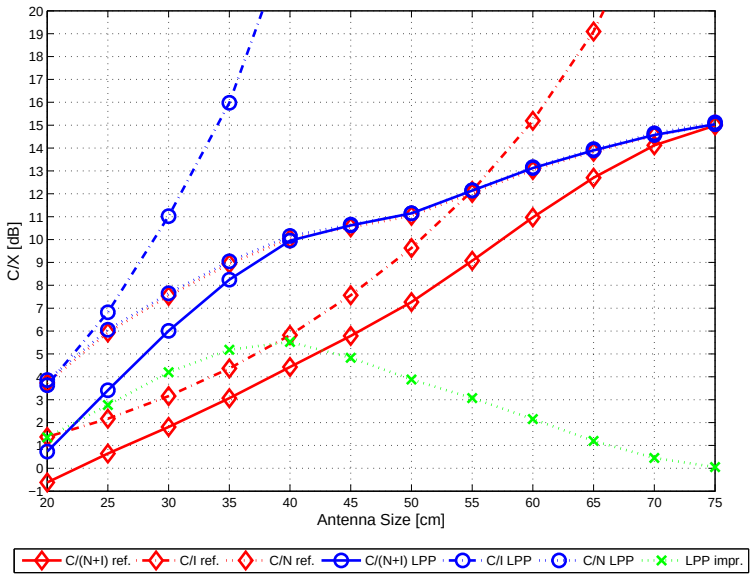

Figure 3.4: Performance of the LPP step compared to a reference antenna system for a three input MLNB system and assuming only one interferer at +3 degrees offset. C/X refers to the signal and noise and interference ratios as defined in the labels below the Figure. The labels are defined as in Figure 3.2. ($M = 3$,$N_C = 2$)

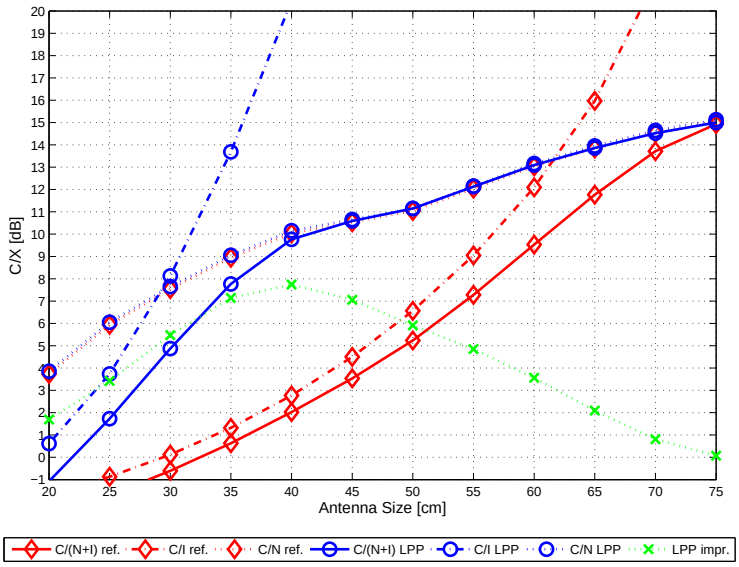

Figure 3.5: Performance plot for three input MLNB as on Figure 3.4, but assuming two interferers at +3 degrees offset and -3 degrees offset. C/X refers to the signal and noise and interference ratios as defined in the labels below the Figure. The labels are defined as in Figure 3.2. ($M = 3$,$N_C = 3$)

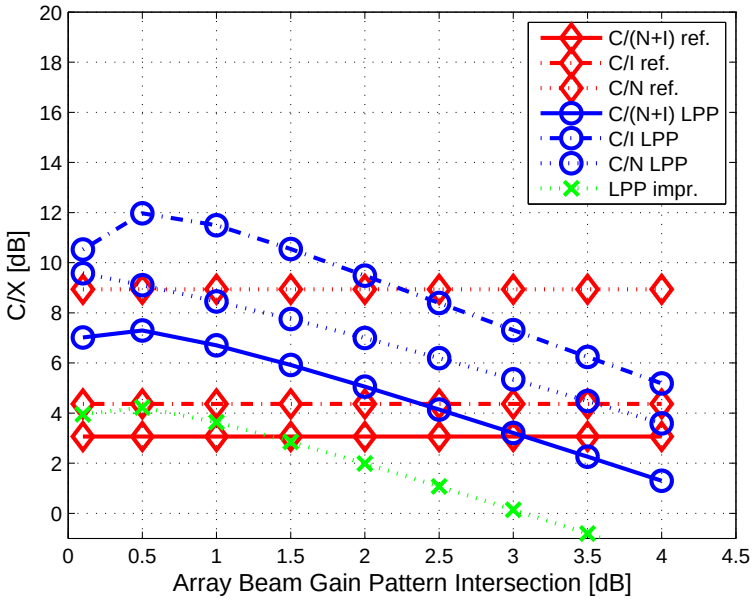

Figure 3.6: Performance of a two element MLNB system with an LPP step as a function of the intersection point of the gain patterns of the different input elements. A single interferer at +3 degrees offset is assumed. Here a 35cm antenna aperture is assumed. C/X refers to the signal and noise and interference ratios as defined in the labels of the Figure. The labels are defined as in Figure 3.2. ($M = 2$, $N_C = 2$)

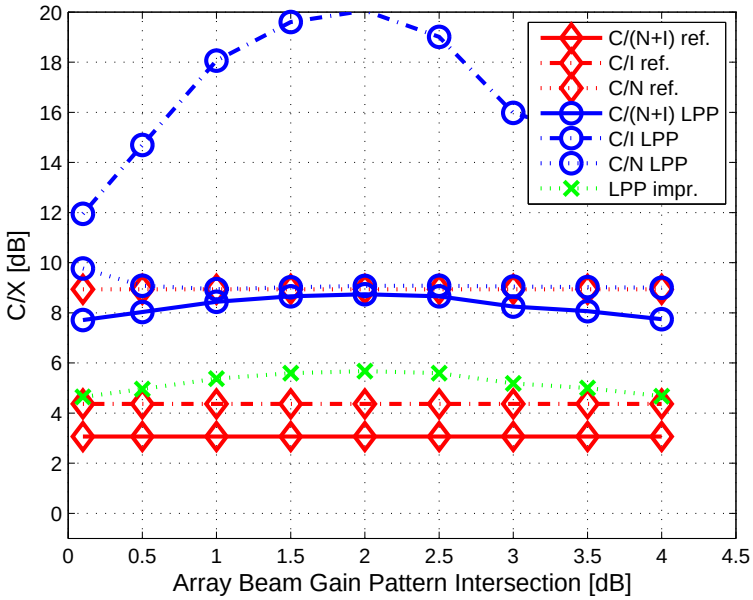

Figure 3.7: Performance of a three element MLNB reception system as a function of the intersection point of the gain patterns of the different input elements. A single interferer at +3 degrees offset is assumed. A 35cm antenna aperture is assumed. C/X refers to the signal and noise and interference ratios as defined in the labels of the Figure. The labels are defined as in Figure 3.2. ($M = 3$, $N_C = 2$)

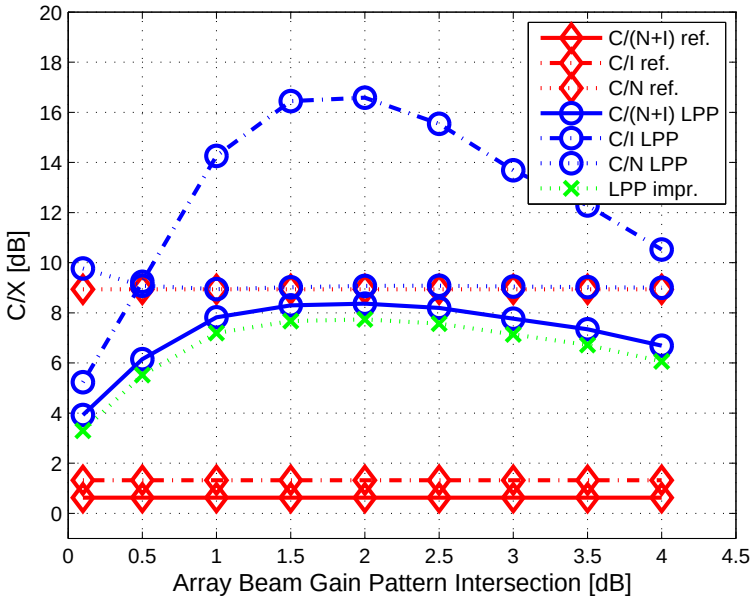

Figure 3.8: Performance of a three element MLNB reception system as a function of the intersection point of the gain patterns of the different input elements. Two interferer at +3 degrees and -3 degrees offset are assumed. A 35cm antenna aperture is assumed. C/X refers to the signal and noise and interference ratios as defined in the labels of the Figure. The labels are defined as in Figure 3.2. ($M = 3$,$N_C = 3$)

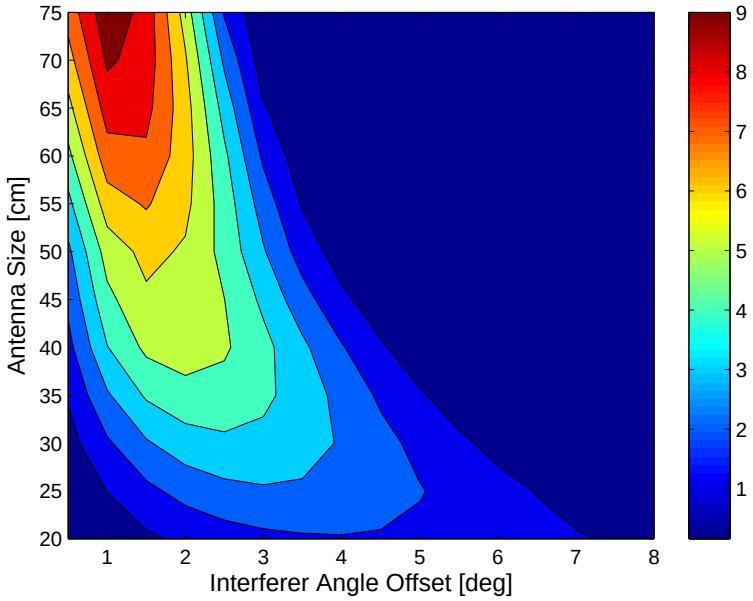

Figure 3.9: LPP improvement in dB as a function of the antenna size and the interferer offset from the wanted signal. A two element MLNB is assumed with an element spacing that optimized the LPP gain as outlined on Figure 3.6. A single interferer is assumed at the offset on the x-axis. The LPP performance improvement over a reference antenna system is indicated in dB. The *LPP improvement* is defined as the difference in dB between the signal to noise and interference ratios of the proposed LPP based antenna system compared to the reference antenna system. ($M = 2$,$N_C = 2$)

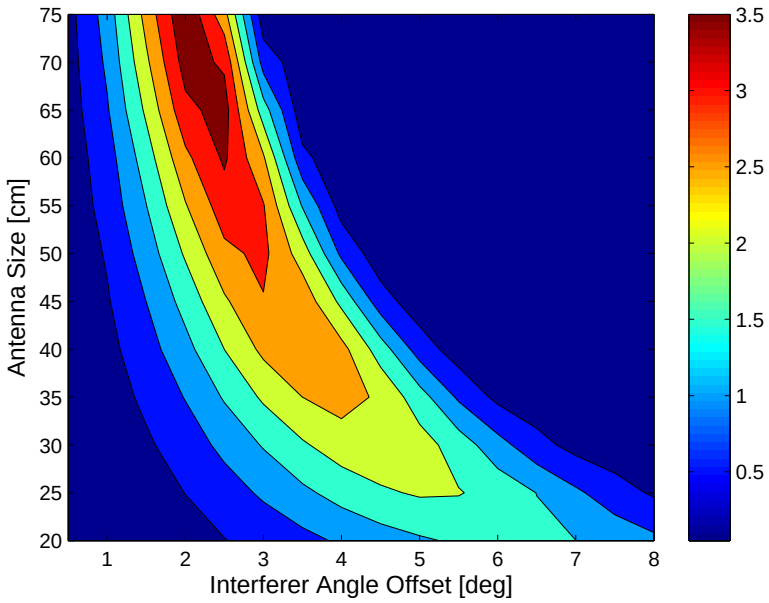

Figure 3.10: LPP improvement (in dB) plot as in Figure 3.9, assuming two interferer spaced on either side of the wanted signal at the offset angle indicated on the x-axis. A two element MLNB is assumed with an element spacing that optimized the LPP gain as outlined on Figure 3.7. The LPP performance improvement over a reference antenna system is indicated in dB. The *LPP improvement* is defined as the difference in dB between the signal to noise and interference ratios of the proposed LPP based antenna system compared to the reference antenna system. ($M = 2$,$N_C = 3$)

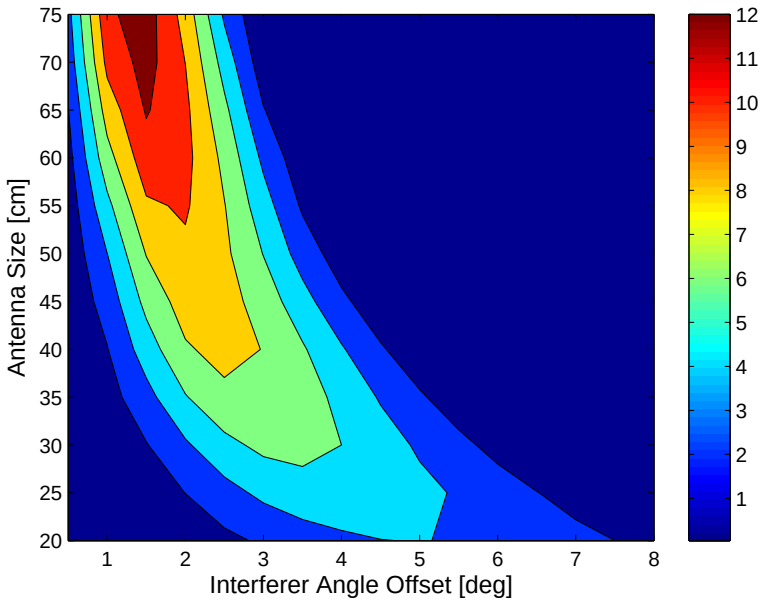

Figure 3.11: LPP improvement (in dB) plot as in Figure 3.9, assuming two interferer spaced on either side of the wanted signal at the offset angle indicated on the x-axis. A three element MLNB is assumed with an element spacing that optimizes the LPP gain as outlined on Figure 3.8. The LPP performance improvement over a reference antenna system is indicated in dB. The *LPP improvement* is defined as the difference in dB between the signal to noise and interference ratios of the proposed LPP based antenna system compared to the reference antenna system. ($M = 3$,$N_C = 3$)

3.4 Conclusion

We have investigated the linear pre-processing step in this chapter and simulated the expected gain in terms of signal to noise and interference ratio at the output of the system. As expected from results from previous work, under non-overloaded conditions the LPP step alone provides a significant interference suppression performance improvement. The LPP provides a spatial degree of freedom that helps suppress interference to a certain extend. However for overloaded scenarios this spatial filtering alone proves insufficient and an additional temporal step is required to achieve better performance. This additional temporal procedure is the topic of the following Chapters 4 and 5.

Chapter 4

MMSE Based Interference Cancellation

4.1 Introduction

The interference limited broadcast reception scenario is considered in this chapter for standard conform DVB-S/S2 signals. An MMSE based iterative soft-decision based interference cancellation method based on work by Beidas et al. [BGK02], is derived and adapted to the broadcast reception scenario. The performance is assessed through simulations, taking into account different symbol rates on the main signal and interferer and also phase noise impairments.

A single input system ($M = 1$) is the basis for this Chapter. The spatial filtering with the LPP linear pre-processing step is not considered in the framework of this chapter. Instead an MMSE based iterative detection method based on [BGK02] is adapted to the specific problem considered here. This implies an adaptation of the symbol rates of main signal and interferer as well as the consideration of the synchronization impact.

The iterative interference processing algorithm is analyzed here in isolation of other receiver components. A wanted signal and a single interferer is assumed in the framework of this chapter.

4.2 Signal Model

We are considering a DVB-S or DVB-S2 compliant wanted signal $s(t)$ at power level E_s that is interfered by $i(t)$ from an adjacent satellite, received at power level E_i. The frequency offset Δf can be any value between 0 to 1 times the symbol rate. The figure 4.1 illustrates the considered scenario in the frequency domain.

The digital broadcast signal received $r(t)$ can be modeled as a linearly modulated signal:

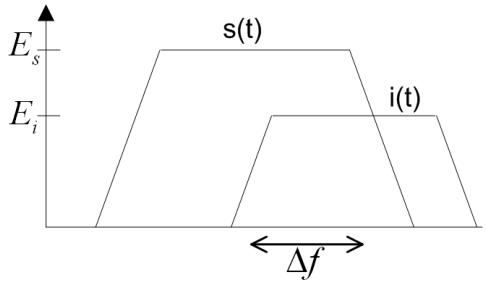

Figure 4.1: Illustration of the wanted signal $s(t)$ and the interfering signal $i(t)$ with a certain frequency offset Δf and assumed respective power levels E_S and E_i.

$$r(t) = s(t) + i(t) + n(t) \tag{4.1}$$

Where $s(t)$ represents the digital PSK modulated wanted signal, $n(t)$ the additive white Gaussian noise and $i(t)$ the additional interference. The signal and interference is assumed digitally modulated according to commonly used broadcast standards, ie. DVB-S [ETS98] or DVB-S2 [ETS05a]. This implies that the signals are shaped with a root-raised cosine filter (RRCF) of a given Rolloff factor. Denoting with $d_{1,k}$ the k^{th} symbols of the signal $s(t)$ and with $d_{2,k}$ the k^{th} symbol of the interferer, using a similar signal model as in [BGK02] the desired signal and interference can be modeled as:

$$\begin{aligned} s(t) &= \sum_{k=-\infty}^{+\infty} \sqrt{E_{s,1}} d_{1,k} g_{MF}(t + kT_1 - \epsilon_s T_1) \\ i(t) &= \sum_{k=-\infty}^{+\infty} \sqrt{E_{s,2}} d_{2,k} g_{MF}(t + kT_2 - \epsilon_i T_2) e^{j(2\pi\Delta f t + \theta + \phi_n(t))} \end{aligned} \tag{4.2}$$

The signal shaping $g_{MF}(t)$ is a square root-raised cosine filter and the signal and interferer power levels are denoted $E_{s,1}$ and $E_{s,2}$ respectively. Note that the same rolloff factor for both $s(t)$ and $i(t)$ is assumed here. However the general case of different rolloff factors can well be considered in a similar manner, taking into account different matched filters $g_{MF}(t)$ for $s(t)$ and for $i(t)$.

In general, the signal and interference are not synchronized and the symbol timing T_1 and T_2 respectively are not aligned. The interference can be on any offset frequency compared to the main signal of interest, denoted with Δf. Also the phase difference θ is an arbitrary value between 0 and 2π.

In addition to the additive white noise $n(t)$, the received signal suffers from jitter on the symbol timing epoch ϵ_1 and ϵ_2 and additional phase noise $\phi_n(t)$.

Using the formalism introduced in [BGK02], the mutual impact of the symbols on the main and interfering channel can be expressed as follows for a symbol time

t_1 for the wanted signal $s(t)$ and a symbol time t_2 for the interfering signal $i(t)$:

$$C_{l,j}(t_1,t_2) = \left[\int g^*_{MF}(\alpha) g_{MF}(\alpha + t_2 - t_1) e^{-j2\pi(\Delta f_j - \Delta f_l)\alpha} d\alpha\right] \times e^{-j(2\pi(\Delta f_j - \Delta f_l)t_2 + (\theta_j - \theta_l))} \times \sqrt{E_{s,j} E_{s,l}} \tag{4.3}$$

which models the influence from a symbol in channel $l = 1, 2$ at time t_1 onto the symbol in channel $j = 1, 2$ at time t_2, where Δf_l and Δf_j are the normalized frequencies of the channels. (Note: $\Delta f_m = 0$ for $m = 1$ and $\Delta f_m = \Delta f$ for $m = 1$.)

Then the filtered signal at the receiver output, sampled at sampling time t_s can be expressed as:

$$\begin{aligned} x_s[t_s] =& r(t) \star g_{MF}(t)|_{t=t_s} \\ x_s[t_s] =& \sum_{j=-\infty}^{+\infty} (d_{1,j} C_{1,1}((j+\epsilon_s)T_1, t) \\ & + d_{2,j} C_{2,1}((j+\epsilon_i)T_2, t)) + n(t)|_{t=t_s} \end{aligned} \tag{4.4}$$

Here also, the index 1 denotes the wanted signal and 2 the interfering signal and the operator $\star$ denotes convolution.

The sequence of symbols on the wanted signal and interfering signal, which are assumed to be both received coherently by the receiver, are subdivided into equal blocks of symbols. Figure 4.2 illustrates the stacking of N_s symbols from a wanted signal with N_i symbols of the interfering signal into a common symbol matrix. A symbol synchronous transmission is assumed in this context. It is assumed that the synchronous transmission can be approximated for a short symbol block of N_s symbols on the wanted signal.

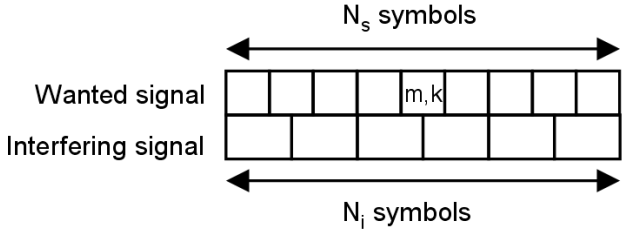

Figure 4.2: Illustration of the considered block of N_s symbols on the wanted signal and N_i symbols on the interfering signal around a considered symbol (m, k).

In the sequel we assume a finite number of N_s symbols of the wanted signal with N_i symbols of an interfering signal. A specific symbol of interest is considered on signal $m = 1, 2$ and symbol sequence k. Let $\mathbf{d}$ be a vector which contains a block of transmitted symbols from the wanted signal and the interferer:

$$\mathbf{d} = [\mathbf{d_s}^T \quad \mathbf{d_i}^T]^T \tag{4.5}$$

with

$$\mathbf{d_s} = [d_{1,1} \quad d_{1,2} \quad \dots \quad d_{1,N_s}]^T \tag{4.6}$$

$$\mathbf{d_i} = [d_{2,1} \quad d_{2,2} \quad \dots \quad d_{1,N_i}]^T \tag{4.7}$$

These numbers can be different, if the symbol rate is different on the wanted and interfering signal. The ratio of N_s/N_i corresponds to the ratio in symbol rates between the main signal and the interferer.

The received vector $\mathbf{x_s}$ of the wanted signal and $\mathbf{x_i}$ of the interfering signal can be expressed as follows:

$$\mathbf{x_s} = \mathbf{C}^I_{1,1}\mathbf{d_s} + \mathbf{C}^I_{1,2}\mathbf{d_i} + \mathbf{n_s} \tag{4.8}$$

$$\mathbf{x_i} = \mathbf{C}^I_{2,1}\mathbf{d_s} + \mathbf{C}^I_{2,2}\mathbf{d_i} + \mathbf{n_i} \tag{4.9}$$

Combining the symbol sequence to a common vector $\mathbf{x} = [\mathbf{x_s}^T \quad \mathbf{x_i}^T]^T$, the noise samples to $\mathbf{n} = [\mathbf{n_s}^T \quad \mathbf{n_i}^T]^T$ and defining the combined matrix $\mathbf{C^I}$ as follows:

$$\mathbf{C^I} = \begin{bmatrix} \mathbf{C}^I_{1,1}\mathbf{C}^I_{1,2} \\ \mathbf{C}^I_{2,1}\mathbf{C}^I_{2,2} \end{bmatrix} \tag{4.10}$$

then the combined received symbol vector for the wanted and interfering signal can be written as:

$$\mathbf{x} = \mathbf{C^I}\mathbf{d} + \mathbf{n} \tag{4.11}$$

This model can be applied to all received symbols m, k on the wanted and interfering sequence. (Without loss of generality and to preserve clarity we omit in the indexing to m and k.)

Now we can define the matrix $\mathbf{C^{Io}}$, which corresponds to the $\mathbf{C^I}$ matrix with the main diagonal elements set to zero. The matrix $\mathbf{C^{Is}}$ is defined as the matrix with only the diagonal elements. ($\mathbf{C^I} = \mathbf{C^{Is}} + \mathbf{C^{Io}}$)

The expression 4.11 can then be reformulated as follows:

$$\mathbf{x} = \mathbf{C^{Is}}\mathbf{d} + \mathbf{C^{Io}}\mathbf{d} + \mathbf{n} \tag{4.12}$$

The vector with the soft-decision based interference estimations of the received symbols can be expressed as:

$$\mathbf{i} = \mathbf{C^{Io}}E(\mathbf{d}|\mathbf{x}) \tag{4.13}$$

In the sequel, the proposed method, based on a minimum mean square error approach as in [GG00] and [BGK02], is adapted to the above mentioned interference problem. The linear minimum mean square error (MMSE) criteria can be expressed

as follows for a given considered symbol d of the symbol vector $\mathbf{d}$ and for a given received symbol sequence $\mathbf{x}$:

$$\min E(|y-d|^2|\mathbf{x}) = \min_{\mathbf{p},q} E(|\mathbf{p}^T\mathbf{x}+q-d|^2|\mathbf{x}) \tag{4.14}$$

Here $\mathbf{p}$ represents the feed-forward coefficients and q the feed-back coefficient of the linear filter $y = \mathbf{p}^T\mathbf{x} + q$.

$$\begin{aligned} \mathbf{p} &= \mathbf{C^{I_S}}^T(\mathbf{C^{I_S}}\mathbf{C^{I_S}}^T + \mathbf{C^{I_O}}E(\mathbf{d}\mathbf{d}^T|\mathbf{x})\mathbf{C^{I_O}}^T \\ &\quad -\mathbf{C^{I_O}}E(\mathbf{d}|\mathbf{x})E(\mathbf{d}|\mathbf{x})^T\mathbf{C^{I_O}}^T)^{-1} \qquad (4.15) \\ q &= -\mathbf{p}^T\mathbf{C^{I_O}}E(\mathbf{d}|\mathbf{x}) \qquad (4.16) \end{aligned}$$

The soft interference cancellation update for each symbol on the wanted and interfering signal sequence follows directly from the MMSE results and can be expressed as:

$$y = \mathbf{p}^T(\mathbf{x} - \mathbf{C^{I_O}}E(\mathbf{d}|\mathbf{x})) \tag{4.17}$$

The matrix inversion in (4.15) can be avoided by approximating the signal and interference autocorrelation, as suggested in [BGK02], leading to the considered simplified expression for the soft interference cancellation update for each symbol on the main and interfering signal.

Regrouping all the filtered symbol estimates y for the main and interfering signal in the vector $\mathbf{y}$, the first estimation of the transmitted symbols can be expressed as:

$$\mathbf{y} \approx \mathbf{x} - \mathbf{C^{I_O}}E(\mathbf{d}|\mathbf{x}) \tag{4.18}$$

This interference processing is subsequently repeated for all symbols on the wanted and interfering signal sequence within the considered symbol block.

For the following iterations over the considered symbol block, the outcome of the previous iteration ($\mathbf{y}^p$) is used:

$$\mathbf{y} \approx \mathbf{x} - \mathbf{C^{I_O}}E(\mathbf{d}|\mathbf{y}^p) \tag{4.19}$$

Simulation Results

This section contains Monte Carlo simulation results of the MMSE method. One single simulation observed 100 symbols. For each BER value calculation several simulations with random phase and timing difference were used. The transmit filter used is the root raised cosine with 35% roll-off and a filter length of 6 symbol times.

The accuracy of the BER results is usually better than ± 20% for the 95% confidence interval. This is realized by taking at least 100 bit errors for each BER value. If 1000 simulations are reached the simulation was stopped. QPSK

was assumed for these simulations, which is the modulation of interest here in the context of DVB-S [ETS98] and also DVB-S2 [ETS05a]. As the proposed algorithm works on detection level, the uncoded BER is used as comparison basis to assess the performance. The required uncoded BER level depends on the used coding of the wanted signal of interest.

Table 4.1 shows the BER results simulations for different E_b/N_0 and CIR[1] values of relevance. The phase was assumed as a random parameter with uniform distribution on the wanted signal and interferer, the symbol timing offset is as well considered a random parameter for each simulation run.

A considerable performance improvement is experienced for the considered signal to noise ration and frequency offsets. A maximal improvement is experienced for staggered interference signals, when the frequency offset is around 0.1-0.5 times symbol rate. Indeed, the noise correlation decreases between the wanted signal and the interferer for increasing frequency offsets, while the mutual interference decreases. It can also be noted that the detection performance after the processing is largely independent of the interferer power level.

A performance threshold can be deduced from the simulation results, see Table 4.1. Indeed, at a certain signal-to-interference ratio at low frequency offsets, the proposed processing will decrease the performance of the detection process. This is due to the fact that the interferer-to-noise ratio is not high enough to improve the detection by subsequent processing. Especially for co-channel interference, with a very small frequency offset, the interference to noise level determines whether a processing is possible.

For signals with similar power level, the impact of the frequency offset is illustrated in Figure 4.3. The improvement is maximum around a frequency offset of 0.4-0.5 times the symbol rate, but in general a considerable improvement can be noticed for other possible offset regions, which indicates the the proposed mechanism is well suited for the case of interest with signals at any frequency offset between wanted and interfering signal. For completely overlapping signals the possible improvement with this method vanishes, which is in line with expectations for the considered scenario of a single input system and an equally powered signal and interferer.

To address this problem of reduced performance under frequency overlapping conditions an additional effort is required in the form of a spatial filtering step (LPP) and/or joint decoding of the signals. These aspects are addressed in the sequel of this thesis.

The impact of symbol timing ratios was investigated and is illustrated in Figure 4.4. For a given block size of symbols of the wanted signal N_s, the symbol timing ratio T_i/T_s was changed. It can be noticed that the proposed mechanism works better for a higher ratio, which corresponds to a slower interferer compared to the wanted signal.

[1] CIR represents the signal to interference ratio.

Synchronization Impact

The influence of timing and phase synchronization errors on the performance of the MMSE mechanism has been verified. The timing synchronization error is assumed to be a Gaussian random variable with a given mean around the ideal symbol detection timing epoch ϵ. For the phase noise a Gaussian random variable was assumed in a first approach and the mask proposed in the DVB-S2 standard [ETS05a] was considered as a second step.

The figure 4.5 illustrates the impact of the timing error on the detection performance for a signal to noise ratio of $\frac{E_b}{N_0} = 6$dB and a very small frequency offset. For a symbol timing error variance of 0.1, a significant performance degradation is experienced. Consequently a good symbol synchronization, with a symbol timing standard deviation significantly better than 0.1 is required for the mechanism to work well.

The phase synchronization performance is depicted on figure 4.6. Also in this case, a significant degradation can be experienced when a phase noise is assumed to exceed $\frac{\pi}{16}$.

Note that in practice the phase will typically be tracked by a closed-loop synchronization mechanism at the receiver. However an acquisition of the phase is necessary for the tracking system to lock under the considered interference conditions. To assess specifically the impact of the phase error on the detection performance result no additional phase tracking system has been assumed in this context.

The phase noise mask recommended in the DVB-S2 standard [ETS05a] has been used to generate worst case phase noise scenarios. The figure 4.7 illustrates the performance of the MMSE method when the worst case phase noise mask is applied. In the region of interest $\frac{E_b}{N_0} = 6$ to 7 dB, a considerable degradation can be observed from the optimal possible performance. This underlines the sensitivity of the considered mechanism with respect to synchronization performance.

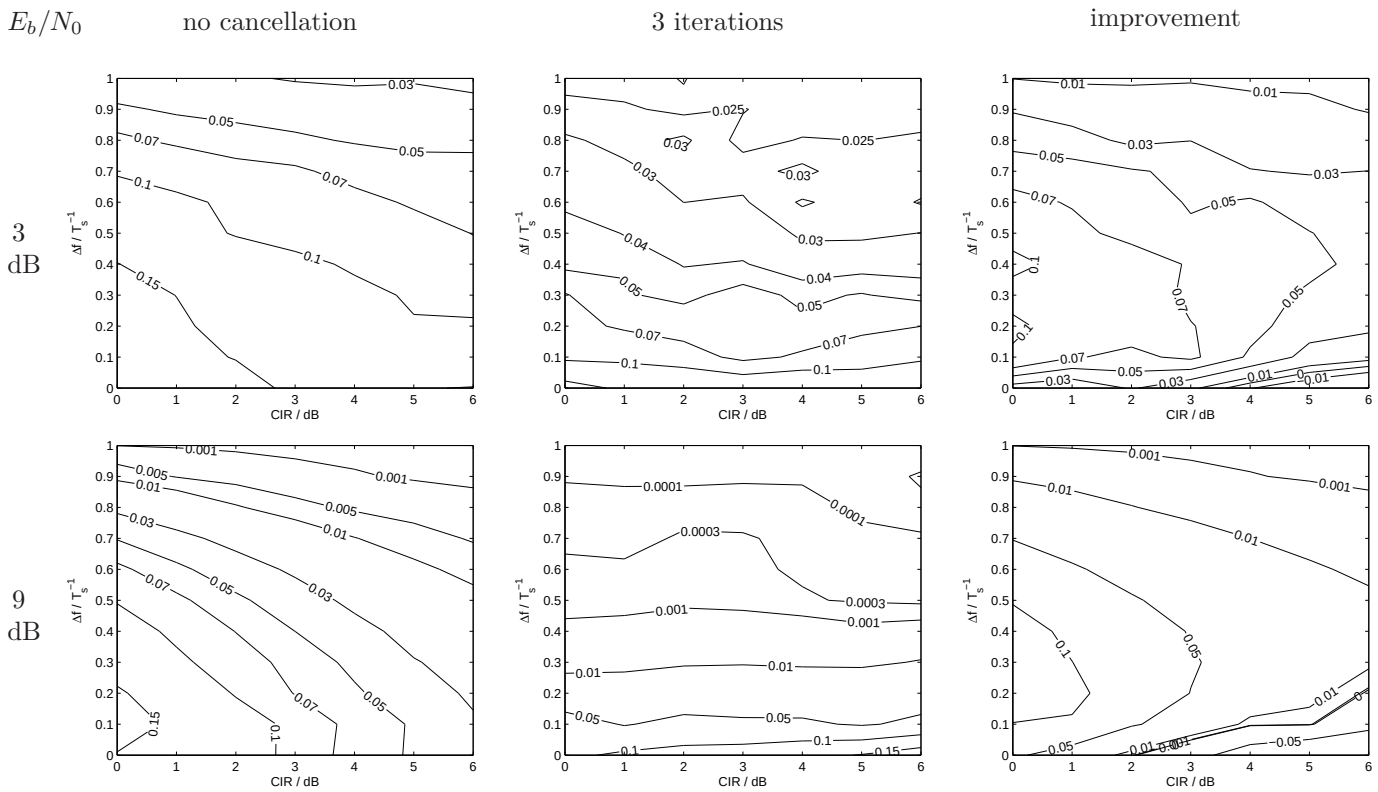

Table 4.1: BER results without interference cancellation, after 3 iterations and the related improvement in terms of BER. The results are plotted as countour plots of BER with respect to signal to interference power density ratio (CIR) in dB and relative frequency offset $\Delta f/T_S^{-1}$. Note that here CIR is the ratio of the power densities E_S/E_i as illustrated on Figure 4.1. The results are plotted for a signal to noise ratio (relative to the wanted signal) Eb/N_0 of 3dB (top row) and 9dB (bottom row). The *improvement* column illustrates the regions where the maximal possible gain is achieved and where the method fails to provide gain (negative values).

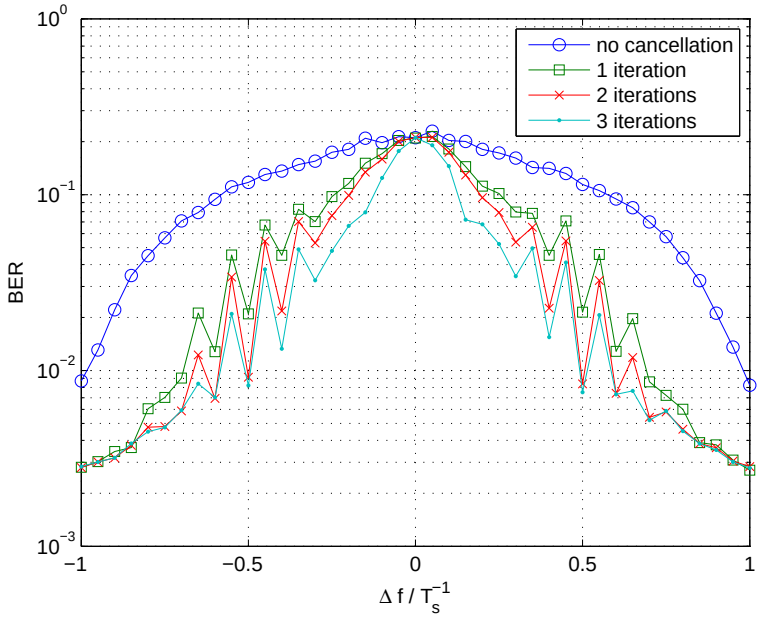

Figure 4.3: Bit Error Rate (BER) performance as a function of the frequency offset Δf for 0 to 3 iterations. The wanted and the interfering signals have equal power density levels. The performance with *no cancellation* is compared to the soft-decision method proposed for 1, 2 and 3 iterations.

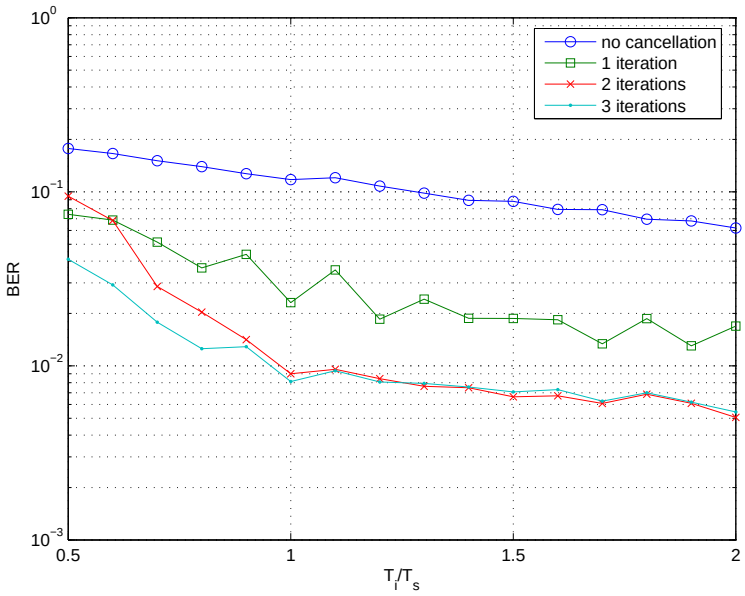

Figure 4.4: Bit Error Rate (BER) performance for different symbol timing ratios T_i/T_s between interferer and wanted signal. $E_b/N_0 = 6$dB. Equal power is assumed for the wanted signal and interferer. A frequency offset Δf of 0.5× Symbol Rate T_S^{-1} is assumed here and equal power density levels of wanted signal and interferer. The relative timing offset is illustrated on Figure 4.2. The resulting performance for *no cancellation* is compared to the proposed soft-decision based iterative procedure for 1, 2 and 3 iterations.

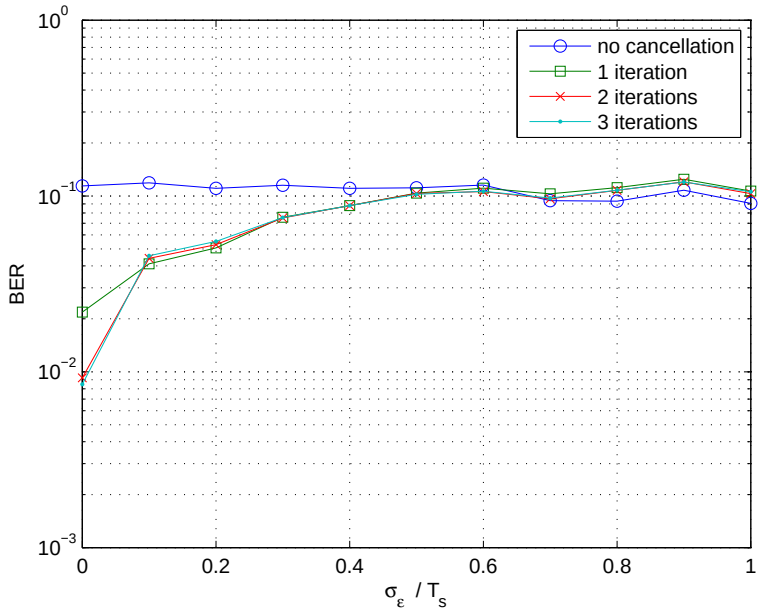

Figure 4.5: Bit Error Rate (BER) performance as a function of timing error relative standard deviation. The performance of the proposed soft-decision based iterative system is compared to the case of no interference cancellation. The main signal and the interferer are assumed at the same power level. The frequency offset Δf is 0.5× Symbol Rate.

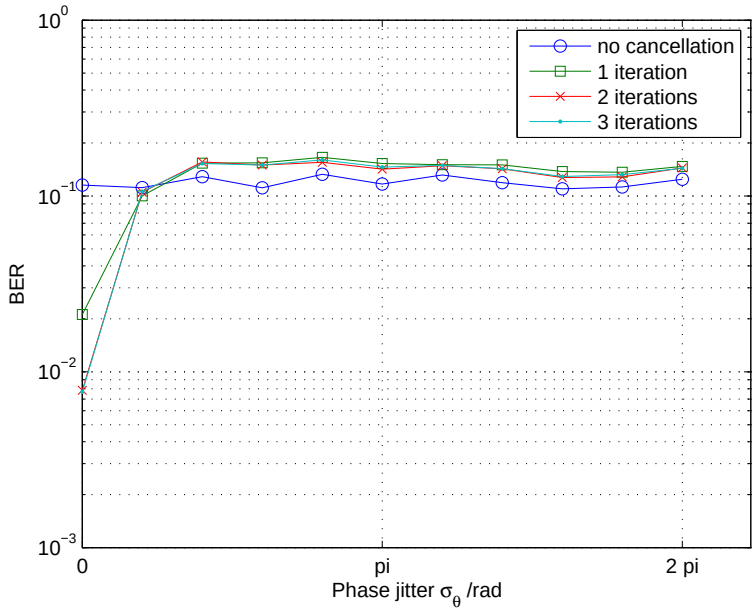

Figure 4.6: Bit Error Rate (BER) as a function of the assumed phase noise standard deviation. The power levels of the main signal and the interferer are assumed the same. The frequency offset Δf is fixed to 0.5× Symbol Rate. The performance of the proposed soft-decision based iterative interference cancellation procedure is compared to the case of *no cancellation*.

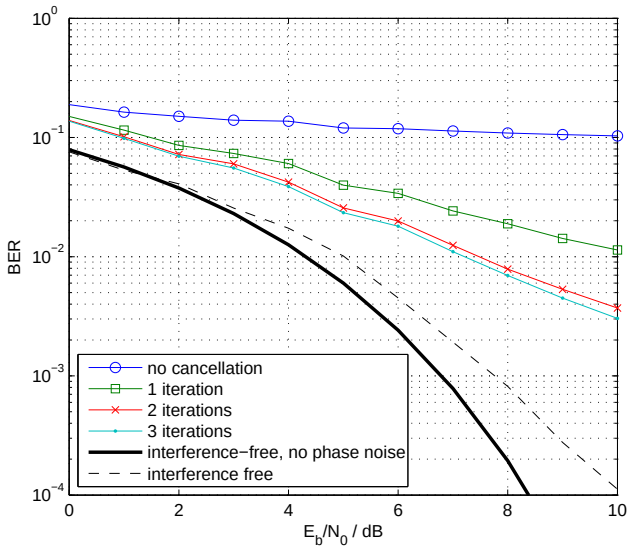

Figure 4.7: Bit error rate (BER) performance for different E_b/N_0 ratios and for different iteration steps (0 to 3). As reference, the interference-free performance is also indicated. Phase noise according to the recommended mask in [ETS05a] was assumed. The frequency offset Δf has been fixed to 0.5× Symbol Rate and the power density levels of the wanted signal and interferer are the assumed the same.

4.3 Conclusion

In this chapter we have reviewed the soft-decision based interference processing approach proposed by Beidas at al. [BGK02] in the context of the introduced broadcast reception scenario. The main additional analysis that have been performed include the consideration of an arbitrary frequency offset between main signal and interferer, an arbitrary symbol rate of the interfering signal relative to the main signal as well as analysis of a number of nuisance parameters, including phase noise and timing jitter.
Simulation results have shown that the considered soft-decision based iterative interference processing is well suited also for broadcast reception scenarios as considered here. However the mechanism is sensitive in performance to synchronization errors and an accurate synchronization is required to achieve the full potential of improvement possible with this approach. The synchronization problem is subsequently studied in Chapter 7 and 8.

Chapter 5

Spatio-Temporal Interference Processing

5.1 Introduction

Since the considered receiver system is assumed overloaded, a nonlinear multiuser detection receiver is proposed in this chapter. A joint spatio-temporal iterative procedure is developed for joint estimation and detection. Based on iterative least squares with projection (ILSP), a soft-decision based iterative detection system is derived from the signal model and detection problem introduced in Chapter 2 proposed and analyzed in performance for the considered reception scenarios.
Note that we refer in this Chapter also to the same formalism introduced in Chapters 2 and 3.
An overloaded system is assumed in the context of this chapter. It has been shown in Chapter 3 that for overloaded systems ($N_C > M$) the LPP spatial filtering step is not sufficient. Here, an additional temporal filtering is proposed in conjunction with the spatial filtering step.

5.2 Interference Cancellation Step

ILSP method

The estimate of the weighting factors $\mathbf{T}$, as defined for (3.6), can be computed directly from the expression (2.21), assuming that an estimate of $\hat{\tilde{\mathbf{d}}}[N]$ is known:

$$\hat{\mathbf{T}} = \mathbf{G}^{\dagger}\mathbf{p}[N]\hat{\tilde{\mathbf{d}}}[N]^{\dagger}\mathbf{S}^{\dagger} \tag{5.1}$$

In a similar manner, for a given estimate of $\hat{\mathbf{T}}$ the symbol sequence estimate $\hat{\tilde{\mathbf{d}}}[N]$ can be extracted linearly from the problem (2.21) or (7.1) respectively:

$$\hat{\tilde{\mathbf{d}}}[N] = \mathbf{S}^{\dagger}\hat{\mathbf{T}}^{\dagger}\mathbf{G}^{\dagger}\mathbf{p}[N] \tag{5.2}$$

The iterative procedure to sequentially compute a novel estimate for $\mathbf{T}$ and then for $\mathbf{d}$ leads to the well known iterative least square with projection ILSP method, as introduced in [TPV96] and [TPV97]. This principle is the basis for the subsequent proposed method, which extends the ILSP method and improves its performance for the considered problems by replacing the second step (5.2) by a successive interference cancellation (SIC) step as improved symbol estimation procedure, as detailed in the subsequent Section 5.2. Note that initial estimates are required for the ILSP method to initialize the iterative estimation over $\hat{\mathbf{T}}$ and $\hat{\bar{\mathbf{d}}}$.

The authors of [TPV96] and [TPV97] also introduce an improved method with a subsequent enumeration step (ILSE). This approach is however not feasible in the considered scenario since the set of symbol choices to enumerate grows exponentially with the number of symbols considered in one sequence. The temporal spread of the inter symbol interference makes the full enumeration intractable. Instead of the enumeration step, a soft-decision based interference cancellation step is considered as alternative which is of tractable complexity.

Using this formalism, a soft-decision based interference processing approaches is derived in the sequel.

Turbo SIC step, (SIC step)

Based on the minimization of the mean square error, soft-decision based techniques have been derived in previous work, e.g. [WP99], [BGK02], [KVKM07].
Wang, [WP99], has described the iterative soft-decision based approach to determine the soft decision estimate $\hat{\bar{\mathbf{d}}}[N]$ of $\bar{\mathbf{d}}[N]$ in the expression (3.6). The present approach uses a similar method to efficiently solve the stated problem. From the cost function in (3.6) we can derive:

$$\mathbf{p}[N] = (\mathbf{G}_S + \mathbf{G}_I)\mathbf{TS}\hat{\bar{\mathbf{d}}}[N] \tag{5.3}$$

Here, $\mathbf{G} = \mathbf{G}_S + \mathbf{G}_I$, where $\mathbf{G}_S$ consists of only the diagonal elements of $\mathbf{G}$ and $\mathbf{G}_I$ of all the off-diagonal elements, which represents the interference impact from neighboring symbols in time and frequency.

Then, using the Jacobian method to solve linear systems of equations, an iterative symbol estimation method can be derived from (5.3). The iteration updates can be expressed for the ith step as:

$$\hat{\bar{\mathbf{d}}}_i[N] = \mathbf{G}_S^{-1}\big(\mathbf{p}[N] - \mathbf{G}_I\mathbf{TS}\hat{\bar{\mathbf{d}}}_{i-1}[N]\big) \tag{5.4}$$

Observing furthermore that the diagonal elements of $\mathbf{G}$ are close to 1, we can simplify (5.4) using the approximation $\mathbf{F}_S \approx \mathbf{I}$:

$$\hat{\bar{\mathbf{d}}}_i[N] \approx \mathbf{p}[N] - \mathbf{G}_I\mathbf{TS}\hat{\bar{\mathbf{d}}}_{i-1}[N] \tag{5.5}$$

The index i denotes the iteration step. Note that a similar related approximation approach has been considered by Beidas (et al.) in [BGK02] for an MF-TDMA

multi-user access system via satellite. The expression 5.5 includes the spatial processing parameters and has been conditioned to the specific problem of overloaded systems, as derived in Chapter 2.

Improved Joint LPP-SIC step

Based on the ILSP method outlined in Section 5.2 here above, the SIC step introduced in the previous section is used to estimate the data sequence $\hat{\tilde{\mathbf{d}}}[N]$ in combination with the update of the weighting factor. In addition, the weighting factor used in the LPP step is updated iteratively in accordance with the iterative ILSP steps. The weighting to determine $\hat{\mathbf{p}}$ is defined as $\mathbf{W}_1$. The weighting factor for the data sequence is defined as $\mathbf{W}_2$, (3.4).

For the subsequent processing the joint weighting factor $\mathbf{W}_1$ is used to compute $\hat{\mathbf{q}}$ and the weighting for best signal-to-noise-and-interference ratio (SNIR), $\mathbf{W}_2$, is used to determine $\hat{\tilde{\mathbf{d}}}_i[N]$ for each iterative step in (5.5). This improves the gain on the main wanted signal for $\hat{\mathbf{p}}$ while iterating on the best data estimates for both wanted signal and interferer.

The SIC procedure described in Section 5.2 is repeated iteratively leading to a symbol sequence estimation $\hat{\tilde{\mathbf{d}}}[N]$ that is used in (5.1) to update the weighting matrix $\mathbf{W}_2$. This approach is similar to the ILSP as outlined in Section 5.2 with the exception that the hard-decision based symbol estimation (5.2) is replaced by the improved soft-decision based iterative SIC procedure as described above. A hard-decision is applied to the symbol sequence $\hat{\tilde{\mathbf{d}}}[N]$ before it is used in (5.1) to estimate the weighting factors $\mathbf{W}_2$.

The proposed improved joint LPP-SIC method can be summarized in the following steps (k is the iteration index):

1. Initialize estimates of $\mathbf{W}_1$ and $\mathbf{W}_2$ obtained from the generalized eigenvalue problems in (3.3) and (3.4) or from values stored in the memory. The covariance matrices $\mathbf{R}$, $\mathbf{R}^{\mathbf{d}}$, $\mathbf{R}_j^d$ are obtained from $\mathbf{R}_n$, $\mathbf{A}^d$, $E\{\mathbf{s}^d(t)\mathbf{s}^{d*}(t)\}$, which are assumed known or measurable.

2. Iterate with iteration index i over the SIC step defined in (5.5) with the weighting matrices $\mathbf{W}_1$ for $\hat{\mathbf{p}} = \mathbf{G}(\mathbf{W}_1)\mathbf{S}\hat{\tilde{\mathbf{d}}}[N] + \bar{\mathbf{n}}[N]$, using (3.5) and $\mathbf{W}_{2,k}$ for $\mathbf{T} = \mathbf{V} \otimes \mathbf{I}_{N_d^2} \approx (\mathbf{W}_{2,k}^* \mathbf{A}^d) \otimes \mathbf{I}_{N_d^2}$. Stop iteration if maximal number of iterations is reached or if the SNIR estimate on $\hat{\tilde{\mathbf{d}}}_i[N]$ does not yield and improvement anymore.

3. Take hard-decision estimates of the symbol sequence outcome from the SIC steps $\hat{\tilde{\mathbf{d}}}_i[N]$ based on the result of the iterative SIC steps, (5.5).

4. Refine the weighting matrix estimation $\mathbf{W}_{2,k+1}$ with the estimated symbol sequence and using (5.1) and $\mathbf{T} \approx (\mathbf{W}_{2,k+1}^* \mathbf{A}^d) \otimes \mathbf{I}_{N_d^2}$.

5. Increment iteration index k and repeat from step 2 onwards as long as a SNIR improvement can be measured, based on the SNIR estimate as defined in the cost function of the expression (3.4).

The initial rough estimates are defined during the installation procedure of the receiver. An SNIR based scanning mechanism can be used to tune to the best possible initial weighting matrix. The updated, improved weighting matrices $\mathbf{W}_1$ and $\mathbf{W}_2$ can be stored in memory and serve as initial estimates for future tuning processes.

Note that the stopping criterion is an important part of the iterative technique. Indeed, it has been shown by previous work, see [MFRC07], that a joint iterative technique on overloaded systems with a linear first step tends to amplify noise after an optimal number of iterations. For similar reasons this problem has also been observed with the proposed method. An improvement measure after each iteration helps control the mechanism and prevents the noise amplification effect. In practice the optimal number of iterations depends on the number of interferers considered and the number of input elements, M. Typically the system reaches the best possible improvement after 2 to 5 iterations.

5.3 Simulation Results, Detection Performance

We assess the performance of overloaded systems using a simulation environment that allows to model the antenna front-end with M elements and combine it with a joint LPP-SIC iterative detection step, as outlined in Section 5.2. For that purpose we assume in the context of these numerical evaluations $M = 2$ input elements in an environment of $N_C = 3$ signals, one wanted signal and two interferer on either of the wanted signal.

Figure 5.1 illustrates the antenna pattern of a dual input LNB system with a 35cm parabolic reflector. The antenna size varies over the simulation runs but if not otherwise stated, the spacing of the LNB elements is fixed so that the beam element gain patterns overlap at the -3dB from maximal gain. Using this antenna pattern characteristic, the performance of the interference processing system depends on the resulting signal to noise and interference ratios (SNIR) for an assumed pointing direction.
The filter impulse response length was set to 12 symbol periods and the Rolloff factor to 35%. The processing block length N_d has been configured for 12 symbols, taking into account all significant inter-symbol interferences.

The SNIR at the output of the LPP step is displayed in Figure 5.2 together with the reference performance without LPP. A minimum SNIR of 6dB can be guaranteed between -3 and $+3$ degrees pointing offset when LPP is used. In a similar manner, the adjacent interference signal can be received with a minimal SNIR,

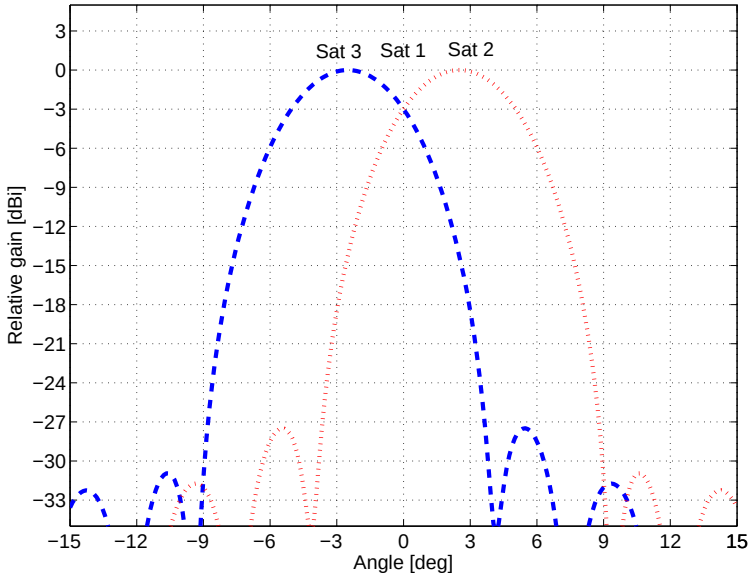

Figure 5.1: Example antenna pattern plot: Dual LNB front-end and a 35cm parabolic reflector antenna and LNB input elements spaced such that the gain patterns intersect at -3dB. The satellite directions assumed are marked. We assume a wanted signal on satellite 1 and interferers on the adjacent satellites.

which provides the adequate conditions for the joint LPP-SIC step to generate improvement in the detection process.

The joint LPP-SIC step performs well in the pointing angle offset region between -3 and $+3$ degrees, as illustrated in Figure 5.3 by the simulated SNIR ratios compared to the computed levels of the main signal ($j = 1$), using the SNIR expression as defined in (3.4). The proposed joint LPP-SIC scheme improves consistently the SNIR over a pointing angle range from -3 to $+3$ degrees. This illustrates well the pointing error robustness of the proposed scheme. The proposed joint LPP-SIC step provides an additional 2-3dB improvement over the separate use of LPP with a subsequent SIC step (one single iteration in the defined method in Section 5.2.

The bit error rate (BER) performance illustrated in Figures 5.4 and 5.7 for an overloaded scenario of one wanted signal at 0 deg offset and two interferers located at -3 and $+3$ degrees offset angle, assuming two input elements M. Here, the signals are assumed synchronized. The pointing error robustness is confirmed in the BER evaluation. An improvement is recorded for an aperture size between 15cm and 45cm and significant performance increase of one order of magnitude (10^{-1} to 10^{-2}) is achieved for an aperture size of 30cm, for this specific scenario.

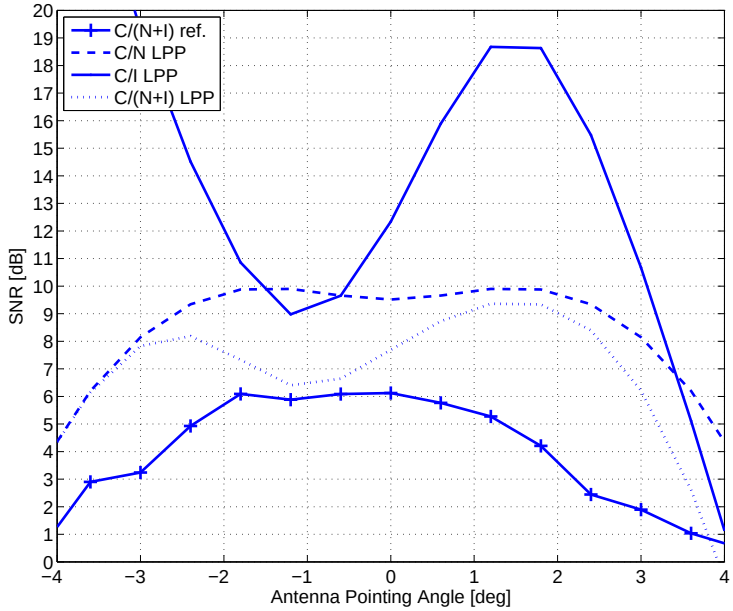

Figure 5.2: Signal to noise and interference ratios, SN(I)R, in dB over the antenna pointing angle for a 35cm antenna and computed after the LPP step and simulated without LPP (+), labeled *C/(N+I) ref.* All with an interferer at 0.5 x Symbol Rate ($\Delta f_2 = 0.5 \cdot R_S$) and at +3 degrees offset with the same power level. A two input element MLNB has been considered here. The reference performance *C/(N+I) ref* reflects a single input stream (left blue dashed pattern on Figure 5.1). The pointing offset is defined with the performance on Figure 5.1 as reference pointing direction. The achievable performance after the LPP step is indicated in terms of signal to noise ratio *C/N LPP*, signal to interference ratio *C/I LPP* and signal to noise and interference ratio *C/(N+I) LPP*.

Figure 5.7 compares also two possible MLNB configurations, one with a spacing of the elements fixed at the 3dB intersection point and one with a smaller element spacing at the 1dB intersection point of the antenna gain patterns. Due to the fact that a multiple input system is more sensitive in off-axis regions than a single input system and that the multi-input system is overloaded and cannot spatially filter the interference, the resulting performance can be worse than the reference system with a single input antenna.
Figures 5.6 and 5.5 illustrate the performance of the considered system over the pointing angle of the reception antenna. The proposed *Joint LPP-SIC* system is

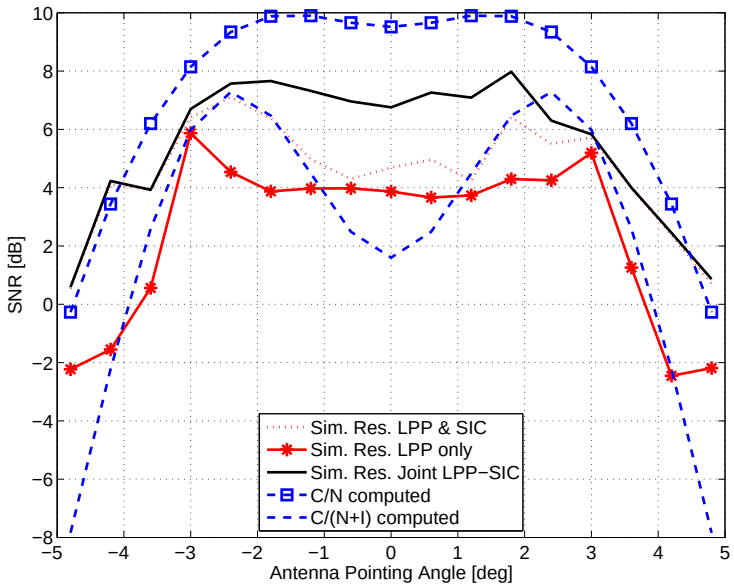

Figure 5.3: Signal to noise and interference ratios computed and simulated for assumed interferers with 0.5 x Symbol Rate frequency offset ($\Delta f_2 = 0.5 \cdot R_S$, $\Delta f_3 = -\Delta f_2$) and at +3 and -3 degrees offset with the same power level as the main signal and for a 40cm aperture antenna. The computed values labelled "C/N computed" and "C/(N+I) computed" were evaluated using the signal-to-noise ratio expression, see objective function of (3.4).

compared to the *Successive LPP & SIC* approach, which is a simple combination of the spatial filtering as described in Chapter 3 with the successive interference processing step as described in Chapter 4. The fact that the iterations of the *Joint LPP-SIC* reach over both the spatial and temporal parameters is the reason that the *Joint LPP-SIC* outperforms the *Successive LPP & SIC*.
Comparing the results of Figure 5.6 and 5.5 it can further be concluded that the element spacing of the MLNB has to be adapted to the interferer locations, which is also related to the fact the in overloaded systems the spatial filtering is not sufficient to suppress the interference impact.

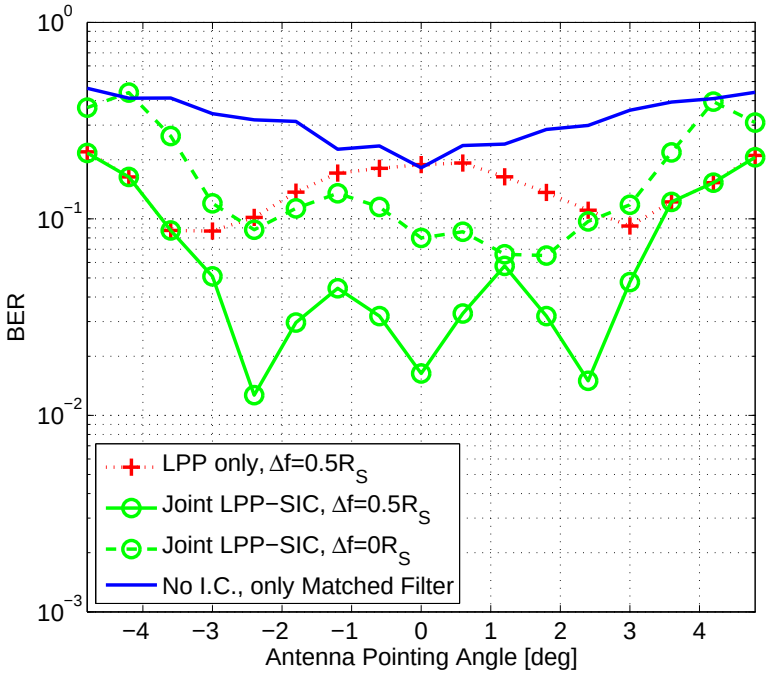

Figure 5.4: Bit error rate (BER) performance comparison of a 35cm dual-input antenna ($M = 2$) with two interferers spaced at +3 and -3 degrees offset, at the same power level as the main signal and one at a frequency offset of 0.5 x Symbol Rate R_S ($\Delta f_3 = 0.5 \cdot R_S$) and the second at co-channel $\Delta f_2 = 0 \cdot R_S$ (dashed-line) and staggered in frequency ($\Delta f_2 = 0.5 \cdot R_S$) (solid line).

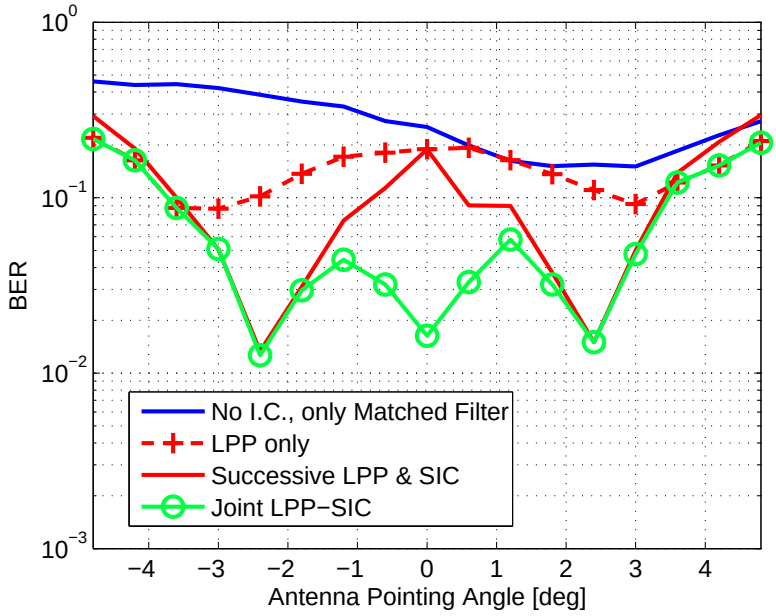

Figure 5.5: Bit error rate (BER) performance comparison of a 35cm dual-input antenna ($M = 2$) with the same configuration as for Figure 5.4 and with the two interferers at +3 and -3 degrees with a frequency offset of 0.5 x Symbol Rate R_S ($\Delta f_3 = 0.5 \cdot R_S$). The 'Joint LPP-SIC' method is compared to the 'Successive LPP & SIC'.

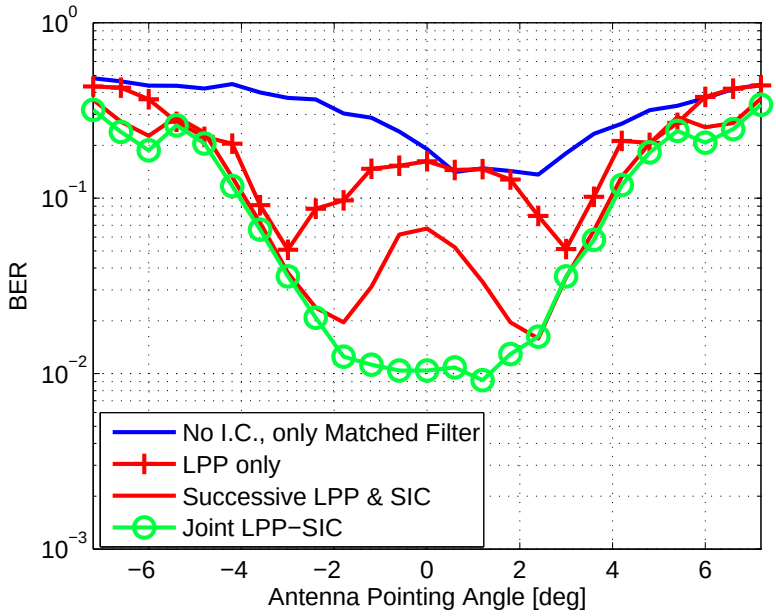

Figure 5.6: Bit error rate (BER) performance comparison of a 35cm dual-input antenna ($M = 2$) with the same configuration as Figure 5.4. The spacing between the two antenna elements is reduced to generate a gain-pattern crossing at 2dB instead of 3dB as for Figures 5.4 and 5.5.

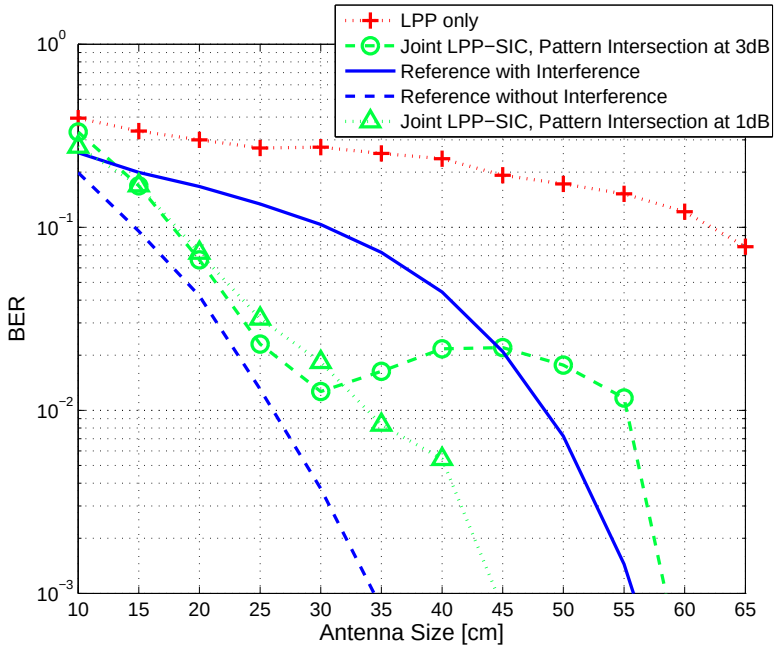

Figure 5.7: Bit error rate (BER) performance comparison of the proposed scheme (joint LPP-SIC) for different equivalent aperture sizes of the front-end. A dual input system ($M = 2$) receiving one wanted signal on-axis and two interferers at +3 degrees and -3 degrees offset with same signal power as the wanted signal are assumed. The interferers are assumed staggered in frequency at halve symbol rate R_S, $\Delta f_2 = 0.5 \cdot R_S$, $\Delta f_3 = -\Delta f_2$.

5.4 Conclusion

An interference tolerant and robust receiver front-end, designed to receive satellite broadcast signals from geostationary satellites under the presence of interference from adjacent satellites was presented. A multi-input antenna with linear pre-processing was introduced to condition the signals prior to the subsequent processing to achieve best possible performance. The proposed method helps minimize the required aperture of the reception antenna and provides a pointing error tolerant reception solution. Overloaded reception conditions were considered.
The performance of the proposed method was verified by simulation of a Ku-band based reception scenario. Common scenarios of fixed satellite systems in other frequency bands, C-band and Ka-band, were also considered with similar performance results (although not presented here because of space constraints).

Note that the spatial filtering is useable for any type of signal while the subsequent temporal interference cancellation step assumes continuous signals of the DVB-S or DVB-S2 [ETS05a] nature.

5.A Derivation of Mapping Matrix S

The mapping matrix $\mathbf{S}$ in the equation (2.17) is defined here below. We can develop equation (2.17) as follows:

$$\mathrm{vec}\{\mathbf{D}^T(t)\} = \mathrm{vec}\{[\mathbf{d}^d(t)\cdots\mathbf{d}^d(t-N_d+1)]^T\} \tag{5.6}$$

with $\mathbf{d}^d(t) = [\mathbf{d}_1(t)^T\cdots\mathbf{d}_M(t)^T]^T$. From the definition of $\bar{\mathbf{d}}(t)$ in equation (2.18), it follows that:

$$\bar{\mathbf{d}}(t) = [d_1(t)\cdots d_1(t-2N_d+2)\cdots d_M(t)\cdots d_M(t-2N_d+2)]^T \tag{5.7}$$

The $MN_d^2 \times M(2N_d-1)$ mapping matrix $\mathbf{S}$ is defined as:

$$\mathrm{vec}\{\mathbf{D}^T(t)\} = \mathbf{S}\bar{\mathbf{d}}(t) \tag{5.8}$$

We first introduce the $N_d^2 \times 2N_d - 1$ matrix $\mathbf{S}_C$, defined as follows:

$$\mathbf{S}_C = \begin{bmatrix} & \mathbf{I}_{N_d} & \mathbf{0}_{N_d\times(N_d-1)} \\ \mathbf{0}_{N_d\times 1} & \mathbf{I}_{N_d} & \mathbf{0}_{N_d\times(N_d-2)} \\ \vdots & & \vdots \\ \mathbf{0}_{N_d\times(N_d-2)} & \mathbf{I}_{N_d} & \mathbf{0}_{N_d\times 1} \\ \mathbf{0}_{N_d\times(N_d-1)} & \mathbf{I}_{N_d} & \end{bmatrix} \tag{5.9}$$

Here $\mathbf{I}_{N_d}$ is the $N_d \times N_d$ identity matrix and $\mathbf{0}_{a\times b}$ is a matrix containing only 0 elements in all entries and with dimension $a \times b$.

The $MN_d^2 \times M(2N_d - 1)$ mapping matrix $\mathbf{S}$ can then be defined as follows:

$$\mathbf{S} = \begin{bmatrix} \mathbf{S}_C & \mathbf{0}_{N_d^2 \times (2N_d-1)} & \cdots & \mathbf{0}_{N_d^2 \times (2N_d-1)} \\ \mathbf{0}_{N_d^2 \times (2N_d-1)} & \mathbf{S}_C & \cdots & \mathbf{0}_{N_d^2 \times (2N_d-1)} \\ \vdots & & \ddots & \vdots \\ \mathbf{0}_{N_d^2 \times (2N_d-1)} & \cdots & \mathbf{0}_{N_d^2 \times (2N_d-1)} & \mathbf{S}_C \end{bmatrix} \tag{5.10}$$

Chapter 6

Interference Processing with Decoding

6.1 Introduction

In this Chapter a channel decoding step is taken into account in a hard-decision based interference cancellation step and compared in performance to a conventional hard-decision based interference cancellation. The aim is to analyze the practicality and achievable gain of an additional decoding step within the interference processing broadcast scenario as discussed. For this purpose it is assumed that the interfering signal is compliant to a DVB-S [ETS98] signal. A convolutional inner code is foreseen in that standard, which is straightforward to decode using Viterbi decoding methods for example. In this context a dual input system is assumed.
In a second part the DVB-S2 decoding is considered in the framework of an interference processing step and the performance is assessed for a single input system and one dominating interferer.
The aim here is to make a first assessment of the potential of additional decoding steps in an interference cancellation loop.

6.2 Interference Cancellation with DVB-S Decoding

In this part a decoding based interference processing is analyzed. Based on known multi-user detection techniques, as outlined in Verdu [Ver98] or Hagerman [Hag95], decision directed interference cancellation is applied to successively subtract the unwanted signals from the desired base-band symbol sequence and consequently increasing the detection performance of the wanted signal. This signal processing technique will allow the requirements on the reflector size and/or on the RF performance of the dual-feed reception system to be reduced. Ideally, this can be integrated cheaply into a single box for mass market production. This means that digital signal processing in the receiver is traded for RF reception quality, which

should help reduce the pricing for consumer equipment.
Common used signal standards for satellite communications are DVB based transmission schemes and it is assumed here that the interference is DVB-S compliant. The inner channel coding of the DVB-S [ETS98] is a simple convolutional based forward error correcting (FEC) code with foreseen puncturing rates of 1/2, 2/3, 3/4, 5/6 and 7/8.
Based on the moderate complexity involved with convolutional decoding ,a decision based detection with subsequent decoding and remodulation step is considered. Similar to the hard-decision based interference cancellation approach proposed by Janssen [JS02], a nonlinear parallel detection step is complemented with a subsequent decoding and remodulation of the signal prior interference subtraction. Figure 6.1 illustrates the considered setup.

This DVB-S based hard-decision interference cancellation has been a first assessment of the potential gains of decoding based interference mitigation. The presented approach is suboptimal but has the considerable practical advantage that a conventional decoding step is used with moderate complexity.

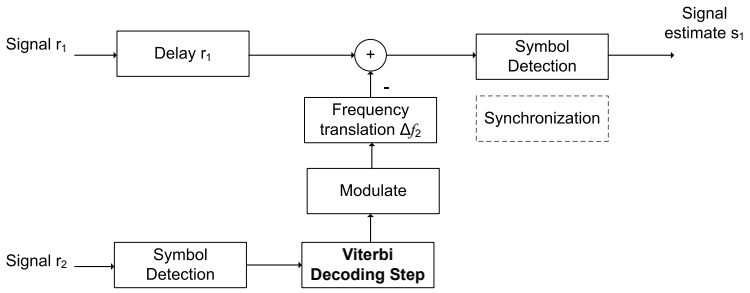

Figure 6.1: Functional system overview of the considered interference processing receiver. A receiver for $r_1(t)$ is tuned to receive the wanted signal $s_1(t)$, whereas a receiver for $r_2(t)$ is tuned to receive the main interfering signal $s_2(t)$. The main interfering signal is detected and decoded to allow a subtractive correction of the received signal $r_1(t)$.

A wanted signal $s_1(t)$ is interfered by one main dominating interferer $s_2(t)$. The interferer is assumed a DVB-S compliant signal. The received signal $r_1(t)$ is assumed configured for spatial selection of signal $s_1(t)$, while $r_2(t)$ is set for the reception of the main interferer $s_2(t)$. After a hard-decision symbol detection step, a conventional Viterbi decoding of the inner code is used to reconstruct the bit

sequence of s_2. The Viterbi decoding uses a sliding window size of 10 symbols. The reconstructed signal $s_2(t)$ is adjusted in amplitude, phase ϕ_2 and frequency Δf_2 and then subtracted from the received signal of the wanted signal and interferer.
The synchronization step has to adjust the frequency offset Δf_2, the signal delay and symbol timing. The task is simplified by the fact that the interference situation is static and is changing only slowly over time.
For numerical evaluations one signal of interest is assumed and a maximum of one simultaneous interferer. In general the interferer can be at different center frequencies, symbol rates and signal power levels compared to the main signal of interest. Synchronization in frequency and symbol timing has to be achieved on both the wanted signal and the main interferer. For the wanted signal, it is assumed that typical linear modulation with common broadcast parameters are used, such as QPSK or 8-PSK in combination with square root raised cosine filtering (SRRCF) at the transmitter and at the receiver.
As a baseline for performance comparison, the following Figure 6.2 illustrates the symbol error rate (SER) performance of the considered hard-decision based interference cancellation at detection level without the decoding step and for signal to noise and interference to noise levels that are well reachable by the first LPP step as described in Section 3.3. A marginal improvement is achieved for signal to noise ratios below 10dB, while a significant improvement is reached only for higher signal to noise ratios of 12dB and for high signal to interference ratios. This is in accordance with the expected suboptimal performance of hard-decision based interference processing.

The use of the decoding step as outlined above has been considered in the Figure 6.3. The use of a decoding step increases considerably the interference mitigation performance for lower signal to interference ratios (C/I) and lower signal to noise ratios (C/N).

Considering that typically 10^{-2} to 10^{-3} is considered as target symbol error rate detection performance prior to decoding, depending on the code rate used. To reach 10^{-2} SER a significant C/I level has to be reached by the front-end of the reception system, the requirements on which can be significantly reduced with the introduction of SIC as illustrated in Figure 6.3.

6.3 Interference Cancellation with DVB-S2 Decoding

In the context of joint work in collaboration with *Space Engineering S.p.A.* [GG07] [CGG08], the context of DVB-S2 based reception has been considered and the use of LDPC based decoding step within the interference cancellation has been evaluated. DVB-S2 frames with a predefined modulation and coding rate have been evaluated in different reception scenarios.

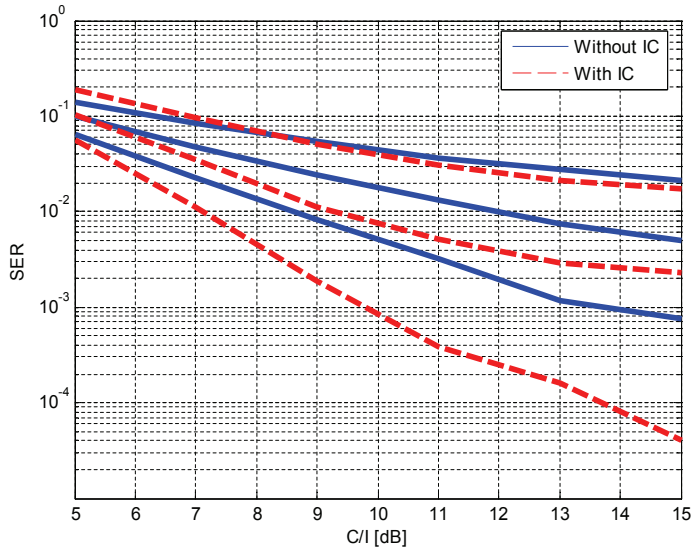

Figure 6.2: Detection performance as Symbol Error Rate (SER) versus C/I levels for different C/N levels assumed. C/N ranges assumed (from top to bottom curves) are 8, 10 and 12 dB. The signals were assumed fully overlapping in frequency $\Delta f_2 = 0$ and the wanted signal is a QPSK here. The reference case without interference suppression (blue solid line) is compared to hard-decision based interference cancellation at detection level (red dashed line).

In the context of this evaluation a single port antenna system has been assumed. The evaluation has been done for staggered signals at the same power density level and for unbalanced signals with 3dB power unbalance. The DVB-S2 decoding step is based on the defined frame structure and the results illustrate the bit error rate after decoding as well as the frame error rate after decoding (FER). The DVB-S2 based LDPC decoding step is used in an iterative interference cancellation (IIC) step as outlined in Chapter 4.
Figure 6.4 illustrates results based on a single input antenna system and two signals staggered in frequency. The results are based on considering LDPC decoding in the interference cancellation step. For comparison, the quasi error free (QEF) performance for QPSK 1/2 is reported in [ETS05a] to be close to $E_S/N_0 = 1.00$dB and for QPSK 3/4 around $E_S/N_0 = 4.03$dB.
It is interesting to note that these results are in principle in line with the results of Chapter 4, which also reported single input antenna results. Specifically the

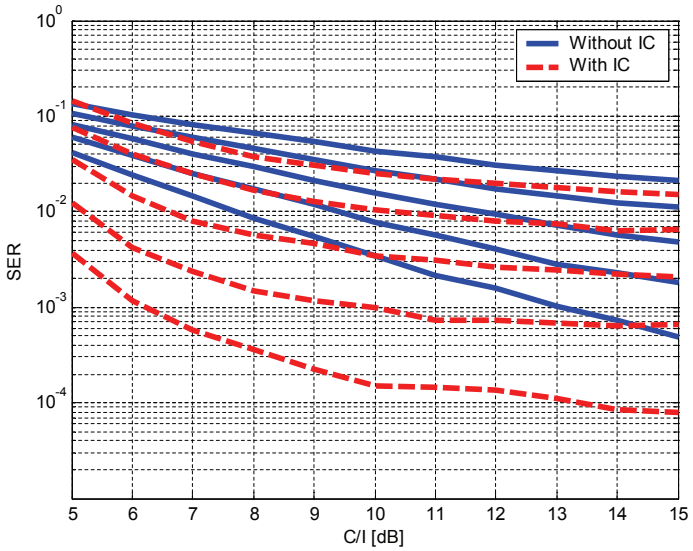

Figure 6.3: Detection performance with additional decoding (1/2 puncturing rate) for different C/N levels ranging from 8, 9, 10, 11 and 12 dB (curves from top to bottom), with and without I.C. The signals are fully overlapping in frequency $\Delta f_2 = 0$ and the wanted signal is QPSK. The reference performance without interference cancellation (blue solid line) is compared to the considered interference processing with decoding of the interfering signal (red dashed line).

performance sensitivity to frequency overlapping signals is of interest. Indeed for fully overlapping signals it is only possible under specific high enough power unbalance conditions to recover the strongest or both signals, depending on the noise floor also. A possible combination with the proposed spatial filtering as defined in Chapter 3 provides the required additional flexibility to adjust the power unbalance at the interference processing input.

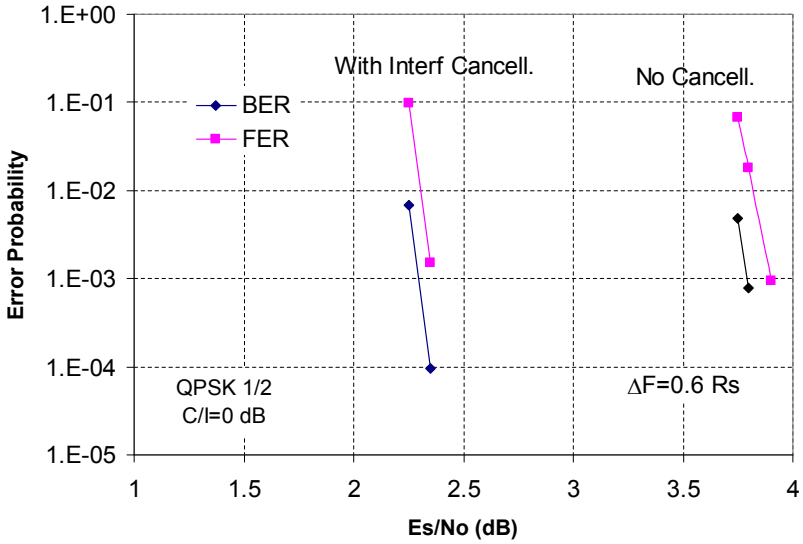

Figure 6.4: Performance comparison of DVB-S2 based interference cancellation steps for QPSK 1/2. The signals are assumed staggered in frequency $\Delta f = 0.6 \cdot R_S$ and the signals are assumed balanced in power density. The reference signal performance without interference cancellation is also measured at the LDPC decoding output. The bit error rate (BER) as well as the frame error rate (FER) are shown as result.

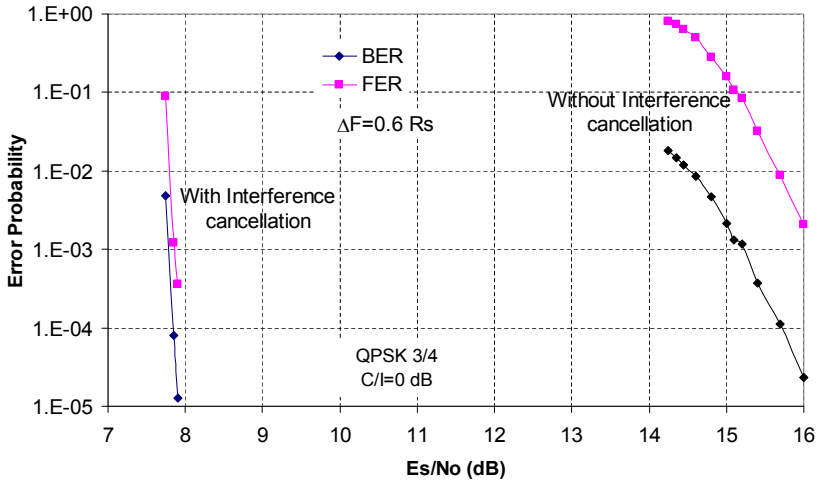

Figure 6.5: Performance comparison of DVB-S2 based interference cancellation steps for QPSK 3/4. The signals are assumed staggered in frequency $\Delta f = 0.6 \cdot R_S$ and the signal power densities are assumed equal. As comparison basis the reference performance is without interference cancellation and only using LDPC decoding after the wanted signal. The bit error rate (BER) as well as the frame error rate (FER) are shown as result.

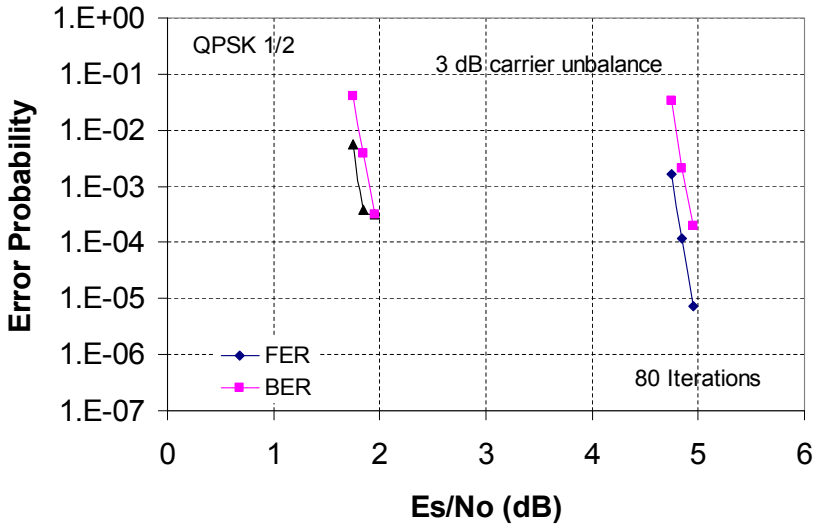

Figure 6.6: Performance comparison of DVB-S2 based interference cancellation steps for QPSK 1/2. Here the carriers are assumed on the same frequency and an unbalance in power density of 3dB is assumed. Both the bit error rate (BER) as well as the frame error rate (FER) are shown. The results on the left (BER and FER) illustrate the performance of the wanted signal, which has a 3dB higher power density level as the considered interferer. The interferer performance after the interference cancellation step are the two curves (BER and FER) on the right.

6.4 Conclusion

The use of DVB-S based convolutional decoding step has been considered in this chapter to verify the achievable gain compared to an interference processing step at detection level. A DVB-S based inner FEC has been decoded prior reconstruction and subtraction of the interfering signal. A significant gain is achieved from a certain signal to noise and signal to interference ratio on that is achievable with an LPP based front-end as outlined in Chapter 3 to condition the signal and interferer prior this interference cancellation step.
Furthermore DVB-S2 based LDPC decoding has been considered in conjunction with a iterative interference cancellation as defined in Chapter 4. The results illustrate that a significant gain is achieved as long as one of the signals (wanted signal or interferer) is decoded well and the signal to noise level is high enough. A more detailed outline of these results is reported in [GG07].
A single port antenna has been used for these evaluations. A possible combination with the considered spatial filtering as defined in Chapter 3 is however straightforward.
An obvious next step is the joint decoding of the wanted signal and the interferer, see for example [Ras08] [BC02]. An important additional problem that has to be addressed in the framework of this scenario is the relative synchronization between the wanted signal and the interferer.

Chapter 7

Synchronization in Broadcast Systems

7.1 Introduction

In this chapter the required synchronization steps at frequency estimation and symbol timing level are included in the presented interference processing method as defined in Chapter 5. The synchronization method presented is based on the detailed outline for broadband synchronization in the next Chapter 8. For this part specifically, it is assumed that the interference signals are DVB-S2 compliant and that the pilot sequence is used, which is optional in the standard. Based on this defined sequence, a joint frequency and timing data-aided (DA) synchronization method is proposed that is based on the extension of the iterative Joint LPP-SIC method presented in the previous Chapter 5.
Note that this chpater builds upon the same mathematical notation than Chapters 2, 3 and 5.

7.2 Joint Interference Processing and Synchronization

The proposed interference processing methods in Chapter 5 work on detection level and require adequate timing and frequency synchronization to perform well. The synchronization parameters $\boldsymbol{\theta}$ enter nonlinearly into the general considered minimization problem (7.1).
A related problem of jointly synchronizing to symbol level timing and frequency and symbol detection has been studied in [GOK07] for satellite multiuser systems. A data-aided two step approach was considered which relies on first rough estimates of timing and frequency offsets on a symbol level and second refined estimate consisting of a Gauss-Newton step on the derived maximum likelihood (ML) expression of the joint synchronization problem.
A similar synchronization approach is considered here. A DVB-S2 based pilot se-

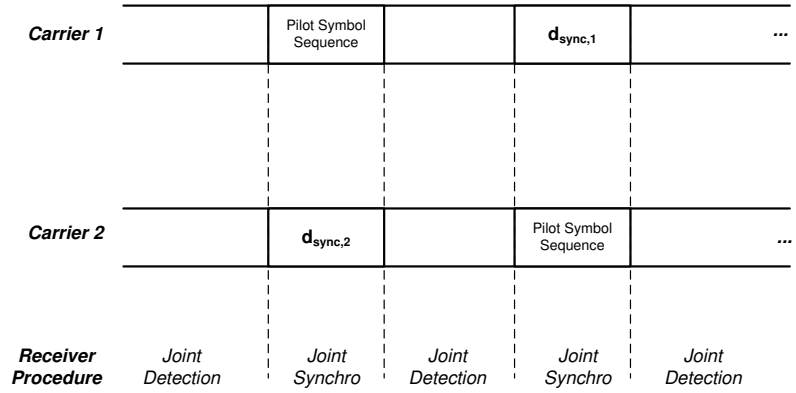

Figure 7.1: Outline of regular joint synchronization steps using regular pilot sequences in main signal (carrier 1) and main interferer (carrier 2).

quence is assumed to be present on the main signal and interferer. This implies a predefined 36 symbol sequence at regular intervals, according to physical layer framing in the specification [ETS05a], every 16 slots.

A joint synchronization processing procedure is proposed for the main signal and interference. For that purpose, we combine the frequency offsets, which include the frequency inaccuracies in a $M \times 1$ vector $\Delta\mathbf{f} = [\Delta f_1 \dots \Delta f_M]^T$ and the unknown signal phases in the $M \times 1$ vector $\boldsymbol{\phi} = [\phi_1 \dots \phi_M]^T$. The $2M \times 1$ vector with nuisance parameters is denoted $\boldsymbol{\theta} = \left[\boldsymbol{\phi}^T \ \Delta\mathbf{f}^T\right]^T$.

7.3 Synchronization Problem Formulation

The detection problem defined in Chapter 2 is the basis for this part. The detection problem (2.21) requires prior frequency and symbol timing synchronization. This synchronization is crucial in practice but can be incorporated in the optimization step as formulated above.

Based on the expression (2.21), the general joint detection and temporal and spatial filtering problem can be formulated as:

$$[\hat{\mathbf{W}}, \hat{\bar{\mathbf{d}}}] = \arg \min_{\mathbf{W},\boldsymbol{\theta},\bar{\mathbf{a}}[N] \in \boldsymbol{\Omega}^{M(2N_d-1)\times N}} ||\mathbf{p}[N] - \mathbf{G}(\mathbf{W},\boldsymbol{\theta})\mathbf{S}\bar{\mathbf{d}}[N]||_F^2 \qquad (7.1)$$

where $\mathbf{G}(\mathbf{W},\boldsymbol{\theta}) = \mathbf{G}^{RX}[\mathbf{W}^{*}\mathbf{A}^{d}\mathbf{G}^{TX,d}(\boldsymbol{\theta}) \otimes \mathbf{I}_{N_d}]$. The optimal symbol sequence detection of the sequences of the M carriers $\bar{\mathbf{d}}$, constrained to the constellation points (generally QPSK) in the set $\boldsymbol{\Omega}$, is of main interest. The additional spatial degrees of freedom in $\mathbf{W}$ can further be exploited for the detection of $\bar{\mathbf{d}}$.

The fact that the cost function in (7.1) has many local minima as a function of $\boldsymbol{\theta}$ and that the symbol sequence $\bar{\mathbf{d}}$ is constrained to the discrete set of constellation points $\boldsymbol{\Omega}$ makes the optimal solution to the problem intractable in its general formulation. Reduced complexity simplified approaches suitable for the considered problem are presented in Section 7.2. A suboptimal joint detection and synchronization method is presented in the sequel that outperforms the separate synchronization and detection procedures.

In a similar manner the synchronization can be included in the LPP optimization process as derived in Chapter 3.3 and using the expressions (2.6), the expression (7.1) becomes:

$$[\hat{\mathbf{T}},\hat{\bar{\mathbf{d}}}] = \arg \min_{\boldsymbol{\theta},\mathbf{T},\bar{\mathbf{d}}[N]\in\boldsymbol{\Omega}^{M(2N_d-1)\times N}} ||\mathbf{p}[N] - \mathbf{G}(\boldsymbol{\theta})\mathbf{T}\mathbf{S}\bar{\mathbf{d}}[N]||_F^2 \tag{7.2}$$

The pilot sequence of the main sequence is interfered by an arbitrary data sequence on the interfering neighboring signals, see outline in Figure 7.1. Using the hard-decision based symbol estimates $\hat{\bar{\mathbf{d}}}$ on all considered M carriers of the detected sequence after the LPP step, $\hat{\mathbf{q}}$, on the interferers, the synchronization mechanism refines the frequency offset estimation. The derived synchronization problem from (7.1) can then be expressed as follows:

$$\hat{\boldsymbol{\theta}} = \arg\min_{\boldsymbol{\theta}} ||\mathbf{p}[N] - \mathbf{G}(\boldsymbol{\theta})\hat{\mathbf{T}}\mathbf{S}\hat{\bar{\mathbf{d}}}[N]||_F^2 \tag{7.3}$$

A synchronization step is triggered by the arrival of a pilot sequence on the main signal or interferer, on j-th signal and the frequency estimation is refined using a first tentative estimate, e.g. the Luise & Reggiannini (L&R) frequency estimation method [LR95] and a second step of a single Gauss-Newton step to refine the search based on the cost function defined in (7.3). Note that the j-th row in $\hat{\bar{\mathbf{d}}}$ corresponds to the pilot sequence.

This synchronization step can be well integrated in the iterative Joint LPP-SIC steps defined, after iteration step 3. Indeed, the arrival of a pilot sequence will trigger the update of the synchronization parameters instead of the data sequence. In the algorithm defined in Section 5.2, this encompasses the iteration over the following steps:

A. As long as no pilot sequence is received, update data sequence estimation $\hat{\bar{\mathbf{d}}}[N]$ using the iterative method defined in Section 5.2.

B. If a pilot sequence is received on either of the M carriers, perform - subsequent to the data $\hat{\bar{\mathbf{d}}}[N]$ estimation step defined in Section 5.2 - a

parameter estimation step as defined in (7.3) with $\mathbf{G}(\boldsymbol{\theta}) = \mathbf{G}^{RX}(\mathbf{G}^{TX,d}(\boldsymbol{\theta}) \otimes \mathbf{I}_{N_d})$, $\mathbf{G}^{TX,d}(\boldsymbol{\theta})$ is defined by (2.6) and (2.3). For this step, the known pilot sequence is used in $\hat{\hat{\mathbf{d}}}[N]$ in place of the symbol estimates on the carrier it was detected.

Note that in practice the presence of the pilot sequence will increase the spatial accuracy as well, through better estimates in (5.1).

7.4 Simulation Results, Synchronization Performance

The feasibility of the proposed synchronization mechanism was assessed by taking into account timing and frequency synchronization mechanism as outlined in Section 7.2. A typical DVB-S2 [ETS05a] pilot sequence of 36 known symbols was considered. The synchronization was performed over 10 consecutive pilot sequences. The sequence was chosen to be a known random bit sequence, different on each simulation run. Simulation performance results are illustrated in Figure 7.4.

A measurable degradation of the BER performance was recorded due to the sensitivity of the joint LPP-SIC scheme to synchronization imprecisions, however a significant performance improvement is still possible within a considerable aperture range.

The frequency estimation performance is presented on Figure 7.2. As can be deduced from these results, an improvement of the synchronization performance is achieved compared to efficient techniques that perform well under noise conditions, like the Luise & Reggiannini method (L&R), which served as comparison here.

Also the timing performance has been recorded in this joint estimation step and is presented on Figure 7.3 as variance of the timing relative to the symbol duration and compared to the modified CRB (MCRB). This result illustrates that the proposed procedure works as expected in terms of timing estimation performance.

In general it has been noted that the detection performance of the Joint LPP-SIC procedure is significantly more sensitive to synchronization errors than non iterative detection systems. This is due to the fact that a synchronization error enters also in the iterative inter-symbol interference estimation and amplifies its impact on the detection result through each iteration step.

For continuous stream signals, like the DVB-S2 broadcast signals, it should however be possible to reach the required synchronization accuracy over a longer sequence of consecutive pilot sequences.

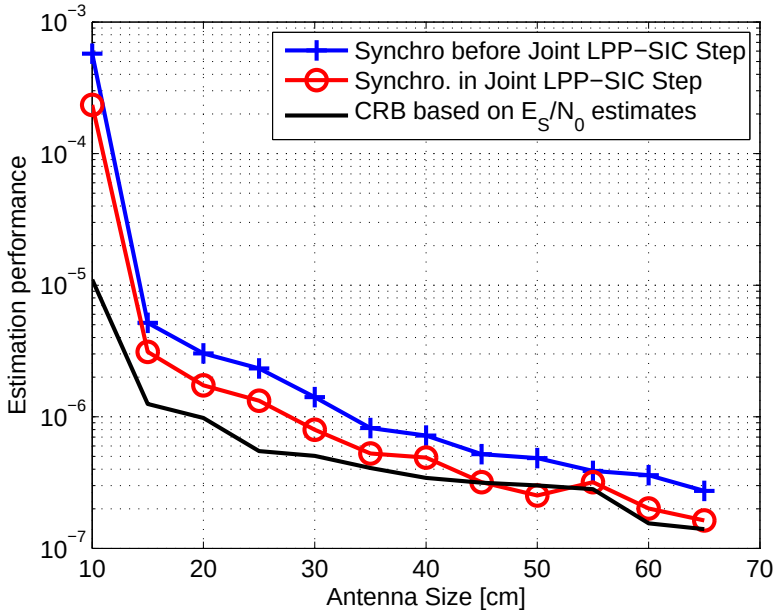

Figure 7.2: Frequency estimation performance (variance) as a function of the assumed antenna size for a dual-input MLNB system. Synchronization is done jointly to the main signal and one interferer at +3 degrees offset from the wanted signal with a frequency offset of $0.5 \cdot R_S$, 50% of the Symbol Rate. The CRB is also plotted, computed using the expression (8.27) and using estimated E_S/N_0 values after processing.

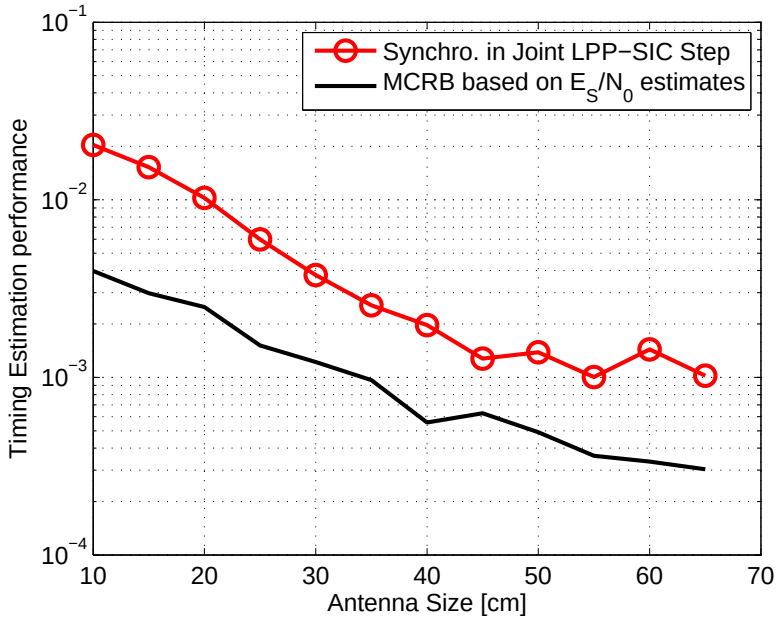

Figure 7.3: Timing estimation performance as a function of the assumed antenna size for a dual-input MLNB system. Synchronization is done jointly to the main signal and one interferer at +3 degrees offset from the wanted signal with a frequency offset of $0.5 \cdot R_S$, 50% of the Symbol Rate. The MCRB is also plotted, computed using the expression (8.28) and using estimated E_S/N_0 values after reception processing.

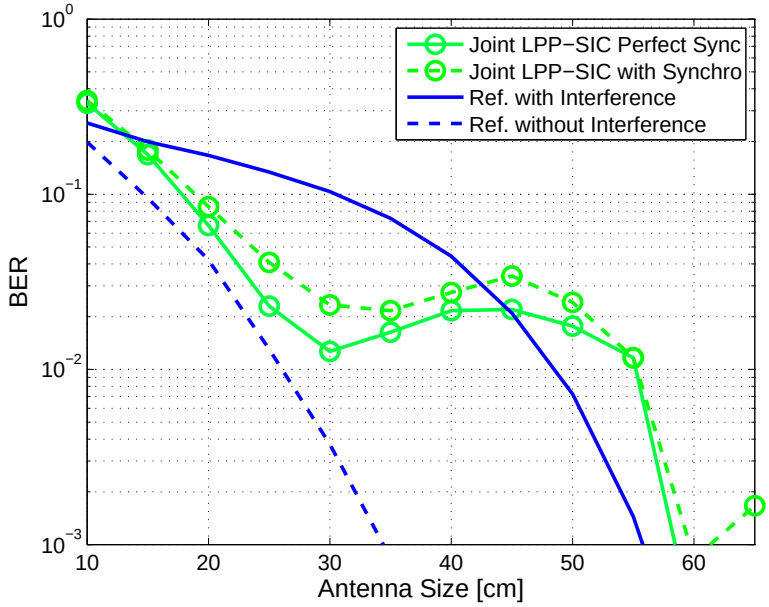

Figure 7.4: Bit error rate (BER) performance comparison of the proposed scheme (joint LPP-SIC) for different equivalent aperture sizes of the front-end and taking into account frequency and phase synchronization as outlined in Section 7.2. Same conditions as for Figure 5.7.

7.5 Conclusion

Synchronization aspects in frequency and symbol timing have been taken into account in the proposed joint LPP-SIC method introduced in Chapter 5. The synchronization method proposed for MF-TDMA broadband return channels introduced in the next Chapter 8 has been included in this context of broadcast reception with the assumption that both signals are DVB-S2 based and include pilot sequences to aid synchronization steps. The combined interference cancellation with synchronization has been simulation under realistic reception conditions. It has been demonstrated that the synchronization procedure is sensitive to synchronization errors. The fact that the signals are time-continuous makes it possible to reach this high synchronization accuracy.

Chapter 8

Synchronization in Broadband Systems

8.1 Introduction

The return channel of a satellite broadband system is the focus in this chapter. Assuming that the system uses DVB-RCS [ETS03a] based MF-TDMA as access strategy, we focus on the channel efficiency improvement achieved with a joint synchronization of the parallel received channels. Specifically the spacing between the MF-TDMA channels is reduced from the interference avoiding level of approx. $> 1.0\times$ Symbol Rate to a level below $< 1.0\times$ Symbol Rate, deliberately taking into account co-channel interference. The received burst sequence is detected with an multi-user detection system that jointly detects adjacent bursts interfering with each other. Known techniques are considered for the detection task, [Ver98] [BGK02]. The synchronization in frequency and symbol timing is investigated in details.

In general the synchronization task is well studied under different digital modulation and channel conditions, see [MA90], [MM97], [MD97] and [MMF98] for example. Applicable estimation performance limits, especially the well known Cramér-Rao Bound, have also been studied intensively under different reception conditions and assumptions, see [JSB03] [TT06] [NSM02] and [NSM04] for example.

However the specific problem of jointly synchronizing to signals received from different users under interference conditions has not been investigated much by previous work. Some work has been done in the context of multi-antenna systems, where an additional spatial degree of freedom permits to mitigate the interference, see for example [AJS99]. The only independently published related work known to the author of this thesis is authored by Yachil, Davidson and Bobrovsky [YBD02] [YDB06], where also the synchronization of a burst-mode transmission with adjacent channel interference is investigated. The proposed low

complexity joint synchronization approach is comparable in concept but differs in the exact cost function derived and in the complexity reduction considered. The complexity reduction proposed by Yachil consists in a simplified *channelization*, in an Expectation and Maximization (EM) approach based on [FW88]. Whereas the approach taken in this work is based on a simplification of the derived maximum likelihood (ML) approach. The achieved performance results are largely comparable.

In the sequel the burst synchronization problem at the receiver side is developed and analyzed in details. A joint synchronization method with tractable complexity is proposed that uses the structure of the interference scenario to improve the data-aided (DA) timing and frequency estimation performance. The performance of this joint estimation method is compared to applicable theoretical estimation limits and evaluated in conjunction with the considered detection techniques. Simulation results are presented that illustrate the achieved estimation improvement and the expected detection performance improvement.

8.2 System Description

We consider a system that uses an MF-TDMA channel as multi user access system. A large number of user terminals are considered accessing the same channel to transmit information to a common receiving hub. In practice these multi access configurations occur for example in DVB-RCS satellite communication where a very large number of users may have to share the same receiving hub. Since spectrum is a scarce resource, the spectral efficiency of the system is an essential performance criterion. Efficiency can be increased by reducing carrier spacing. As demonstrated in [BGK02], data detection and decoding performance can be maintained at channel spacing below 1 x Symbol Rate with joint detection of frequency adjacent and synchronized bursts.

Typically, the multi access terminals are loosely synchronized to the common receiver clock to allow for a minimal guard band in the MF-TDMA grid. The detection of the burst parameters such as power, timing offset, phase and residual frequency error are performed using a unique word sequence at the beginning of the burst.

Tight feedback control-loop systems could be considered in practice in order to facilitate synchronization, but requires additional processing power in the terminal and frequent retransmission of control information to the terminals. Eventually this feedback can be done only at the moment of network-access of the terminals, if a significant signalling traffic is to be avoided. The control loop option is not taken into account in the present framework and can be considered as an additional method to maintain synchronization beyond the acquisition phase for a user terminal.

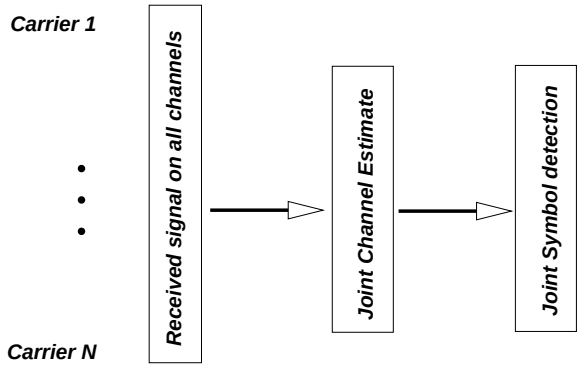

Figure 8.1: System overview for joint multi-user synchronization.

The problem of joint synchronization can be outlined as illustrated on Figure 8.1.

A common entity in the receiver estimates the channel parameters (timing, frequency, amplitude, phase) of all adjacent bursts in a frame. The subsequent detection can be performed in a joint or in separate estimation steps. The Figure 8.1 illustrates the main steps of the proposed scheme, joint channel estimation with subsequent detection on each channel.

8.3 Signal Model

The signal received on a given frame comprising N_C carrier frequencies can be modeled as follows:

$$s(t) = \sum_{i=1}^{N_C} a_i s_i(t) + n(t) \tag{8.1}$$

where the signal $s_i(t)$ can be expressed as follows:

$$s_i(t) = c_0(t - \Delta t_i) e^{2\pi j (t - \Delta t_i)(f_i^c + f_i)} \tag{8.2}$$

Here, the modulated signal on channel i is denoted $s_i(t)$ and the additive noise process is denoted $n(t)$. The shaped symbol sequence is represented by a power-normalized sequence, $c_0(t)$. The complex amplitudes, a_i, model amplitude as well as phase impact on the received signal for channel i, $1 \leq i \leq N_C$. The timing of each burst is offset with respect to the start of the slot by a random time offset Δt_i. The nominal frequency of a given carrier i is denoted with f_i^c and its residual burst frequency offset is f_i.

The time and frequency reference of every transmitter is derived from a common clock at the hub side within certain accuracy. The time-offset, Δt_i, of the carrier i is a function of the time synchronization of the transmitters and can be subject

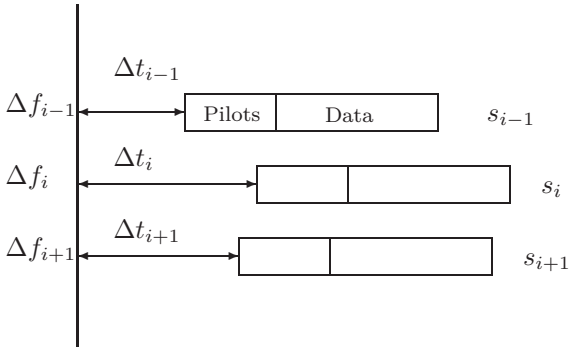

Figure 8.2: Considered frequency estimation problem with adjacent burst interference.

to a certain offset and random deviation, reflecting the residual timing error of the transmission start control loop.

The frequency-offset, f_i, is assumed to be constant over the length of the burst. This is a reasonable approach since short bursts are considered compared to the typical longer oscillator drifts. For longer bursts, oscillator drifts can be tracked using known techniques, see [MD97]. It is assumed that the burst synchronization is based on a unique-word detection of L symbols located at the beginning of the burst, which is the same for all users. Figure 8.2 illustrates the scenario considered ($\Delta f_i = f_i^c + f_i$).

Every user has the possibility to transmit within a certain transmit window beginning with the predefined *start of slot* time. The timing parameter of relevance is the relative difference in timing offset between adjacent carriers. For a given carrier j of interest, this can be expressed as follows, $\tau_i = \Delta t_i - \Delta t_j, i = j-1, j, j+1$. Note that $\tau_j \equiv 0$.

The receiver performs matched filtering (matched to the shaping filter of the transmitter) of the received signal. The impulse response of the filter of the ith channel is denoted $g_{MF}(t)$. The filtered signal can then be expressed as a convolution as follows:

$$s_i^f(t, \tau_i, f_i) = g_{MF}(t) \star s_i(t, \tau_i, f_i) \ . \tag{8.3}$$

Typically, the signal shaping is done by a root raised-cosine filtering (RRC) with a Rolloff factor of 0.35.

The known unique-word sequence received $x(1)...x(L)$ can then be expressed in vector form as follows for the signal of interest on channel i:

$$x(m) = g_{MF}(t) \star \sum_{k=1}^{N_C} s_k\,(t) a_k + n'\,(t)\,|_{t=mT_S} \tag{8.4}$$

The constant T_S represents the symbol duration. The filtered noise process is expressed as $n'(t) = g_{MF}(t) \star n(t)$. With normal carrier spacing, the matched filtering would provide good suppression of the adjacent frequency channels. However, as the carrier spacing decreases, ACI increases significantly.

Channel interference from direct adjacent channels clearly dominates and consequently the received signal sequence on a given channel with index i can be well approximated by a three signal system. This yields the following expression:

$$\mathbf{x} = \begin{bmatrix} x(1) \\ \vdots \\ x(L) \end{bmatrix} \simeq \begin{bmatrix} \mathbf{s_{i-1}^f} & \mathbf{s_i^f} & \mathbf{s_{i+1}^f} \end{bmatrix} \cdot \begin{bmatrix} a_{i-1} \\ a_i \\ a_{i+1} \end{bmatrix} + \mathbf{n}' \tag{8.5}$$

With the $L \times 1$ vector $\mathbf{s_i^f}$ regrouping the L symbol samples of carrier i, where L is the number of symbols in the known word sequence. The filtered noise process is represented by $\mathbf{n}'$:

$$\mathbf{n}'(t) = g_{MF}(t) \star \mathbf{n}(t) \tag{8.6}$$

which is of dimension $(L \times 1)$. Regrouping the following frequency and timing parameters in vector form, we define:

$$\boldsymbol{\tau} = \begin{bmatrix} \tau_{i-1} & \tau_i & \tau_{i+1} \end{bmatrix}^\top \tag{8.7}$$

$$\mathbf{f} = \begin{bmatrix} f_{i-1} & f_i & f_{i+1} \end{bmatrix}^\top \tag{8.8}$$

$$\mathbf{a} = \begin{bmatrix} a_{i-1} & a_i & a_{i+1} \end{bmatrix}^\top \tag{8.9}$$

Using (8.5)-(8.9), the received signal vector can then be formulated as follows:

$$\mathbf{x}(\boldsymbol{\tau}, \mathbf{f}, \mathbf{a}) = \mathbf{S}(\boldsymbol{\tau}, \mathbf{f})\mathbf{a} + \mathbf{n}' \tag{8.10}$$

where $\mathbf{S}$ regroups the filtered signals in an $L \times 3$ matrix as follows:

$$\mathbf{S}(\boldsymbol{\tau}, \mathbf{f}) = \begin{bmatrix} s_{i-1}^f(1) & s_i^f(1) & s_{i+1}^f(1) \\ \vdots & \vdots & \vdots \\ s_{i-1}^f(L) & s_i^f(L) & s_{i+1}^f(L) \end{bmatrix} \tag{8.11}$$

8.4 Joint Parameter Estimation

Maximum Likelihood Criterion

The synchronization problem amounts to estimating the unknown parameters $\boldsymbol{\tau}, \mathbf{f}, \mathbf{a}$ from the noisy observations $\mathbf{x}(\boldsymbol{\tau}, \mathbf{f}, \mathbf{a})$. From the above defined signal model, a joint estimator can be derived for any subcarrier i, taking into account the two adjacent carriers $i-1$ and $i+1$. The goal is to accurately estimate $\boldsymbol{\tau}, \mathbf{f}, \mathbf{a}$ based on

the knowledge of the unique word sequences of the three carriers. This will allow reliable joint detection of the data within the received burst.

It is assumed that the direct neighboring channels of the channel i considered represent the dominating interference. Furthermore we make the reasonable assumption of sampling at Symbol Rate, which implies that the additive noise remains a white noise contribution after reception filtering. Under these conditions the expressions (8.1)-(8.11) lead to the following Maximum Likelihood (ML) criterion for the estimation problem, under the assumption of Gaussian noise:

$$\left[\begin{array}{ccc} \hat{\boldsymbol{\tau}} & \hat{\mathbf{f}} & \hat{\mathbf{a}} \end{array} \right] = \arg \min_{\mathbf{a},\boldsymbol{\tau},\mathbf{f}} \left\| \mathbf{x} - \mathbf{S}\left(\boldsymbol{\tau},\mathbf{f}\right)\mathbf{a} \right\|_F^2 \tag{8.12}$$

The complex amplitude vector, $\mathbf{a}$, enters linearly into (8.10) and the problem in (8.12) is known as a separable least squares problem [GP73]. It is possible to optimize (8.12) with respect to $\mathbf{a}$ and obtain an explicit expression of the form:

$$\hat{\mathbf{a}} = \left(\mathbf{S}^*\mathbf{S}\right)^{-\mathbf{1}} \mathbf{S}^*\mathbf{x} = \mathbf{S}^{\dagger}\mathbf{x} \tag{8.13}$$

which depends on the known frequency and timing. This expression may be substituted back into (8.12) leading to the concentrated ML problem depending only on the frequency and timing:

$$\left[\begin{array}{cc} \hat{\boldsymbol{\tau}} & \hat{\mathbf{f}} \end{array} \right] = \arg \min_{\boldsymbol{\tau},\mathbf{f}} \left\| \mathbf{P}^{\perp}\mathbf{x} \right\|_F^2 = \arg \min_{\boldsymbol{\tau},\mathbf{f}} \mathbf{x}^*\mathbf{P}^{\perp}\mathbf{x} \tag{8.14}$$

where $\mathbf{P}^{\perp}$ is a projection matrix given by,

$$\mathbf{P}^{\perp} = \mathbf{I} - \mathbf{S}\left(\mathbf{S}^*\mathbf{S}\right)^{-\mathbf{1}}\mathbf{S}^* = \mathbf{I} - \mathbf{S}\mathbf{S}^{\dagger} \tag{8.15}$$

The cost function of the concentrated problem (8.14) depends on the timing and frequency parameters of the main and the two interfering carriers and is denoted

$$V(\boldsymbol{\Theta}) = \mathbf{x}^*\mathbf{P}^{\perp}(\boldsymbol{\Theta})\mathbf{x} \tag{8.16}$$

with the following parameter vector definition:

$$\boldsymbol{\Theta} = \left[\begin{array}{cccccc} \tau_{i-1} & \tau_i & \tau_{i+1} & f_{i-1} & f_i & f_{i+1} \end{array} \right]^T \tag{8.17}$$

The optimization problem in (8.14) is highly non-linear and an explicit solution for the optimal parameters does not exist in general. The cost function has many local minima and a global search for the optimum is very costly for this multi dimensional criterion. Below, we propose an efficient second order search technique based on initial estimates of the unknown parameters. Provided sufficiently accurate initial estimates, this procedure results in the ML estimates of the frequency and timing parameters with reasonable computational complexity.

ML Optimization Procedure – Gauss-Newton Method

The problem (8.14) is differentiable and suitable for search techniques provided initial frequency and timing estimates are sufficiently close to the global optimum. We will investigate the use of known single signal synchronization methods, see [BGK02] and [LR95] to initiate a multi dimensional search technique in the next section.

From the signal model outlined in Section 8.3, the gradient $\mathbf{g}$ and the Hessian $\mathbf{H}$ of the cost function with respect to the unknown parameters can be derived. With knowledge of these quantities, a damped Newton method to iteratively update the parameter estimate can be formulated [GMW81].

$$\mathbf{\Theta}_{k+1} = \mathbf{\Theta}_k + \gamma_k \mathbf{H}^{-1}\mathbf{g} \tag{8.18}$$

where k is the iteration index and the gradient and Hessian are evaluated at θ_k. Here, γ_k is a real valued step length parameter.

If the initial estimates of the frequency and timing are sufficiently accurate, the Newton method will converge to the optimal solution allowing synchronization of a particular carrier and taking the direct adjacent interferers into account. Note that the synchronization procedure must be repeated for each carrier of interest.

The cost function in (8.16) may be expressed as

$$V(\mathbf{\Theta}) = \mathbf{x}^*\mathbf{P}^{\perp}(\mathbf{\Theta})\mathbf{x} = \left|\mathbf{P}^{\perp}(\mathbf{\Theta})\mathbf{x}\right|^2 = |\mathbf{r}|^2 \tag{8.19}$$

where $\mathbf{r} = \mathbf{P}^{\perp}\mathbf{x}$ is an $L \times 1$ vector. To establish the gradient of the cost function, consider the first order derivative with respect to θ_l of $\mathbf{\Theta}$. The derivative may be expressed as

$$\frac{\partial V(\mathbf{\Theta})}{\partial \theta_l} = 2\mathrm{Re}\left\{\left(\frac{\partial \mathbf{r}}{\partial \theta_l}\right)^* \mathbf{r}\right\} = 2\mathrm{Re}\left\{\mathbf{r}_l^*\mathbf{r}\right\} \tag{8.20}$$

Next, the Hessian is obtained by considering the second order derivative of the cost function. Differentiating (8.20) with respect to θ_j results in

$$\frac{\partial^2 V(\mathbf{\Theta})}{\partial \theta_l \partial \theta_j} = 2\mathrm{Re}\left\{\mathbf{r}_l^*\mathbf{r}_j + \mathbf{r}_{lj}^*\mathbf{r}\right\} \tag{8.21}$$

The Gauss modification of the Newton method approximates the Hessian by dropping the second term above. This modification is often motivated by noting that the residual $|\mathbf{r}(\hat{\mathbf{\Theta}})|$ is often small compared to the first term in (8.21) for reasonable SNR ranges. The so-call Gauss-Newton (GN) method has the added advantage of always supplying an estimate of the Hessian matrix that is positive semi-definite which is required in (8.18). In addition, the approximate Hessian requires fewer operations to compute and only involves first order derivatives of the known signal sequence. Analytic expressions of the gradient and Hessian are derived in Appendix 8.B.

Consequently, a highly efficient (second order convergence) Gauss-Newton (GN) [GMW81] descent method can be considered for the synchronization problem.

Since the iterative procedure described above may be time consuming at the receiver side, we propose to reduce the complexity by only taking one GN step from the initial estimate. Indeed, the major part of the improvement is typically reached after the first GN iteration. As will be demonstrated in the simulation section, this leads to a significant improvement in estimation performance at a reasonable additional complexity at the receiver side.

Below, an initialization procedure is proposed where the timing and frequency offsets are estimated for the individual carriers. The initial estimate is obtained with the conventional L&R method for the three signals separately and then refined with a single GN step on the cost function as outline above.

8.5 Initialization of Synchronization Method

For the proposed method to converge, it requires the initial timing and frequency estimates for all channels to be close enough to the overall minimum of the ML cost function defined above. This means that frequency and timing offset should be within the region of attraction (ROA) of the cost function. This depends on the channel spacing, the signal shaping (Rolloff factor for the Root-Raised Cosine Method) and the pilot length. The following table summarizes the ROAs of the typical scenarios considered (for a channel spacing of 0.75×Symbol Rate and a Rolloff factor of 35%). The values are relative to the Symbol Time or Rate.

*	128 Symbols	64 Symbols	32 Symbols
$Var\{\tau\}$	$\backsim 0.03$	$\backsim 0.025$	$\backsim 0.020$
$Var\{\Delta f\}$	$\backsim 6 \cdot 10^{-3}$	$\backsim 0.015$	$\backsim 0.03$

Initial Frequency and Timing Estimation

For a rough first frequency and timing estimate, known estimation methods, which are well documented in literature, can be used. Many frequency estimation methods have been developed in the past, the most commonly used are the L&R method, [LR95], Kay's Method [MD97], and the ML approximation method [MD97]. The initial timing estimate can be obtained from a correlation based procedure, see [MD97]. Herein, initial timing is achieved using a correlation based estimator of the delay, comparing the known word sequence with the received signal, see [MS84].

It is interesting to note that the L&R method can be seen as a special case of the ML estimator developed above. Assuming that the timing is known and only one carrier in additive white Gaussian noise, the ML expression, (8.14)- (8.16), reduces to:

$$\max_{f_i} \mathrm{Tr}\{\mathbf{s}_i^f(f)\mathbf{s}_i^{f*}(f)\mathbf{x}\mathbf{x}^*\} \Leftrightarrow \max_{f_i} |\mathbf{s}_i^{f*}(f)\mathbf{x}| \tag{8.22}$$

This expression corresponds to the maximum likelihood expression for the special case of a single signal. This criterion involves the optimization over a single

parameter f_i and in general, an exhaustive search is still required, since the function $V(f) = |\mathbf{s}_i^{f*}(f)\mathbf{x}|$ has still many local maxima.

Luise and Reggiannini, [LR95], have derived a simple method from this expression under certain limiting conditions on the frequency error f_i, taking the derivative with respect to f leads to the following expression:

$$\frac{dV}{df} = \sum_{k=1}^{L}\sum_{m=1}^{L}(k-m)x(k)x^*(m)c_0(k-m)e^{2\pi j f_i(\Delta t_k - \Delta t_m - \Delta t_i)} \tag{8.23}$$

Using the definition of the correlation function $R(k)$,

$$R(m) = \frac{1}{L-m}\sum_{k=m}^{L-1} x(k)x^*(m-k) \tag{8.24}$$

and using the same approach as in [LR95], the following expression for the frequency estimate can be derived:

$$\hat{f}_i \equiv \frac{1}{2\pi}\frac{\sum_{k=1}^{M}\mathrm{Im}\{R(k)\}}{\sum_{k=1}^{M}k\mathrm{Re}\{R(k)\}} \simeq \frac{1}{\pi(M+1)}\arg\{\sum_{k=1}^{M}R(k)\} \tag{8.25}$$

The performance of the L&R method depends on the frequency error itself [LR95], but approaches the optimum for very small frequency errors, $f_i << 1/T_S$. The window size M is a design parameter that can be selected between 1 and L. For initial estimation $M = L/2$ has been chosen, which is a commonly used compromise, see [LR95].

8.6 Numerical Results

The pilot sequence aided synchronization techniques described in the previous sections have been evaluated on simulated data. The numerical examples are based on a multi-frequency time division multiple access system as typically used in DVB-RCS systems. Synchronization performance as well as the resulting detection accuracy are investigated for different scenarios.

GN Iteration Initialization

Using the rough frequency and timing estimates based on the proposed single carrier method, the iterations defined in (8.18) are applied for all parameters on all N_C carriers. A single GN step is taken with $\gamma_k = 0.9$. For an initial estimate the amplitude is assumed at its nominal level and the phase an unknown uniform random variable between 0 and 2π. After each GN step on a given carrier, estimates of amplitude and phase are obtained using (8.13). As illustrated in the examples below, the initial estimates are sufficiently accurate in these cases for the GN method to provide an iteration towards the global optimum. No cases were observed where the GN method produced large errors as would be the case with inaccurate initial estimates.

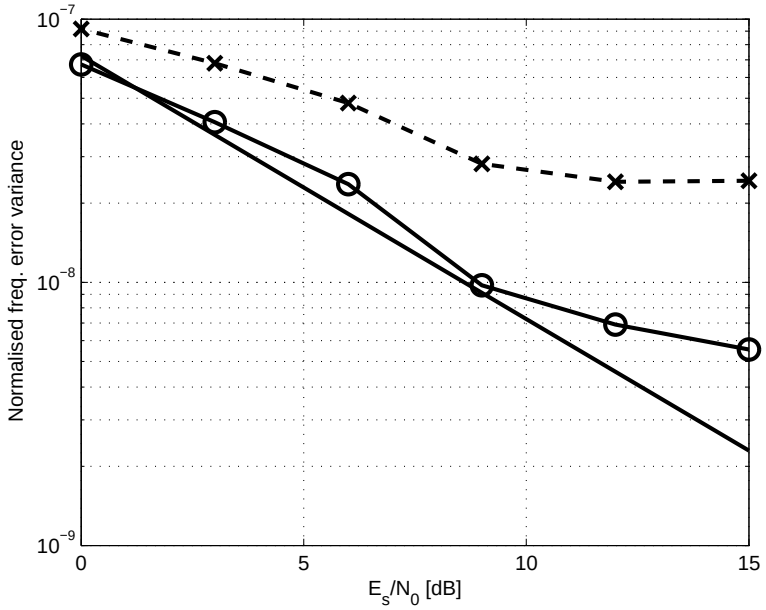

Figure 8.3: Normalized variance of the carrier frequency estimation for channel spacing of 0.7 x Symbol Rate. Dashed Line (x): L&R Method; Solid Line (o): L&R Method with one GN Step. A known-sequence of 128 symbols sequence was assumed and the CRB is also plotted for reference.

Estimation Performance

The proposed mechanism has been evaluated numerically over an additive white Gaussian noise (AWGN) channel. A frame structure of 5 carriers was assumed. The statistics presented were recorded on the carrier in the middle. A training pilot sequence of 64 or 128 symbols was assumed. The timing and frequency errors were assumed to be Gaussian random variables on each carrier. The timing offset variance has been assumed to range between 0.2 to 1.0 $\times$ Symbol Duration and the frequency error was also assumed to be very small compared to the channel spacing. The amplitude of the bursts were chosen to be of equal mean and varying as a Gaussian random variable with standard deviation 1%. This is reasonable in the perspective that a power regulation system will align the terminal transmit power levels to a nominal value.

The results as a function of the signal to noise level are illustrated on Figures 8.3–8.6. In Figures 8.3–8.4 the pilot sequence lenth is 128 and the results are displayed for carrier spacing 0.7 and 0.9. In Figures 8.5–8.6 also illustrate the results for carrier spacing 0.7 and 0.9 while the pilot sequence lenth is 128. In addition, the

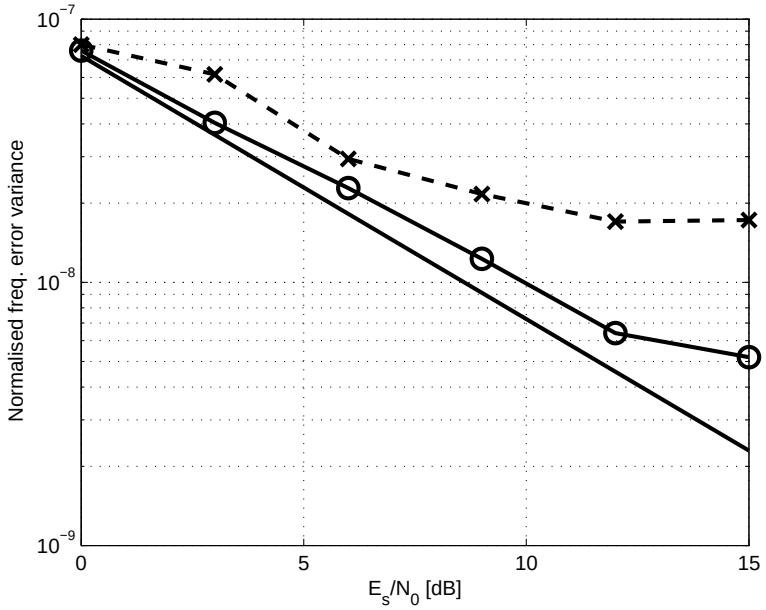

Figure 8.4: Normalized variance of the carrier frequency estimation for channel spacing of 0.9 x Symbol Rate. Dashed Line (x): L&R Method, Solid Line (o): L&R Method with one GN Step. A known-sequence of 128 symbols sequence was assumed and the CRB is also plotted for reference.

Cramér-Rao lower Bound (CRB) on the estimation accuracy is display in the figures to provide a bench mark. The derivation of the CRB is provided in Appendix 8.A for the signal model in use.

A considerable improvement is noticed which increases with the signal to noise ratio. For example at $E_S/N_0 = 10$dB the estimation variance is reduced to half with the proposed method, compared to the single carrier approach. This leads to an increased channel efficiency through the reduction in pilot sequence length or closer carrier spacing.

Comparing the frequency estimation variance as a function of the pilot sequence length, see Figure 8.8, the possible reduction in pilot sequence can be deduced for a given minimal estimation accuracy. For example to maintain a frequency estimate of variance better than 10^{-7}, it would be necessary to foresee a pilot sequence of at least 85 symbols, whereas with the proposed method 65 symbols would be sufficient.

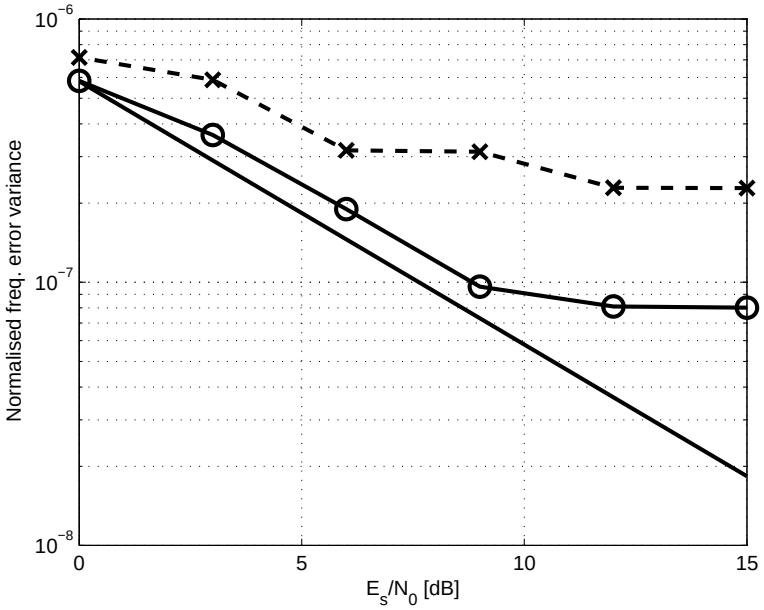

Figure 8.5: Normalized variance of the carrier frequency estimation for channel spacing of 0.7 x Symbol Rate. Dashed Line (x): L&R Method; Solid Line (o): L&R Method with one GN Step. A known-sequence of 64 symbols sequence was assumed and the CRB is also plotted for reference.

Detection performance

To verify the improvement of the proposed method also on the subsequent data detection, a reference burst receiver has been implemented. A hard-decision based successive interference cancellation (SIC) method, based on the previously proposed methods, see [JS02], has been implemented. The impact of frequency, timing, amplitude, and phase inaccuracy is investigated.

As reference method, a short burst length of 128 symbols is assumed, as no frequency or phase tracking mechanism is implemented over the burst. In practice, of course, longer bursts would be considered including phase tracking methods which are well known.

For this evaluation, the estimation was performed on a 64 symbol pilot sequence. The results are illustrated in Figure 8.9 as a function of signal to noise ratio and in Figure 8.10 as a function of channel spacing. Three successive SIC steps were performed. A significant improvement of the detection performance results from the application of the proposed synchronization method. Indeed, a SER of 6×10^{-3} can be reached compared to 3×10^{-2} if a single carrier synchronization method is

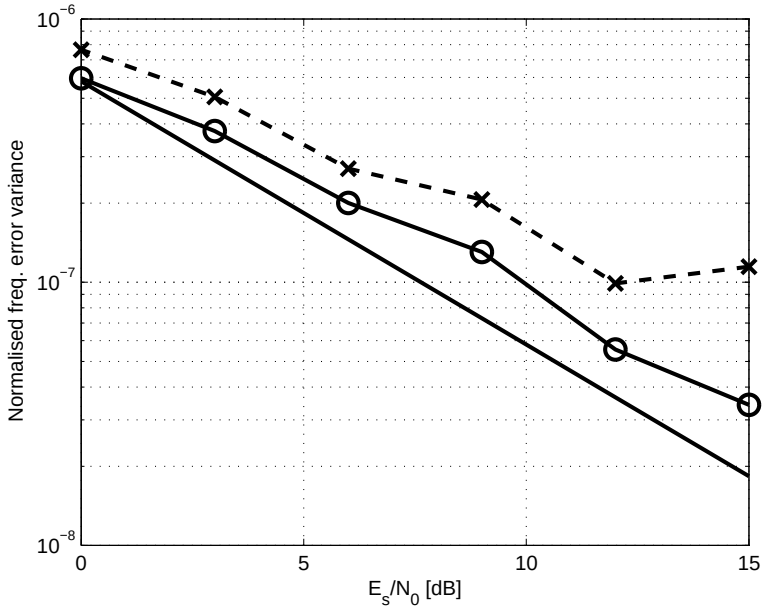

Figure 8.6: Normalized variance of the carrier frequency estimation for channel spacing of 0.9 x Symbol Rate. Dashed Line (x): L&R Method, Solid Line (o): L&R Method with one GN Step. A known-sequence of 64 symbols sequence was assumed and the CRB is also plotted for reference.

used for channel spacing 0.7, pilot sequence length 64, and $E_S/N_0 = 15$dB.

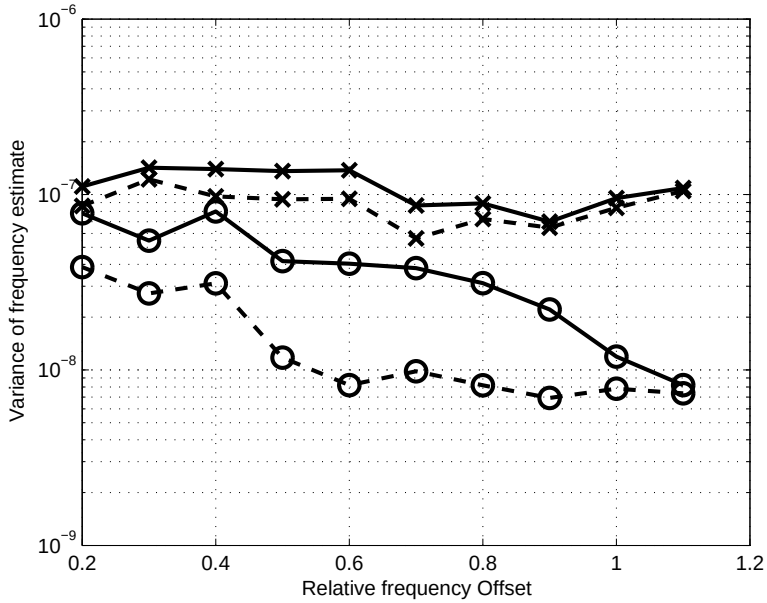

Figure 8.7: Frequency synchronization improvement versus Channel Spacing (Relative frequency Offset). Dashed Line: L&R Method with one GN Step; Solid Line: L&R Method. 128 symbols were assumed as known word length. Results for $E_S/N_0 = 0$dB (+) and $E_S/N_0 = 10$dB (o) are plotted.

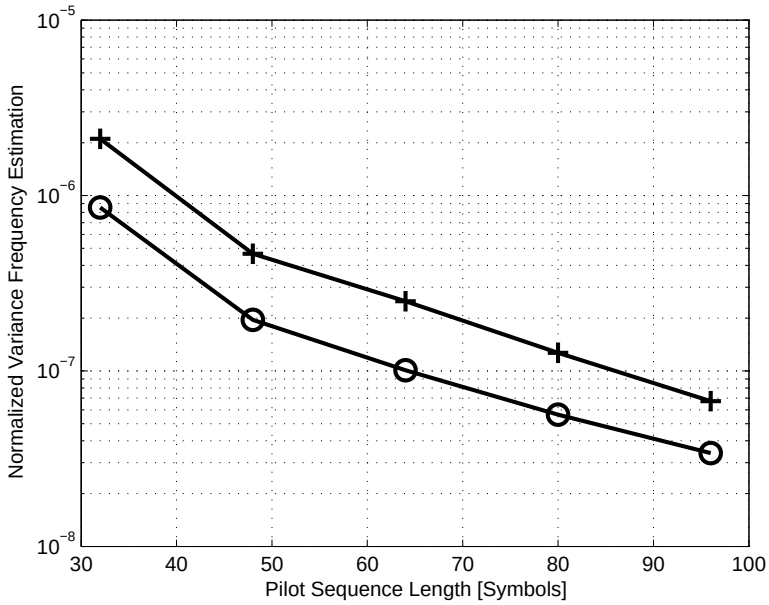

Figure 8.8: Estimation improvement as a function of the pilot sequence length. (+): L&R Method. (o): L&R Method with one GN step. A channel spacing of 0.7 was assumed and $E_S/N_0 = 10$dB.

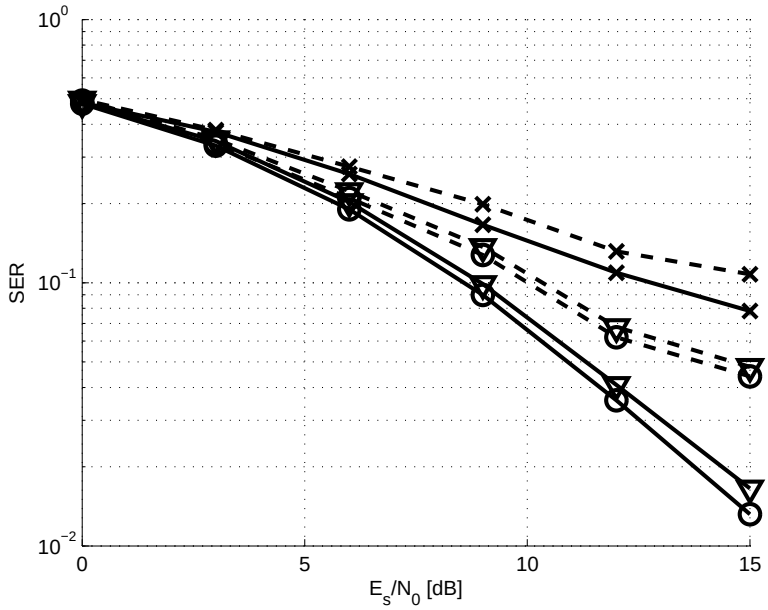

Figure 8.9: Impact on error rate performance of the frequency offset and the improvement achieved with the proposed method. Assuming 0.7 x Symbol Rate channel spacing, the Dashed Line corresponds to the single carrier synchronization approach, the Solid Line to the proposed improvement with one GN step. (+): Before SIC, ($\bigtriangledown$): First SIC Step, (o): Second and Third SIC Step. Synchronization was done on a 64 symbols long unique word and a 128 symbols data section was assumed.

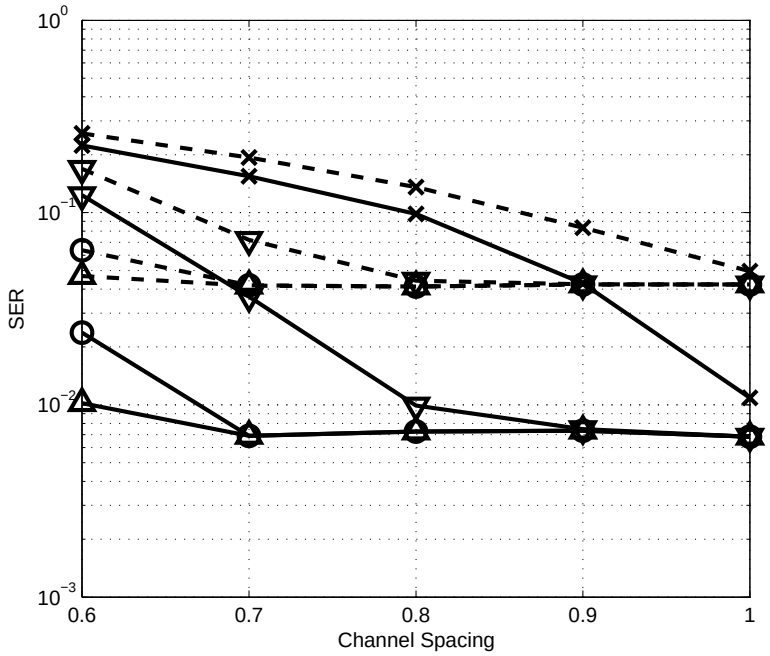

Figure 8.10: Symbol Error Rate (SER) Vs Channel Spacing for $E_S/N_0 = 15$dB. Successive Interference Cancellation (SIC) was used to improve the detection performance. The Dashed Lines illustrate the performance with synchronization on each channel individually and the Solid Lines show the improvement with the proposed joint synchronization method. (+): Before SIC, ($\bigtriangledown$): First SIC Step, (o): Second SIC Step, ($\bigtriangleup$): Third SIC Step. A 64 symbol unique word was assumed for synchronization.

8.7 Conclusion

The problem of joint synchronization of multi-user access systems has been considered. A novel data-aided synchronization method is proposed functioning under interference limited conditions to allow increased spectral efficiency. The method is based on the ML criterion for joint channel parameter estimation of the carrier of interest and the adjacent interfering carriers.

The performance of the proposed method was analyzed and compared to standard single carrier synchronization and the CRB. The impact of the parameter estimation on the detection performance was considered and a significant improvement has been demonstrated. Using the proposed synchronization technique, improved spectral efficiency was displayed. This may be manifested either through a reduction in pilot sequence length or tighter carrier frequency spacing. Especially for systems with short data bursts (as may be expected on the return channel of DVB-RCS systems), significant improvement in efficiency are expected.

The performance improvement depends on the signal-to-noise ratio that can be achieved by the system. Typical satellite multi-user systems will work at high signal-to-noise ratios, e.g. ($\frac{E_S}{N_0} >> 6dB$) for well over 90% of the time and experience fading as a result of rain or atmospheric conditions for only small periods over the average year. During these periods the system may fall back to slower rates or higher channel coding conditions (see e.g. [ETS03b]). This means that for a significant amount of time the system operates at high signal-to-noise ratios, which allows considerable improvements by performing joint synchronization in conjunction with a joint detection scheme.

8.A Cramér-Rao Bound Derivation

CRB for Frequency Estimation

Lower bounds on the estimation accuracy of timing and frequency synchronization have been studied for different types of signal models. D'Andrea [DMR94] *et al.* have studied the Cramér-Rao lower bound for the joint problem of frequency, timing and phase synchronization for a unique information carrier. Under the assumption that the signal phase is unknown and the signal timing is estimated or known, the modified CRB coincides with the CRB for the here applicable constraints, see [DMR94].

From the expression of the signal model, as outlined in section 8.3, the analytical expression for the CRB can be derived.

Starting form the asymptotic expression derived in [CTO89], the Fisher Information Matrix (FIM) can be expressed as follows:

$$\{\mathbf{J}^{-1}\}_{\theta_k,\theta_l} = \frac{2}{\sigma^2}\, Re(\mathrm{Tr}((\frac{\partial}{\partial\theta_k}\mathbf{S}^*)\mathbf{P}^{\perp}(\frac{\partial}{\partial\theta_l}\mathbf{S})\mathbf{c_0^*c_0})) \tag{8.26}$$

Applying the result to the frequency offset estimation results in:

$$\begin{aligned}\{\mathbf{J^{-1}}\}_{f_i f_i} =& \frac{2}{\sigma^2}\, Re\{\mathrm{Tr}\{\mathbf{s}_i^{f*}\left(2\pi j\left(t-\tau_i\right)\right)^* \\ & \left(I-\mathbf{s}_i^f\left(\mathbf{s}_i^{f*}\mathbf{s}_i^f\right)^{-1}\mathbf{s}_i^{f*}\right)\mathbf{s}_i^f\left(2\pi j\left(t-\tau_i\right)\mathbf{c}_0^*\mathbf{c_0}\right)\}\} \\ =& \frac{2}{\sigma^2}\, Re\{\mathrm{Tr}\{4\pi^2\left(t-\tau_i\right)^*\left(t-\tau_i\right)E_S\}\}\end{aligned}$$

To evaluate the CRB for the frequency estimation, the expectation over the timing offset has to be taken. Also, as we are interested in a lower bound, the maximum over the considered interval is reached for $t \equiv \frac{LT_S}{2}$, see [MD97], Chapter 2.4.3., for details. (Let $T_S = 1$ here.) This then leads to the expression:

$$\begin{aligned}\{\mathbf{J^{-1}}\}_{f_i f_i} =& 4\pi^2\frac{2E_S}{\sigma^2}\int_0^L (t-\tau_i)^2 dt \\ =& 4\pi^2\frac{2E_S}{\sigma^2}\frac{1}{3}\left[(L-\tau_i)^3-(0-\tau_i)^3\right] \\ =& 4\pi^2\frac{2E_S}{\sigma^2}\frac{1}{3}\left[\left(\frac{L}{2}\right)^3+\left(\frac{L}{2}\right)^3\right] \\ =& \frac{2\pi^2 E_S L^3}{3\sigma^2}\end{aligned}$$

A valid CRB for the frequency estimation can then be expressed as follows:

$$\mathrm{CRB}_{f_i f_i} = \frac{3}{2\pi^2\frac{E_S}{N_0}L^3} \tag{8.27}$$

CRB for Timing Estimation

The CRB for the symbol timing estimation of linearly modulated signals has been addressed in past work, e.g. [DMR94] and [TT06]. Using the signal model defined in Section 2.2 and following the same derivation as in [TT06], the modified timing CRB can be formulated as follows:[1]

$$\mathrm{MCRB}_{\tau_i\tau_i} = \frac{1}{2L\frac{E_S}{N_0}(-g_{TX}(-t) \star g_{RX}(t))''} \tag{8.28}$$

8.B Gradient and Hessian Expressions

Based on the signal model defined in the section (8.3), the Gradient and Hessian can be expressed analytically, following similar methods as in previous work, see [VO91]. Note that only the first order derivative of $\mathbf{r}$ is required in order to form the approximate Hessian used in the GN method. This can be expressed as follows:

$$\mathbf{r}_l = \frac{\partial}{\partial\theta_l}\mathbf{P}^{\perp}\mathbf{x} \tag{8.29}$$

to yield the following expressions for the Gradient and the Hessian:

$$\mathbf{g}_l = 2\mathrm{Re}\left\{\mathbf{r}_l^*\mathbf{r}\right\} \tag{8.30a}$$

$$\mathbf{H}_{lj} = 2\mathrm{Re}\left\{\mathbf{r}_l^*\mathbf{r}_j\right\} \tag{8.30b}$$

The expression $\mathbf{r}_l^*\mathbf{r}_j$ can be expressed as follows:

$$\mathbf{r}_l^*\mathbf{r}_j = \mathbf{x}^*\mathbf{P}_l^{\perp *}\mathbf{P}_j^{\perp}\mathbf{x} \tag{8.31}$$

The derivative of the projection matrix $\mathbf{P}^{\perp}$ has the following form:

$$\mathbf{P}_l^{\perp} = \frac{\partial}{\partial\theta_l}\mathbf{P}^{\perp} = -\mathbf{P}^{\perp}\left(\frac{\partial}{\partial\theta_l}\mathbf{S}\right)\mathbf{S}^{\dagger} - \left[\mathbf{P}^{\perp}\left(\frac{\partial}{\partial\theta_l}\mathbf{S}\right)\mathbf{S}^{\dagger}\right]^* \tag{8.32}$$

where $\mathbf{S}$ contains the known pilot sequences. This allows to elaborate expression (8.31) as follows:

$$\mathbf{r}_l^*\mathbf{r}_j = \mathbf{x}^*\left(\mathbf{S}^{\dagger *}\mathbf{S}_l^*\mathbf{P}^{\perp}\mathbf{S}_j\mathbf{S}^{\dagger} + \mathbf{P}^{\perp}\mathbf{S}_l\mathbf{S}^{\dagger}\mathbf{S}^{\dagger *}\mathbf{S}_j^*\mathbf{P}^{\perp}\right)\mathbf{x} \tag{8.33}$$

Using the expression for the nonzero elements of the derivative of the matrix $\mathbf{S}$,

$$\frac{\partial s_l^f}{\partial\tau_l} = s_l^f\left(t, f_l\right)\ \left(-1 - 2\pi j\left(f_l^c + f_l\right)\right) \tag{8.34a}$$

$$\frac{\partial s_l^f}{\partial(f_l^c + f_l)} = s_l^f\left(t, f_l\right)\ 2\pi j\left(t - \tau_l\right) \tag{8.34b}$$

the necessary expressions for the GN Method are defined, which are subsequently used in the defined method in section 8.4.

[1] Here, $(\,)''$ denotes the second derivative with respect to time index t.

Chapter 9

Conclusions and Future Work

9.1 Conclusions

In this thesis the problem of interference limited reception has been studied in details for broadcast reception scenario as well as for broadband satellite systems. Interference mitigation techniques were presented and the related problem of synchronization has been studied. Techniques were derived to improve the synchronization in interference limited reception scenarios and to improve the receiver performance.

In Chapter 2 a receiver design is proposed for the satellite broadcast reception using a multi-input antenna front-end with subsequent spatial linear processing and temporal processing for symbol detection. With the outline of this receiver design, the problem of joint detection of interfering signals from multiple satellites has been posed and presented.

In Chapter 3 the derived problem of the spatial linear pre-processing (LPP) is derived and presented. The performance of the LPP combining results are presented and discussed. It has been shown that the LPP step performs well when the system is not overloaded. A reduction of the antenna diameter in azimuth from the typically recommended 55 to 60cm requirement to 35cm is possible with an LPP pre-processing step if the system is not overloaded with interferers. This means in practice in most scenarios that at least 3 input elements (feeds) are required for the MLNB. However for overloaded systems, in general, there is no significant gain possible with the LPP step alone and an additional processing step is required. Note that the LPP step has the nice advantage of being independent of the nature of the interference signal. Indeed, if the interferer is a multi-carrier signal from different terminals and cannot be coped with in terms of temporal processing, the LPP step provides still the possibility of the spatial filtering step.

In Chapter 4 a temporal interference processing step based on iterative soft-decision symbol detection is proposed. This method is derived from a Minimum Mean Square Error criterion at the symbol detection level. A key complexity reduction, introduced by Beidas et al. in [BGK02], is used that avoids a matrix inversion step based on the assumption that the symbol auto-correlation dominates over the correlation with the interfering symbol sequence. It has been demonstrated through computer simulations that this method is a powerful tool for interference suppression and that a significant improvement can be reached in the current considered scenarios. In a second step of this evaluation the phase noise of the receiver and symbol timing inaccuracies are taken into account. It has been demonstrated through these results that the synchronization requirements are significantly increased at the receiver, compared to a conventional matched filter based symbol detection step, to achieve the potential improvements of the interference cancellation mechanism.

The results of Chapter 3 demonstrated that interference overloaded scenarios cannot be handled by spatial filtering (LPP) alone. An additional temporal interference processing step is required. This proposed supplementary temporal processing step is derived in details in Chapter 5. An ILSP based spatio-temporal processing step is derived in this Chapter. Starting from the presented problem formulation of Chapter 2, an iterative processing method is derived that estimates the symbols of the jointly received data streams by the LPP front-end. Taking into account the spatial estimation in a second iterative loop, the resulting procedure is robust against small initialization errors and also antenna pointing misalignments. The robustness and performance of the proposed method is demonstrated by simulation results. These results underline that for practical scenarios of interference on both sides of the wanted signal, an antenna size reduction to 35cm is practical with the same target performance as a 55cm antenna with conventional single input LNB and no signal processing. The advantage of this approach over successive spatial (LPP) and temporal interference processing is demonstrated.
It has been demonstrated with these results that a 2 input element MLNB system with the proposed joint LPP-SIC processing step can cope well with interference coming from both sides of the wanted signal direction.
An additional advantage of the proposed receiver structure is its inherent capability to receive signals from adjacent satellites that are located within a certain gain-angle reach of approximately 6 degrees for a 3 input element MLNB system.

In Chapter 6 the feasibility to improve the interference cancellation step using a decoded and reconstructed signal based on DVB-S is analyzed. The potential gain of an additional decoding step in the interference cancellation procedure provides especially at lower signal to noise ratio a higher gain potential as detection based interference cancellation. The presented results illustrate specifically that e.g. for a code rate of 1/2, a typical signal to noise ratio (C/N) of 10dB the tolerable signal to interference level to reach a target performance of 10^{-2} in BER can be reduced from 12dB to 7dB. This approach obviously relies on the fact that the

signal complies to a predefined coding standard, here DVB-S.
The work presented in [CGG08] illustrates well that for DVB-S2 based decoding the interference cancellation works very well as long as the decoded signal is above the required decoding threshold in terms of signal to noise ratio. This assumes that the signals are DVB-S2 compliant and that the receiver can master the decoding complexity.

In Chapter 7 the additional problem of synchronization is taken into account. Based on the joint LPP-SIC mechanism introduced in Chapter 6, the synchronization mechanism introduced in the following Chapter 8 for broadband reception is included in the joint LPP-SIC processing step. An slightly improved frequency estimation performance has been demonstrated by simulation results and symbol timing estimation results that are sufficient for the joint LPP-SIC mechanism to work and improve detection. The bit error rate simulations have demonstrated the high sensitivity of the joint LPP-SIC mechanism to synchronization errors. However for time continuous signals a sufficiently high synchronization accuracy can be achieved over the period of 10 pilot sequences to reach a synchronization accuracy that is sufficient for joint LPP-SIC to perform well. This result is in line with the results from Chapter 4, in the sense that the sensitivity of the interference processing step with respect to synchronization errors is demonstrated. The required level of accuracy is however achievable for time continuous signals.

In Chapter 8 a broadband return channel is analyzed. Specifically the burst transmission on the MF-TDMA channel is considered and the receiver synchronization in the case of a dense packing in frequency of the channels on the MF-TDMA frame, which leads inevitably to adjacent channel interference (ACI). A joint synchronization mechanism is proposed that helps the receiver synchronize in symbol-timing and in frequency to the received bursts. The maximum likelihood (ML) criterion is derived. This approach is in practice of intractable complexity and a simplified gradient descent based method is derived with reduced complexity. This joint iterative synchronization method is analyzed in details though simulations. A significantly improved frequency synchronization performance is achieved, compared to efficient synchronization methods that work on a single burst. For example for realistic channel conditions, a pilot (known word) length of 65 symbols can achieve the same estimation performance of 10^{-7} as an 85 symbols sequence for single burst synchronization. In conjunction with a joint detection method, this approach has the potential to improve significantly the return link efficiency and a channel spacing of $0.7 \times R_S$ (70% of the symbol rate) is well feasible with this approach.

9.2 Implementation aspects

The results show that the considered interference mitigation techniques have different performance results but also under different complexity requirements. The LPP method alone provides good interference suppression results under the requirement that the system must not be overloaded and that the reception geometry is optimized. The inherent advantage of the LPP step is its independence from the nature of the interferer. These aspects are specifically attractive in the considered context, where this is the only approach that does not necessarily require a broadcast operator coordination. Furthermore the LPP approach itself does not increase the complexity of the synchronization steps required. For a static interference situation the configuration can be fixed or quasi-static and does not need to be time-dependent on the level of the transmission rate.
The *Joint LPP-SIC* approach considered works at joint detection level and increases the complexity also in the respect that synchronization is required in timing and frequency to the processed signals. The mechanism proposed is robust against small parameter errors and works under overloaded conditions. The increase in complexity is reasonable as it implies reception filtering and iterative joint detection on reasonably short processing frames that span over twice the filter length. The LPP processing needs to be quick and responsive, as the procedure foresees an adaptation of the weighting factors at the rate of the processing. This approach requires the knowledge of some parameters of the interfering signal, mainly the modulation type and symbol rate. This also implies that a minimal level of coordination is required with the operator of the interfering signal.
The use of decoding within the interference processing step increases further the requirements and complexity of the scheme. Indeed it is necessary to coordinate on transmission schemes with operators of interfering systems for this approach to be practical. The decoding complexity is increased by the processing of both the main signal and the interferer for each iteration step of the processing. In combination with the LPP pre-processing this approach provides however a robust and performing interference suppression.
Further work would extend this approach to consider joint decoding approaches that adapt the decoding step to process both the wanted signal and the interference.

Depending on the specific scenario and application considered, a compromise between the low complexity versus performance improvement can be drawn. The practical approach can be different on a case by case basis.

9.3 Future Work

The continuously growing demand for higher throughputs increases the demand also for satellite capacity for broadcast as well as for broadband systems. The

pressure on efficient transmission systems will drive the need for novel receiver designs and satellite constellation approaches. In addition the use of communication tools that are ubiquitously connected requires services that permit mobile and nomadic connection possibilities. The satellite is well suited as gap filler for terrestrial mobile networks, who would have to struggle with high investment costs to provide truly seamless coverages over a large service area.

The presented work on spatial and temporal processing to symbol detection, as outlined in Chapter 2 and Chapter 5, can be extended and improved in different manners. Even so the method provides a processing approach with tangible complexity, the achieved performance is not reaching the optimal level, as can be deduced from the approach and witnessed by the results. Taking into account a decoding step in the temporal processing increases the complexity but provides an additional level of redundancy that can be exploited to improve even further the performance of the system and improve the gain even more.

The presented synchronization procedure in Chapter 8 has been derived with the aim of a practical and computationally tractable synchronization mechanism. A considerable estimation performance improvement has been recorded by simulation results, however the theoretical bound has not been reached at all signal to noise ratio levels. A significant improvement can be reached by improved techniques that exploit further the signal structure received, at the price of higher complexity at the receiver side.

Broadband Systems

To provide more capacity to two way satellite systems, the use of spot-beam based coverage areas with frequency reuse is the most promising next step in addition to the introduction of DVB-S2 Adaptive Coding and Modulation (ACM). This will introduce interference in the forward link to the terminals as each spotbeam uses the same frequency bands and is only separated by the spatial selectivity of the satellite antenna beams. The use of pre-coding techniques has recently been considered as possible downlink interference mitigation technique [DCM+07] in combination with frequency re-used multi-beam satellite systems. The satellite antenna system, comprising shaped reflector and feed-array, is typically designed to minimize the interference between frequency reusing beams and compromise on the maximal gain to achieve target gain masks. The combined use with interference suppressing pre-coding systems provide however possibility to alleviate the need for stringent gain masks and compromise on higher inter-cell interferences to allow higher maximal gains. Work in this area would be of high interest for future satellite broadband systems.
Adapting the proposed space-time reception technique also to broadband systems with multi-beam, frequency re-use satellite coverage areas has the potential to

increase significantly the efficiency of the multi-user access return channel. Indeed, the joint spatio-temporal processing of the interfering users in adjacent cells can be processed in a similar manner as the proposed broadcast reception processing presented in Chapter 5.
Beamforming and multi-antenna techniques have now been well introduced in the context of broadcast systems, see for example [dFCSSL08]. The design of satellite broadcast systems has however still to explore the full potential of these technologies. The forward link of broadband systems using spot-beam coverages with frequency reuse have the potential to improve their efficiency. Especially the approach of downlink beamforming techniques in combination with pre-coding provides a promising level of flexibility to address specific terminals while suppressing interference to other users. Recently, related work has been done in conjunction with the concept of ground based beam-forming (GBBF) [ZK05]. This approach is particularly interesting since the satellite can be conceived as a generic entity with a minimized amount of complexity (and thus risk of failure) weight and power usage, while the complex beamforming system is located on the ground.
The efficiency of next generation broadband satellite systems would benefit from such approaches and further research is required to reach these potential is practice.

Broadcast Systems

With the introduction of DVB-S2 the efficiency of the broadcast channel has approached closely the Shannon theoretical limit. Also the adaptive coding and modulation (ACM) approach provides the required flexibility to achieve both high throughputs and high availability of two-way systems. There are however still fields of potential improvement. The efficiency in mobile broadcast scenarios is often limited at different levels and the channel statistical fading typical to mobile satellite reception has to be taken into account. The use of DVB-SH based mobile broadcast system that jointly use satellite systems and ancillary terrestrial networks are in operation in the U.S. (XM Radio, Sirius Radio) and planned for Europe for the near future. The joint use of spatial and temporal processing techniques, similar to the one presented in this thesis, in combination with satellite diversity and terrestrial diversity provides an interesting field of study. Especially in the perspective of the fading channel characteristics of joint satellite-terrestrial network topologies.

Appendix A

Useful Lemmas and Rules

The following results are used in different places throughout the thesis. Matrix Inversion Lemma.

Lemma A.1. *For the four matrices* $\mathbf{A}$,$\mathbf{B}$,$\mathbf{C}$,$\mathbf{D}$ *it holds that*

$$(\mathbf{A}+\mathbf{BCD})^{-1} = \mathbf{A}^{-1} - \mathbf{A}^{-1}\mathbf{B}(\mathbf{DA}^{-1}\mathbf{B}+\mathbf{C}^{-1})^{-1}\mathbf{DA}^{-1} \tag{A.1}$$

if all matrices involved exist.

Proof. The proof can be computed starting from the equation:

$$(\mathbf{A}+\mathbf{BCD})\mathbf{X} = \mathbf{I} \tag{A.2}$$

where $\mathbf{X}$ is assumed the unknown matrix. We can reformulate this as:

$$\mathbf{X} = \mathbf{A}^{-1} - \mathbf{A}^{-1}\mathbf{BCDX} \tag{A.3}$$

Multiplying this result with $\mathbf{D}$ from the left side yields:

$$\mathbf{DX} = \mathbf{DA}^{-1} - \mathbf{DA}^{-1}\mathbf{BCDX} \tag{A.4}$$

Regrouping this, we can write:

$$(\mathbf{C}^{-1}+\mathbf{DA}^{-1}\mathbf{B})\mathbf{CDX} = \mathbf{DA}^{-1} \tag{A.5}$$

Isolating $\mathbf{CDX}$ yields:

$$\mathbf{CDX} = (\mathbf{C}^{-1}+\mathbf{DA}^{-1}\mathbf{B})^{-1}\mathbf{DA}^{-1} \tag{A.6}$$

Reinserting this result into (A.3) leads to:

$$\mathbf{X} = \mathbf{A}^{-1} - \mathbf{A}^{-1}\mathbf{B}(\mathbf{C}^{-1}+\mathbf{DA}^{-1}\mathbf{B})^{-1}\mathbf{DA}^{-1} \tag{A.7}$$

which leads to the desired, well known and useful expression from A.1. □

Common standard linear algebra rules that are used throughout the thesis are the following [HJ85] [HJ91] [Gra81]:

$$\mathrm{Tr}(\mathbf{A}^*\mathbf{B}) = (\mathrm{vec}(\mathbf{A}))^*\mathrm{vec}(\mathbf{B}) \tag{A.8}$$

$$\mathrm{Tr}(\mathbf{AB}) = \mathrm{Tr}(\mathbf{BA}) \tag{A.9}$$

$$\mathrm{vec}(\mathbf{ABC}) = (\mathbf{C}^T \otimes \mathbf{A})\mathrm{vec}(\mathbf{B}) \tag{A.10}$$

$$(\mathbf{A} \otimes \mathbf{B})(\mathbf{C} \otimes \mathbf{D}) = (\mathbf{AC}) \otimes (\mathbf{BD}) \tag{A.11}$$

$$(\mathbf{A} \otimes \mathbf{B})^{-1} = (\mathbf{A}^{-1} \otimes \mathbf{B}^{-1}) \tag{A.12}$$

Bibliography

[AGB98] H. Arslan, S. C. Gupta, and G. E. Bottomley. Successive cancellation of adjacent channel signals in FDMA/TDMA digital mobile radio systems. *Proceedings of IEEE Vehicular Technology Conference*, December 1998.

[AJS99] D. Astély, A. Jakobsson, and A. L. Swindlehurst. Burst synchronization on unknown frequency selective channels with co-channel interference using an antenna array. *IEEE 49th Vehicular Technology Conference*, 49, May 1999.

[BB83] Sergio Benedetto and Ezio Biglieri. Nonlinear equalization of digital satellite channels. *IEEE Journal on Selected Areas in Communications*, SAC-1:57–62, 1983.

[BBD79] Sergio Benedetto, Ezio Biglieri, and Riccardo Daffara. Modeling and Performance Evaluation of nonlinear Satellite Links - A Volterra Series Approach. *IEEE Transactions on Aerospace and Electronic Systems*, AES-15:494–507, 1979.

[BC02] J. Boutros and G. Caire. Iterative Multiuser Joint Decoding: Unified Framework and Asymptotic Analysis. *IEEE Transactions on Information Theory*, 48:1772–1793, July 2002.

[BC07] A. Barbieri and G. Colavolpe. On Pilot-Symbol-Assisted Carrier Synchronization for DVB-S2 systems. *IEEE Transactions on Broadcasting*, 53, September 2007.

[BG96] Claude Berrou and Alain Glaiveux. Near optimum error correcting coding and decoding: Turbo-codes. *IEEE Transactions on Communications*, 44:1261–1271, October 1996.

[BGK02] B. F. Beidas, H. E. Gamal, and S. Kay. Interactive interference cancellation for high spectral efficiency satellite communications. *IEEE Transactions on Communications*, 50, 2002.

[BHW03] S. Baro, J. Hagenauer, and M. Witzke. Iterative detection of MIMO transmission using a list-sequential (LISS) detector. *Proceedings of the IEEE Conference on Communications*, 4, May 2003.

[BK80] V. M. Bogachev and I. G. Kiselev. Optimum combining of signals in space-diversity reception. *Telecommunication Radio Engineering*, 34/35:83, 1980.

[CCC00] W.-J. Choi, K.-W. Cheong, and J. M. Cioffi. Iterative soft interference cancellation for multiple antenna systems. *IEEE Wireless Communications and Networking Conference*, 1, 2000.

[CdGR08] Stefano Cioni, Riccardo de Gaudenzi, and Rita Rinaldo. Channel estimation and physical layer adaptation techniques for satellite networks exploiting adaptive coding and modulation. *International Journal of Satellite Communications and Networks*, 26:157–188, 2008.

[CFK07] M. Angeles Vazquez Castro, David P. Fernandez, and Sastri Kota. VoIP Transmission cross-layer design over satellite WiMAX hybrid networks. *Military Communications Conference*, October 2007.

[CFL07] Carlo Caini, Rosario Firrincieli, and Daniele Lacamera. PEPsal: A Performance Enhancing Proxy for TCP Satellite Connections. *IEEE Aerospace and Electronic Systems Magazine*, 22:B9–B16, August 2007.

[CFP04] L. Chisci, R. Fantacci, and T. Pecorella. Predictive bandwidth control for GEO Satellite Networks. *IEEE International Conference on Communications*, 7:3958–3962, June 2004.

[CFS97] Jian Cui, David D. Falconer, and Asrar U. H. Sheikh. Performance evaluation of optimum combining and maximum ratio combining in the presence of co-channel interference and channel correlation of wireless communication systems. *Journal of Mobile Networks and Applications*, 2:315–324, 1997.

[CGG08] Enrico Casini, Gennaro Gallinaro, and Joel Grotz. Reduced front-end reception requirements for satellite broadcast using interference processing. *IEEE Transactions on Consumer Electronics*, 54, November 2008.

[Col07] G. Colavolpe. On LDPC Codes over Channels with Memory. *IEEE Transactions on Wireless Communications*, 5(7):1757–1766, July 2007.

[CTO89] H. Clergeot, S. Tressens, and A. Ouamri. Performance of High Resolution Frequencies Estimation Methods compared to the Cramér-Rao Bound. *IEEE Transactions ASSP*, 37(11), November 1989.

[DCB00] M. O. Damen, A. Chkeif, and J.-C. Belfiore. Lattice code decoder for space-time codes. *IEEE Communications Letters*, 4, May 2000.

[DCM+07] Marcos Alvarez Diaz, Nicolas Courville, Carlos Mosquera, Gianluigi Liva, and Giovanni E. Corazza. Non-linear interference mitigation for broadband multimedia satellite systems. *Proceedings of the International Workshop on Satellite and Space Communications*, pages 61–65, September 2007.

[dFCSSL08] Ruben de Francisco Claude Simon, , Dirk T. M. Slock, and Geert Leus. Beamforming for correlated broadcast channels with quantized channel state information. *SPAWC 2008, The 9th IEEE International Workshop on Signal Processing Advances in Wireless Communications*, July 2008.

[DMR94] A. N. D'Andrea, U. Mengali, and R. Reggiannini. The Modified Camer-Rao Bound and its application to synchronization problems. *IEEE Transactions on Communications*, 42(2/3/4), February 1994.

[ETS98] ETSI. EN 300 421 v1.1.2: Digital Video Broadcasting (DVB); framing structure, channel coding and modulation for 11/12GHz satellite services. *ETSI Standard*, 1998.

[ETS03a] ETSI. EN 301 790: DVB-RCS Standard v1.4.1: Digital Video Broadcasting (DVB); Interaction Channel for Satellite Distribution Systems. *ETSI Standard*, 2003.

[ETS03b] ETSI. TR 101 790: Digital Video Broadcasting (DVB); Interaction channel for satellite distribution systems; Guidelines for the use of EN 301 790. *ETSI Standard*, 2003.

[ETS05a] ETSI. EN 302 307 : Digital Video Broadcasting (DVB); second generation framing structure, channel coding and modulation systems for broadcast, interactive services, news gathering and other broadband satellite applications. *ETSI Standard*, 2005.

[ETS05b] ETSI. TR 102 376 v1.1.1.: Digital Video Broadcasting (DVB) user guide for second generation system for broadcasting, interactive services, news gathering and other broadband satellite applications (DVB-S2). *ETSI Standard*, 2005.

[FLR94] S. T. Fu, L. F. Lester, and T. Rogers. Ku-band high power high efficiency pseudomorphic HEMT. *IEEE International Microwave Symposium Digest*, 2:793–796, 1994.

[FMI99] M. Fossorier, M. Mihaljevic, and H. Imai. Reduced complexity iterative decoding of low-density parity check codes based on belief propagation. *IEEE Transactions on Communications*, 47(5):673–680, May 1999.

[FW88] M. Feder and E. Weinstein. Parameter Estimation of Superimposed signals using the EM algorithm. *IEEE Transactions in Acoustics, Speech and Signal Processing*, ASSP-36:477–489, 1988.

[Gal62] R. G. Gallager. Low Density Parity Check Codes. *IRE Transactions on Information Theory*, pages 21–28, January 1962.

[GC98] S. J. Grant and J. K. Cavers. Performance enhancement through joint detection of cochannel signals using diversity arrays. *IEEE Transactions on Communications*, 46, 1998.

[GG00] H. E. Gamal and E. Geraniotis. Iterative Multi-User Detector for coded CDMA signals in AWGN and Reighleigh fading channels. *IEEE Journal on Selected Areas in Communications*, January 2000.

[GG07] Gennaro Gallinaro and Joel Grotz. Reduction of Antenna and Front-End Requirements for DTH Broadcast Reception. *European Space Agency (ESA), Final Report of ARTES-1 Pre-study, Contract Number 18070/04/NL/US*, May 2007.

[GMW81] P.E. Gill, W. Murray, and M.H. Wright. *Practical Optimization*. Academic Press, London, 1981.

[GO05] Joel Grotz and Björn Ottersten. Data-aided frequency synchronisation under interference limited conditions. In *Proceedings IEEE Vehicular Technology Conference, Spring*, May 2005.

[GOK05] Joel Grotz, Björn Ottersten, and Jens Krause. Decision-directed interference cancellation applied to satellite broadcast reception. In *Proceedings IEEE Vehicular Technology Conference, Fall*, September 2005.

[GOK06] Joel Grotz, Björn Ottersten, and Jens Krause. Applicability of interference processing to DTH reception. In *Ninth International Workshop on Signal Processing for Space Communications, September 2006*, ESA/ESTEC, Noordwijk, Netherlands, September 2006.

[GOK07] Joel Grotz, Björn Ottersten, and Jens Krause. Joint channel synchronization under interference limited conditions. *IEEE Transactions on Wireless Communications*, 6(10):3781–3789, October 2007.

[GOK08] Joel Grotz, Björn Ottersten, and Jens Krause. Signal detection and synchronization for interference overloaded satellite broadcast reception. *IEEE Transactions on Wireless Communications*, July 2008. Submitted.

[GP73] G. H. Golub and V. Pereyra. The differentiation of pseudo-inverses and nonlinear least square problems whose variables separate. *SIAM J. Num. Anal.*, 10, April 1973.

[Gra81] Alexander Graham. *Kronecker Products and Matrix Calculus With Applications*. John Wiley & Sons, New York, 1981.

[GSM+97] K. Giridhar, John J. Shynk, Amit Mathur, Sujai Chari, and Richard P. Gooch. Nonlinear techniques for the joint estimation of cochannel signals. *IEEE Transactions on Communications*, 45, April 1997.

[Hag95] B. Hagerman. *Single-user receivers for partly known interference in multiuser environment*. PhD in Telecommunications, Royal Institute of Technology, Stockholm, Sweden, 1995.

[HC05] Y. Hong and J. Choi. A new approach to iterative decoding on coded MIMO channels. *IEEE Vehicular Technology Conference*, 3, May 2005.

[HJ85] Roger A. Horn and Charles R. Johnson. *Matrix Analysis*. Cambridge University Press, New York, 1985.

[HJ91] Roger A. Horn and Charles R. Johnson. *Topics in Matrix Analysis*. Cambridge University Press, New York, 1991.

[HK99] Thomas H. Henderson and Randy H. Katz. TCP Performance over Satellite Channels. *Technical Report No. UCB/CSD-99-1083, EECS, University of California at Berkeley, California 94720, U.S.A.*, December 1999.

[HMF02] Yim Fun Hu, Gérard Maral, and Ernio Ferro. *Service Efficient Network Interconnection Via Satellite: EU Cost Action 253*. John Wiley & Sons, New York, February 2002.

[HtB03] B. M. Hochwald and S. ten Brink. Achieving near-capacity on a multiple-antenna channel. *IEEE Transactions on Communications*, 51, March 2003.

[HTR+02] J.E. Hicks, J. Tsai, J.H. Reed, W.H. Tranter, and B.D. Woerner. Overloaded array processing with MMSE-SIC. *IEEE Vehicular Technology Conference*, 2, May 2002.

[ITU07] ITU-R P.618-9. Propagation data and prediction methods required for the design of earth-space telecommunication systems. *International Telecommunications Union (ITU), Recommendation ITU-R P.618-9*, 2007.

[JS02] G. J. Janssen and B. Slimane. Symbol error probability analysis of a multiuser detector for M-PSK signals based on successive interference cancellation. *IEEE Journal On Selected Areas in Communications*, 20, February 2002.

[JSB03] Yimin Jiang, Feng-Wen Sun, and John S. Baras. On the performance limits of data-aided synchronization. *IEEE Transactions on Information Theory*, 49(1), January 2003.

[KL02] Y. Koo and Y. H. Lee. A joint likelihood approach to frame synchronization in presence of frequency offset. *IEEE International Conference On Communications*, 3, May 2002.

[KLF01] Y. Kou, S. Lin, and M. Fossorier. Low Density Parity-Check Codes Based on Finite Geometries: A rediscovery and new results. *IEEE Transactions on Information Theory*, 47:2711–2736, 2001.

[KO02] Goran Klang and Björn Ottersten. Structured semi-blind interference rejection in dispersive multichannel systems. *IEEE Transactions on Signal Processing*, 50, August 2002.

[KO05] G. Klang and B. Ottersten. Interference robustness aspects of space-time block code-based transmit diversity. *IEEE Transactions on Signal Processing*, 53, April 2005.

[KVKM07] J. Karjalainen, N. Veselinovic, K. Kansanen, and T. Matsumoto. Iterative Frequency Domain Joint-over-Antenna Detection in Multiuser MIMO. *IEEE Transactions on Wireless Communications*, 6, 2007.

[KZC05] C. C. Ko, W. Zhi, and F. Chi. ML-based frequency estimation and synchronization of frequency hopping signals. *IEEE Transactions On Signal Processing*, 53, February 2005.

[Lec07] G. Lechner. Efficient Decoding Techniques for LDPC Codes. *Dissertation TU Vienna*, July 2007.

[LR95] M. Luise and R. Reggiannini. Carrier recovery in all-digital modems for burst-mode transmissions. *IEEE Trans. Comm.*, 43, 1995.

[LX97] H. Liu and G. Xu. Smart antennas in wireless systems: Uplink multiuser blind channel and sequence detection. *IEEE Transactions on Communications*, 45, 1997.

[MA90] H. Meyr and G. Ascheid. *Synchronisation in Digital Communications*. John Wiley & Sons, New York, 1990.

[MB02] Gérard Maral and Michel Bousquet. *Satellite Communications Systems: Systems, Techniques and Technology*. John Wiley & Sons, New York, 4 edition, 2002.

[MD97] U. Mengali and N. D'Andrea. *Synchronisation Techniques for Digital Receivers*. Plenum Press, New York, 1997.

[MFRC07] S. Morosi, R. Fantacci, E. Del Re, and A. Chiassai. Design of turbo-MUD receivers for overloaded CDMA systems by density evolution technique. *IEEE Transactions on Wireless Communications*, 6, 2007.

[MM97] Umberto Mengali and M. Morelli. Data-Aided Frequency Estimation for Burst Digital Transmission. *IEEE Transactions on Communications*, 45(1), January 1997.

[MMF98] Heinrich Meyr, Marc Moeneclaey, and Stefan A. Fechtel. *Digital Communication Receivers, Synchronization, Channel Estimation and Signal Processing*. John Wiley & Sons, New York, 1998.

[MN96] D. MacKay and R. Neal. Near shannon limit performance of low density parity check codes. *Electronics Letters*, 32:1645–1646, 1996.

[Mos96] S. Moshavi. Multi-user detection for DS-CDMA communications. *IEEE Communications Magazine*, October 1996.

[MR04] A. Morello and U. Reimers. DVB-S2, the second generation standard for satellite broadcasting and unicasting. *International Journal on Satellite Communications and Networking*, 22:249–268, 2004.

[MS84] H. Meyr and G. Spies. The structure and performance of estimators for real-time estimation of randomly varying time delay. *IEEE Transactions on Acoustics, Speech and Signal Processing*, ASSP-32(1), February 1984.

[MYBM01] Catherine Morlet, Jungpil Yu, Marie-Laure Boucheret, and Gilles Mesnager. Synchronization algorithms for multimedia satellite communications payloads. *7th International Workshop on Digital Signal Processing Techniques for Space Communications - Sesimbra Protugal*, October 2001.

[NSM02] N. Noels, H. Steendam, and M. Moeneclaey. The True Cramer-Rao Bound for Phase-Independent Carrier Frequency Estimation from a PSK signal. *GLOBECOM 2002 - IEEE Global Telecommunications Conference*, 21, November 2002.

[NSM04] N. Noels, H. Steendam, and M. Moeneclaey. The True Cramer-Rao Bound Frequency Estimation From a PSK signal. *IEEE Transactions on Communications*, 52, 2004.

[ORK89] B. Ottersten, R. Roy, and T. Kailath. Signal waveform estimation in sensor array processing. *Proc. 23rd ASILOMAR Conference on Signals, Systems and Computing*, 2, 1989.

[OSA99] Bjorn Ottersten, Peter Stoica, and David Astely. Spatio-temporal processing for wireless communications. *Radio Vetenskap och Kommunikation*, pages 402–406, June 1999.

[OVK92] Bjorn Ottersten, Mats Viberg, and Thomas Kailath. Analysis of Subspace Fitting and ML Techniques for Parameter Estimation from Sensor Array Data. *IEEE Transactions on Signal Processing*, 40:590–600, March 1992.

[PF94] B. R. Petersen and D. D. Falconer. Suppression of adjacent channel, cochannel and intersymbol interference by equalizers and linear combiners. *IEEE Transactions on Communications*, 42, December 1994.

[PP97] A. Paulraj and C. Papadias. Space-Time Processing for Wireless Communications. *IEEE Signal Processing Magazine*, 14:49–83, November 1997.

[Pro00] John G. Proakis. *Digital Communications.* McGraw Hill, New York, 4 edition, 2000.

[Ras08] Lars K. Rasmussen. Linear Detection in Iterative Joint Multiuser Decoding. *IEEE International Symposium on Communications, Control and Signal Processing*, pages 753–757, March 2008.

[RBL+00] T. Reveyrand, D. Barataud, J. Lajoinie, M. Campovecchio, J.-M. Nebus, E. Ngoya, J. Sombrin, and D. Roques. A Novel Experimental Noise Power Ratio Characterization Method for Multicarrier Microwave Power Amplifiers. *ARFTG Conference Digest - Spring, 55th*, 37:1–5, June 2000.

[RdG04a] Rita Rinaldo and Riccadro de Gaudenzi. Capacity analysis and system optimization for the forward link of multi-beam satellite broadband systems exploiting adaptive coding and modulation. *International Journal of Satellite Communications and Networks*, 22:401–423, 2004.

[RdG04b] Rita Rinaldo and Riccadro de Gaudenzi. Capacity analysis and system optimization for the reverse link of multi-beam satellite broadband systems exploiting adaptive coding and modulation. *International Journal of Satellite Communications and Networks*, 22:425–448, 2004.

[SCD+87] P. M. Smith, P. C. Chao, K. H. G. Duh, L. F. Lester, B. R. Lee, and J. M. Ballingall. Advances in HEMT technology and applications. *IEEE International Microwave Symposium Digest*, 87:749–752, 1987.

[Sch81] Martin Schetzen. Nonlinear system modeling based on the Wiener theory. *Proceedings IEEE*, 69:1557–1573, 1981.

[SGO07] Klaus Schwarzenbarth, Joel Grotz, and Björn Ottersten. MMSE based interference processing for satellite broadcast reception. In *Proceedings IEEE Vehicular Technology Conference, Spring*, March 2007.

[SGS08] Shakti Prasad Shenoy, Irfan Ghauri, and Dirk T. M. Slock. Receiver Designs for MIMO HSDPA. *Proceedings of the IEEE International Conference on Communications (ICC) 2008*, 2008.

[Sha48] Claude E. Shannon. A mathematical theory of communication. *Bell Systems Technical Journal*, 27:379–423, 623–656, October 1948.

[Tan96] R. Tanner. A recursive approach to low complexity codes. *IEEE Transactions on Information*, 32:1645–1646, 1996.

[Tel] TelliTec. Tellinet application module, enhanced TCP. *TelliTec*.

[TKN05] Tarik Taleb, Nei Kato, and Yoshiaki Nemoto. Recent Trends in IP/NGEO Satellite Communication Systems: Transport, Routing, and Mobility Management Concerns. *IEEE Wireless Communications*, 12:63–69, October 2005.

[TPV96] S. Talwar, A. Paulraj, and M. Viberg. Blind separation of synchronous co-channel digital signals using an antenna array. I. Algorithms. *IEEE Transactions on Signal Processing*, 44, 1996.

[TPV97] S. Talwar, A. Paulraj, and M. Viberg. Blind separation of synchronous co-channel digital signals using an antenna array. II. Performance analysis. *IEEE Transactions on Signal Processing*, 45, 1997.

[TR06] Peng Hui Tan and Lars K. Rasmussen. Asymtotically Optimal Nonlinear MMSE Multiuser Detection Based on Multivariable Gaussian Approximation. *IEEE Transactions on Communications*, 54:1427–1438, August 2006.

[TT06] Goncalo N. Tavares and Luis M. Tavares. The True Cramer-Rao Lower Bound for Data-Aided Carrier-Phase-Independent Time-Delay Estimation From Linearly Modulated Waveforms. *IEEE Transactions on Communications*, 54(1), January 2006.

[TV05] D. Tse and P. Viswanath. *Fundamentals of Wireless Communications*. Cambridge University Press, Cambridge, 2005.

[VB96] L. Vandenberghe and S. Boyd. Semidefinite programming. *SIAM Review*, 38, 1996.

[Ver98] S. Verdu. *Multiuser Detection*. Cambridge University Press, London, 1998.

[VO91] M. Viberg and B. Ottersten. Sensor array processing based on subspace fitting. *IEEE Transactions on Signal Processing*, 39(5), May 1991.

[Wei82] S. Weinreb. Low noise technology, 1982 state-of-the-art. *IEEE International Microwave Symposium Digest*, 82:10–12, 1982.

[WFGV98] P. W. Wolniansky, G. J. Foschini, G. D. Golden, and R. A. Valenzuela. V-BLAST: an architecture for realizing very high data rates over the rich-scattering wireless channel. *URSI International Symposium on Signals, Systems, and Electronics*, 1998.

[Win84] J. H. Winters. Optimum combining in digital mobile radio with cochannel interference. *IEEE Journal on Selected Areas in Communications*, SAC-2, 1984.

[WP99] X. Wang and H. V. Poor. Iterative (turbo) soft interference cancellation and decoding for coded CDMA. *IEEE Transactions on Communications*, 47, 1999.

[YBD02] D. Yachil, B. Bobrovsky, and J. Davidson. Multichannel synchronization for burst modems with adjacent channel interference. *Proceedings of the 22nd Convention of Electronics and Electrical Engineers in Israel*, pages 225–227, 2002.

[YDB06] D. Yachil, J. Davidson, and B. Bobrovsky. Low complexity multichannel synchronization for satellite systems with adjacent channel interference. *International Journal on Satellite Communications and Networks*, 24(1), 2006.

[ZK05] Dunmin Zhen and Peter D. Karabinis. Adaptive Beam-Forming with Interference Suppression in MSS with ATC. *Proceedings of the 23rd International Communications Satellite Systems Conference (ICSSC), Rome*, September 2005.